Exploring the electrophysiological responses to sudden sensory events

Richard Somervail

PhD Thesis

Systems Neuroscience

University College London (UCL)

Supervisor:
Professor Giandomenico Iannetti

Dedications

To my family, who gave me passion for knowledge.

To my friends, who nurtured that passion.

To my lab group, who taught me how to use it.

Exploring the electrophysiological responses to sudden sensory events

---

I, Richard Somervail, confirm that the work presented in this thesis is my own. Where information has been derived from other sources, I confirm that this has been indicated in the thesis. Chapters 4 and 7 have been published in the journals Cerebral Cortex in 2020 and Scientific Reports in 2019, respectively, with myself as first author.

Abstract

Living in rapidly changing and potentially dangerous environments has shaped animal nervous systems toward high sensitivity to sudden and intense sensory events - often signalling threats or affordances requiring swift motor reactions. Unsurprisingly, such events can elicit both rapid behavioural responses (e.g. the defensive eye-blink) and one of the largest electrocortical responses recordable from the scalp of several animals: the widespread Vertex Potential (VP). While generally assumed to reflect sensory-specific processing, growing evidence suggests that the VP instead largely reflects *supramodal* neural activity, sensitive to the *behavioural-relevance* of the eliciting stimulus. In this thesis, I investigate the relationship between sudden events and the brain responses and behaviours they elicit. In Chapters 1-3, I give a general introduction to the topic. In Chapter 4, I dissect the sensitivity of the VP to stimulus intensity - showing that its amplitude is sensitive only to the relative increase of intensity, and not the absolute intensity. In Chapter 5, I show that both increases and decreases of auditory and somatosensory stimulus intensity elicit the same supramodal VP, demonstrating that the VP is sensitive to any sufficiently abrupt sensory change, regardless of its direction or sensory modality. In Chapter 6, I observe strong correlations between the magnitudes of the VP and the eye-blink elicited by somatosensory stimuli (hand-blink reflex; HBR), demonstrating a tight relationship between cortical activity and behaviour elicited by sudden stimuli. In Chapter 7, I explore this relationship further, showing that the HBR is sensitive to high-level environmental dynamics. In Chapter 8, I propose an account of the underlying neural substrate of the VP, consistent with my results and the literature, which elucidates the relationship between the VP and behaviour. I also detail future experiments using fMRI and intracranial recordings to test this hypothesis, using the knowledge gained from this thesis.

Impact Statement

Exploring the brain responses to sudden sensory stimuli and their relationship to behaviour is likely to provide insights into a vast range of related topics, such as attention, motor preparation, and the predictive mechanisms of the brain.

In the longer term, this field could have an impact on clinical research. Although it is difficult to predict exact clinical outcomes from basic science research, it is nevertheless critical to form a solid foundation of basic scientific understanding before science can be applied successfully. In particular, having a good understanding of the fundamental networks involved in responding to sudden sensory events may eventually form the basis for a better understanding of a wide range of clinical disorders, including many types of anxiety, ADHD and obsessive-compulsive disorder. Having a deeper understanding of such conditions will allow better (and hopefully more personalised) clinical treatments.

Eventually, this research could also contribute to a broad range of non-medical fields, from emergency services (e.g. the split-second decisions made by firefighters) to law (e.g. in legal cases, understanding human behaviour during emergency situations).

Exploring the electrophysiological responses to sudden sensory events

1 Table of Contents

2 Preface

2.1 Acknowledgements

All data presented were exclusively analysed by myself alone, except for the geometric modelling in Chapter 7 which was done together with Rory Bufacchi.

The data presented in Chapter 4 were collected by myself (Experiments 4.1, 4.2 and 4.C), and Fengrui Zhang (Experiment 4.3; EcoG data from rats) at University of Chinese Academy of Sciences, Beijing. The data in Experiment 4.2 were collected with assistance from Cristina Salvatori. The vibrotactile stimulator used in Experiment 4.2 was built by Claudio Lorini and Marco Crepaldi.

The data presented in Chapter 5 were collected by myself, with assistance from Cristina Salvatori (Experiments 5.1 and 5.3), Sofija Perovic (Experiment 5.2), and Davide Ahmar (Experiments 5.2 and 5.4). The force measurement system used in Experiment 5.4 was set up by Lydia Neary-Zajiczek.

The data presented in Chapter 6 were collected by Rory Bufacchi and James Steckelmacher. Data were preprocessed by myself and Rory Bufacchi.

The data presented in Chapter 7 were collected by Rory Bufacchi (Experiment 7.1) and myself, with assistance from Oliver Eastwood (Experiment 7.2). The Virtual Reality environments used in Experiments 7.1 and 7.2 were programmed by myself and Rory Bufacchi, with assistance from Erin Somervail.

3 General Introduction

3.1 The ethological importance of sudden sensory events

Animals face a rapidly changing and potentially dangerous environment, in which sudden sensory events can indicate situations demanding an immediate behavioural response. Indeed, a ripple in the ocean or the snap of a twig underfoot could signal the arrival of a dangerous predator to avoid, or a crucial opportunity to catch prey. Not every sudden event necessitates a behavioural reaction of course, but the cost of ignoring them altogether would be too great for any organism. Even in modern society, in which we are far too often assaulted with a barrage of irrelevant yet attention-grabbing stimuli (e.g. while being marched through the disorienting 'Duty-Free' section in the airport), sudden events maintain their relevance. While driving, detecting an abrupt sound or flash of light could result in life or death. The ability to detect and appropriately respond to sudden sensory events is therefore key to survival, and these events have shaped nervous systems throughout evolution. Given their importance, it is no surprise that such events elicit one of the largest and most widespread transient electrocortical responses detectable using scalp or epidural recordings. These responses have been described in a number of animals including rats (Knight et al., 1985; Hu et al., 2015; Guo et al., 2016; Xia et al., 2016; Hu and Iannetti, 2019), monkeys (Kulics, 1982; Gardner et al., 1984; Neville and Foote, 1984; Pineda et al., 1989; Beydoun et al., 1997) and humans (Bancaud et al., 1953; Walter, 1964; Mouraux and Iannetti, 2009). In this thesis, I present a series of experiments investigating the relationship between sudden environmental stimuli, the brain responses they elicit, and behaviour. Throughout the work, I use the words "sudden" and "abrupt" interchangeably to refer to such rapid (or fast-rising) sensory changes.

3.2 Sudden sensory events elicit large, widespread and highly supramodal Vertex Potentials in the human EEG

In the human electroencephalogram (EEG), the response to sudden sensory events consists of a large and widespread negative-positive (N-P) event-related potential (ERP), which is maximal at the scalp vertex and sometimes referred to as a Vertex Potential (VP) or Vertex Wave[1] (Bancaud et al., 1953; Walter, 1964; Davis and Zerlin, 1966; Snyder and Hillyard, 1976; Torta et al., 2012; Novembre et al., 2018). The VPs elicited by different sensory modalities have highly similar morphology and scalp distribution (Figure 3.1; Mouraux and Iannetti, 2009; Liang et al., 2010). The average latencies of the N and P waves vary depending on modality, but this can be satisfactorily explained by differences in peripheral conduction: for example, the VP elicited by non-nociceptive electrical stimulation of Aβ fibres using transcutaneous stimuli applied to the hand typically peaks at ~110 and ~250 ms post-stimulus (N and P respectively) while the VP elicited by nociceptive laser stimulation of Aδ fibres in the hand typically peaks at ~200 and ~330 ms (Mouraux and Iannetti, 2009), reflecting the difference in conduction velocity between these fibres (Tran et al., 2001). Similarly, stimulation of different body parts also results in different response latencies (Figure 3.2; Valentini et al., 2012; Hu et al., 2014b).

[1] Not to be confused with the *vertex sharp wave* that is observed in the EEG recorded during the early stage of non-REM sleep (e.g. Kooi et al., 1964).

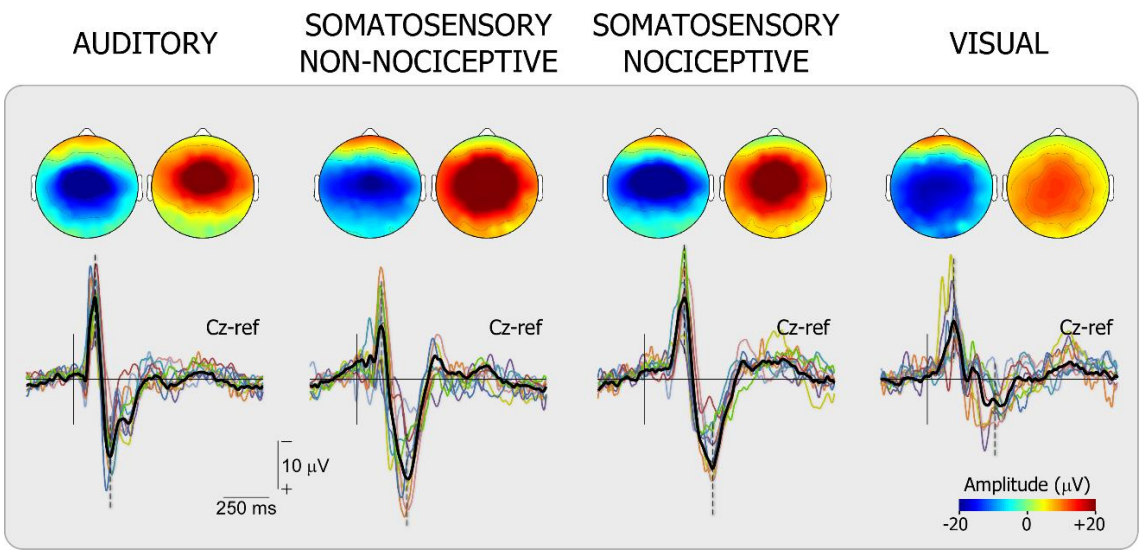

Figure 3.1. The EEG responses to sudden stimuli are highly similar regardless of sensory modality (adapted from Mouraux and Iannetti, 2009)

Black plots show the grand average EEG waveforms (at Cz) elicited by sudden stimuli of four sensory modalities. Coloured plots show the single-participant averages. Vertical lines indicate stimulus onset. Scalp distributions are also shown for the negative and positive peaks of each grand average waveform. Note the similarity of waveform morphologies and scalp distributions across the four modalities. Due to their vertex-maximal scalp distributions, these responses are sometimes labelled 'Vertex Potentials' (VP). However, other labels exist such as 'auditory-evoked potential' for the VP elicited by auditory stimuli or 'visual-evoked potential' for the VP elicited by visual stimuli etc. I use the term 'Vertex Potential' throughout this thesis (see Figure 3.3).

Despite broad similarities in morphology and scalp distribution across modalities, the VP is often interpreted as a response which primarily reflects neural activity specific to the modality of the stimulus used to evoke it, and is more commonly labelled according to that modality. For example, the VP elicited by painful laser stimulation has been referred to as a laser-evoked potential (LEP) and assumed to reflect nociceptive processing and pain perception (e.g. Iannetti et al., 2005; Valeriani et al., 2008; Paloyelis et al., 2016; Staikou et al., 2016; Uglem et al., 2017; Hird et al., 2018; Squintani et al., 2018; Valeriani et al., 2021; Zhang et al., 2021), while the VP elicited by auditory stimuli is usually referred to as an auditory-evoked potential (AEP) and interpreted as a measure of neural activity in auditory cortex (e.g. Jones, 1992; Hegerl et al., 1994; Martin and Boothroyd, 1999, 2000; Shahin et al., 2003; Baumann et al., 2008; Ben-David et al., 2011; Carpenter and Shahin, 2013; Baltzell and Billings, 2014; Han and Dimitrijevic, 2015; Wagner et al., 2016).

This interpretation is sometimes justified by the results of source analysis studies which found neural generators in sensory-modality-specific cortical regions (e.g. Scherg et al., 1989; Hegerl et al., 1994; Picton et al., 1999; Mulert et al., 2002; Pratt et al., 2010; Han and Dimitrijevic, 2015), although generators in other areas are also found, such as the anterior cingulate, supplementary motor, orbitofrontal, occipitotemporal and operculoinsular cortex (e.g. Picton et al., 1999; Garcia-Larrea et al., 2003; Mouraux and Iannetti, 2009; Pratt et al., 2010). However, source analysis of EEG has a very high degree of uncertainty due to the large solution space, and this problem is compounded when the analysis is applied to a widespread EEG response with many subcomponents (Grech et al., 2008), which is likely to be the case for the VP (see Näätänen and Picton, 1987, and below for additional evidence).

An alternative interpretation is that the VP largely reflects neural activity which is supramodal (i.e. independent of the modality-specific sensory systems). This view is informed by studies which use methods that dissect the response into its

underlying subcomponents. These methods range from simple re-referencing of the EEG montage (e.g. Iannetti et al., 2005; Hu et al., 2010) to more sophisticated techniques such as adaptive spatial filtering (local spatial analysis; Bufacchi et al., 2021), microstate analysis (Hu et al., 2014b; Figure 3.2) or probabilistic independent component analysis (Mouraux and Iannetti, 2009; Liang et al., 2010; Figure 3.3). These approaches have revealed that the VP is dominated by a large, supramodal subcomponent which is maximal at scalp vertex, while more local and modality-specific subcomponents account for smaller proportions of the response (Figure 3.3; Mouraux and Iannetti, 2009; Liang et al., 2010; Hu et al., 2014b). For example, the somatosensory N1 and P4 responses which contribute some variance to the earliest and latest parts of the response, and whose scalp distributions suggest that they are generated by neural activity in the primary somatosensory cortex contralateral to the stimulated body part (Figure 3.2; Liang et al., 2010; Valentini et al., 2012; Hu et al., 2014b). When source analysis is performed on the supramodal subcomponents, generators are found in regions outside the modality-specific sensory cortices, such as anterior cingulate and insular cortex (Mouraux and Iannetti, 2009). Further support for this supramodal interpretation comes from direct, interventional evidence in rats: a large vertex-maximal subcomponent of the response elicited by auditory stimuli was largely unaffected by bilateral ablation of the primary auditory cortices, while smaller lateralised subcomponents were completely abolished (Simpson and Knight, 1993).

As the supramodal and vertex-maximal subcomponents make up most of the total variance of the response, I use the term ‘Vertex Potential’ to refer to the ERP throughout this thesis, rather than alternative terms which carry the implication of modality-specificity (such as ‘auditory-evoked potential’).

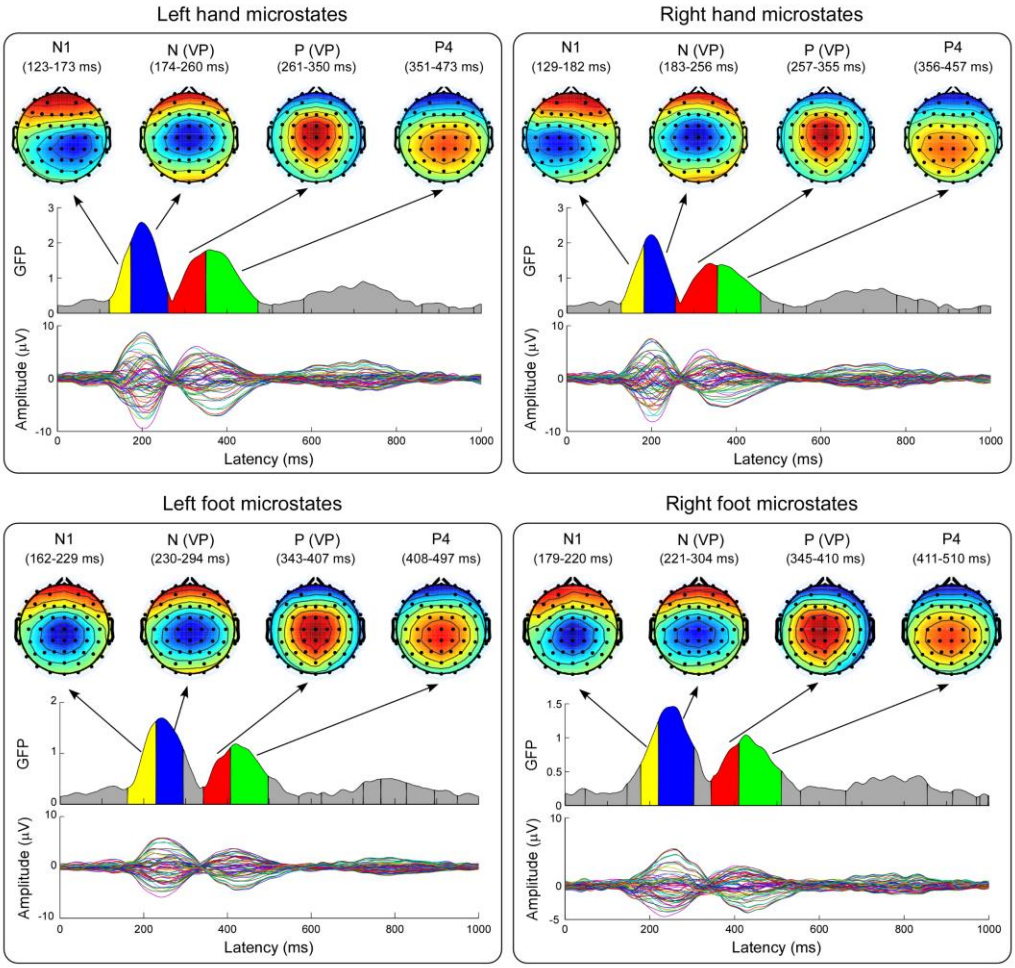

Figure 3.2. Somatosensory-specific N1 and P4 components contribute mostly to the earliest and latest parts of the ERP (adapted from Hu et al., 2014b)
Breakdown of laser-evoked responses into functional microstates. Group-level waveforms, global field power (GFP), and functional microstates of ERPs elicited by the stimulation of the hand dorsum (upper panels) and the foot dorsum (lower panels), on the left side (left panels) and the right side (right panels). Coloured plots show signal at different electrodes superimposed. Four functional microstates (marked in yellow, blue, red, and green) were observed in all four conditions and contributed to the response amplitude at time intervals corresponding to the N1, vertex N wave, vertex P wave and P4 subcomponents. Note that the maximum of the scalp distributions of the N1 and P4 microstates were located above the primary somatosensory cortex (S1) contralateral to the stimulated body part. Importantly, this lateralization was more pronounced for the hand conditions than for the foot conditions, due to the respective locations of the hand and foot regions of S1. This figure shows that modality-specific subcomponents reflecting S1 contribute some variance to the earliest and latest parts of the somatosensory ERP, while the core of the response is dominated by the vertex-maximal N and P components. Note that this analysis does not show the overlap of different subcomponents or the proportions of their contribution to the total signal variance (for this, see Figure 3.3).

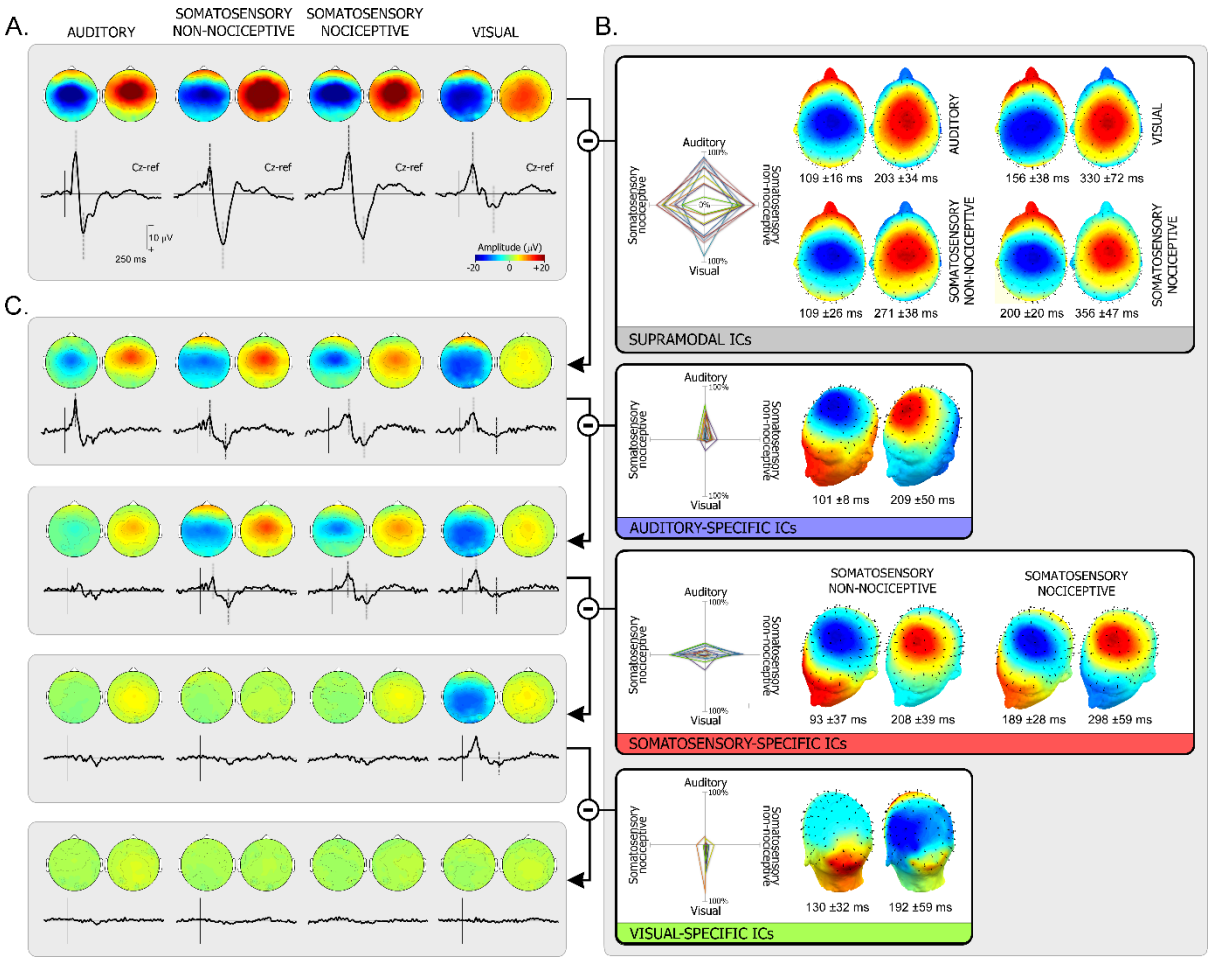

Figure 3.3. Vertex Potentials are largely comprised of supramodal subcomponents (adapted from Mouraux and Iannetti, 2009)

A. The grand average waveforms (at Cz) elicited by four sensory modalities and corresponding scalp distributions at the negative and positive peaks. Vertical lines indicate stimulus onset.

B. Independent components (ICs) resulting from the breakdown of the single-participant averaged responses from each sensory modality. ICs were classified according to their contributions to the total response variance for each modality. Radar plots show these contributions for each participant separately. Scalp distributions are shown for the grand average waveforms for each component category.

C. Sequential subtraction of each IC category from the grand average waveforms for each sensory modality. Note how the subtraction of supramodal components markedly reduces signal amplitude, thereby showing that supramodal neural activity comprises the bulk of the responses to each sensory modality. As such, I use the term 'Vertex Potential' to refer to the response throughout this thesis, rather than alternative terms which carry the implication of modality-specificity (such as 'auditory-evoked potential').

3.3 Vertex Potentials, surprise, and behavioural relevance

VPs are often assumed to reflect sensory-specific processing or processing related to perception (e.g. Chen et al., 1979; Martin and Boothroyd, 1999; Iannetti et al., 2005; Spackman et al., 2006; Baltzell and Billings, 2014; Paloyelis et al., 2016; Staikou et al., 2016; Uglem et al., 2017; Squintani et al., 2018; Valeriani et al., 2021). This assumption has sometimes been justified by the observation that VP amplitude appears to "encode" properties of the sensory stimulus, such as intensity (Davis and Zerlin, 1966; Davis et al., 1968; Schweitzer and Tepas, 1974; Chen et al., 1979; Bromm and Treede, 1991; Beydoun et al., 1993; Arendt-Nielsen, 1994; García-Larrea et al., 1997; Iannetti et al., 2005; Huang et al., 2013; Hu et al., 2014a). However, this relationship with intensity can be disrupted: predictable repetition of identical stimuli at short latency (e.g. at 1 Hz) will substantially reduce the magnitude of the VP (i.e. the response habituates; Figure 3.4) without affecting perceived intensity (Ritter et al., 1968; Chapman et al., 1981; Woods et al., 1984; Treede et al., 2003; Iannetti et al., 2008; Wang et al., 2010; Herrmann et al., 2015). These results indicate that the above sensory-specific interpretation above is incorrect.

Instead of faithfully encoding the sensory percept, the response magnitude appears to instead reflect the degree of change relative to previous stimuli, which could be referred to as *deviance*, *contrast,* or *salience*[2]. A sudden stimulus essentially reflects a rapid change in the environment, giving rise to the large VP response. When that stimulus is repeated at short latency (e.g. a train of stimuli at 1 Hz), *the contrast with the recent sensory input is reduced*, and a smaller VP is elicited (Iannetti et al., 2008). However, when the temporal predictability of the train of stimuli is disrupted by randomly varying the time-interval between

[2] Also called "saliency" by some authors (Novembre et al, 2018).

successive stimuli, the resulting VP is not reduced in amplitude (Wang et al., 2010). This result indicates that the VP is sensitive not only to the low-level contrast with recent sensory input, but also higher-level contrasts with the predictions or expectations[3] that the nervous system makes about forthcoming sensory input. Both of these observations can be interpreted in a common framework: the VP is sensitive to sudden violations of expectations at different levels, ranging from the violation of low-level predictions (e.g. that the sensory input will not suddenly change) to higher-level predictions (e.g. that a sequence of identical changes of sensory input will continue occurring in a regular fashion). In this thesis, I describe this violation of expectations as *unexpectedness* or *surprise.* Importantly, the term "surprise" here does not necessarily imply the conscious experience of surprise. Indeed, the term is used in theories of brain function without this implication (Friston, 2009). As such, factors can be surprising for the brain system underlying the VP without necessarily being surprising for the individual at a conscious level: for example, during an experiment in which participants are informed that sudden stimuli will be delivered.

[3] I use the words "expectation" and "prediction" interchangeably here and throughout the thesis.

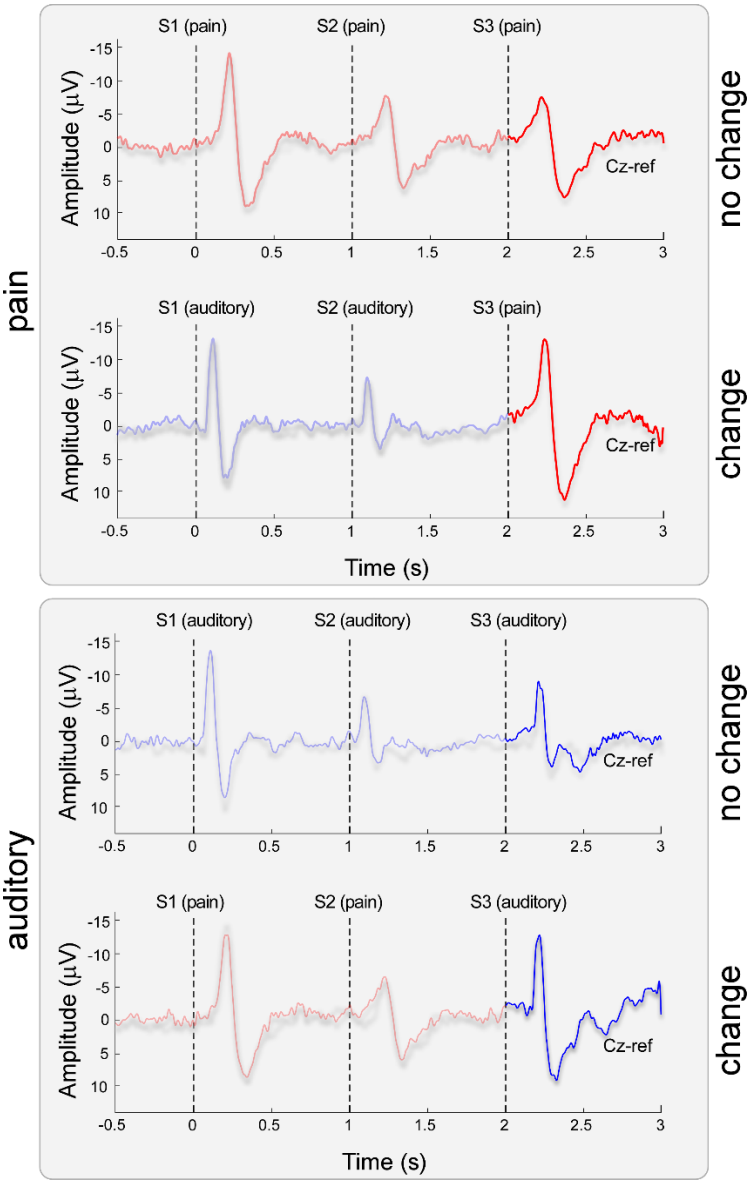

Figure 3.4. Vertex Potentials are highly sensitive to the surprise content of the eliciting stimulus (adapted from Valentini et al., 2011)
Grand average Vertex Potentials (VP) elicited by painful laser stimuli (red) and auditory stimuli (blue) at Cz. Stimuli were delivered in triplets at 1 Hz (S1-S2-S3). Vertical dashed lines indicate stimulus onsets. S1 and S2 always belonged to the same sensory modality, while S3 belonged to either the same modality as S1 and S2 (triplet no change, *top waveforms of each panel*) or to the other modality (triplet change, *bottom waveforms of each panel*). The data show a reduction of VP amplitude when identical stimuli were repeated in sequence (i.e. habituation), and an increase of amplitude when there was a change of modality between S2 and S3 (i.e. *dis*habituation). These results show that VPs are highly sensitive to the surprise content (i.e. the unexpectedness) of the eliciting stimulus.

Indeed, several factors influencing *surprise* at different levels can effectively modulate the VP magnitude: First, more abrupt stimuli (i.e. stimuli with shorter rise-time) elicit a larger VP than less abrupt stimuli (Onishi and Davis, 1968). Second, the VP will habituate at short timescales (as discussed above; Ritter et al., 1968; Chapman et al., 1981; Iannetti et al., 2008; Wang et al., 2010; Herrmann et al., 2015), and this habituation can be reversed by changes of particular stimulus properties, such as changes of sensory modality (Valentini et al., 2011), changes of stimulus location in egocentric, but not somatotopic, coordinates (Moayedi et al., 2016) and successive increases, but not decreases, of stimulus intensity in a sequence of abrupt stimuli (Ronga et al., 2013). Third, the VP will habituate also at longer timescales (i.e. minutes; Fruhstorfer, 1971).

What do these rules determining the sensitivity of the VP to surprise suggest about its function? As discussed earlier (Chapter 3.1), from an ethological perspective sudden sensory events can reflect potentially dangerous situations requiring an *urgent and immediate behavioural response*. More surprising sudden events are therefore more likely to entail less time for an animal to prepare for the necessary behavioural response. As such, the *urgency* of that behavioural response is far higher, resulting in a larger VP amplitude. Ultimately, the importance of the surprise content of an environmental event is due to the *behavioural relevance* of that event.

Given this sensitivity to *behavioural relevance*, our group has previously hypothesised that VP function is related to the preparation for immediate behavioural responses (Iannetti and Mouraux, 2010; Moayedi et al., 2015; Novembre et al., 2018). The rules determining VP magnitude seem to be consistent with this ethological perspective. For example, the importance of abrupt and intense stimuli moving towards the core of the body (Torta et al., 2012; Moayedi et al., 2016) has a clear relevance to survival in a natural environment: such stimuli could represent a threat to the body which demands an immediate behavioural response. Several other results suggest such a relationship with

behaviour. Our group recently described a clear relationship between the VP and the motor system: abrupt stimuli, delivered while participants maintain a constant isometric force with their hand, elicit a multiphasic modulation of the exerted force (Novembre et al., 2018). Importantly, this modulation of force shares several properties with the VP (such as supramodality and sensitivity to the surprise content of the stimulus), and is highly correlated with VP amplitude, indicating a tight coupling between the VP and motor output (Novembre et al., 2018). Additionally, the peaks of the VP are known to correlate with movement reaction time independently of confounding factors such as perceived stimulus intensity (Moayedi et al., 2015; Tiemann et al., 2018), and this relationship is stronger when the stimulus triggers *defensive* movements (Moayedi et al., 2015). A close relationship between the VP and behaviour makes sense given that the abrupt and intense sensory stimuli which elicit this brain response also elicit a large number of defensive reflexes (which are perhaps the simplest examples of urgent behaviours in nature), such as the withdrawal reflex to painful heat stimuli (Creed et al., 1932), various blink reflexes (Miwa et al., 1998; Lucia et al., 2009; Sambo et al., 2012b) and the startle reflex (Cooke and Graziano, 2003).

3.4 Outstanding questions

So far, I have outlined what is known about the functionality of the large, widespread brain response to abrupt sensory stimuli (the Vertex Potential). I have also detailed a central hypothesis about the function of the VP: that it is elicited by surprising and therefore behaviourally-relevant environmental changes, and that it reflects the preparation for immediate behavioural responses to those events.

To test this hypothesis, I explore the following questions:

(1) Which environmental features determining behavioural-relevance can modulate the brain and behavioural responses to sudden sensory events?
(2) What is the relationship between these brain and behavioural responses?

In Chapter 4 (*published in Cerebral Cortex, 2020*), I dissect the sensitivity of the VP to the relative (i.e. differential) and absolute components of stimulus intensity, using both auditory and somatosensory stimuli, in humans and rodents.

In Chapter 5 (*ready to be submitted to Cerebral Cortex*), I investigate whether the same supramodal VP can be elicited by equally sudden increases and decreases of auditory and somatosensory stimuli, whether these responses are similarly sensitive to the behavioural-relevance of the stimulus, and whether they are similarly related to concurrent modulations of motor output.

In Chapter 6, I explore the relationship between the Vertex Potential and behaviour by studying a model reflex (the hand blink reflex; HBR), and test whether the HBR magnitude is correlated with VP amplitude.

In Chapter 7 (*published in Scientific Reports, 2019*), I explore whether high-level environmental dynamics reflecting behavioural-relevance can affect the magnitude of the HBR.

4 Brain sensitivity to differential, not absolute, stimulus intensity is conserved across humans and rats

(This chapter has been published as Somervail et al. in *Cerebral Cortex*, 2020)

4.1 Introduction

In this chapter, I explore which environmental features the Vertex Potential is sensitive to. Understanding these features is crucial for understanding the functional role of the VP – when does an organism require such a large, and therefore physiologically costly, brain response?

It is well-established that stimulus intensity largely determines Vertex Potential magnitude, both in humans (Davis and Zerlin, 1966; Davis et al., 1968; Schweitzer and Tepas, 1974; Bromm and Treede, 1991; Beydoun et al., 1993; Iannetti et al., 2005, 2008; Huang et al., 2013; Hu et al., 2014a) and rats (Hu et al., 2015; Xia et al., 2016). However, what is usually labelled 'stimulus intensity' reflects two distinct components that are often conflated (e.g. in all references above): *differential* and *absolute* intensity. '*Differential* intensity' refers to the difference between the baseline and target intensity. In contrast, '*absolute* intensity' can be formalised as the baseline from which an intensity increase takes place, or the target at which the intensity increase arrives, or any other absolute point inbetween the baseline and the target (here, I formalised absolute intensity as the target intensity (see Methods): for example, a difference of 2 units could occur at a low absolute level (from 2 to 4) or a high absolute level (from 9 to 11).

To the best of my knowledge, the relative importance of these two components in eliciting a VP has not been dissected. Indeed, VPs are usually elicited by impulse stimulation, in which stimulus intensity rises from zero to a desired target value, plateaus for a short time, and then drops back to zero (Davis and Zerlin, 1966; Davis et al., 1968; Schweitzer and Tepas, 1974; Bromm and Treede, 1991; Beydoun et al., 1993; Iannetti et al., 2005, 2008; Huang et al., 2013). Obviously,

with this type of stimulus, *differential* and *absolute* intensity covary, and are therefore indistinguishable.

To this end, I conducted three experiments in humans and rats using a paradigm that allowed clear dissociation of *differential* and *absolute* stimulus intensity. I delivered continuous auditory or somatosensory stimuli with embedded abrupt intensity increases of different sizes occurring at different absolute levels, using a 3x3 factorial design (Figure 4.1). Given that abrupt increases of stimulus intensity and isolated impulse stimuli elicit highly similar VPs and likely reflect the same neural system (Nishihara et al., 2011), the results of these experiments should generalise to the VP elicited by impulse stimuli. In Experiments 4.1 and 4.2 I recorded scalp EEG from 36 human participants while delivering auditory and vibrotactile stimuli respectively. In Experiment 4.3, my collaborator (see Chapter 2.1, *Acknowledgements*) recorded activity directly from the brain surface (EcoG) of 5 rats while delivering auditory stimuli.

I hypothesised that differential intensity would be the main factor determining VP magnitude. While it is well-known that a higher sensitivity to sensory differentials than to absolute intensity is a common property of some peripheral receptors (e.g. muscle stretch receptors; Hulliger et al. 1977; Hunt and Wilkinson 1980; Blum et al. 2017), it remains unknown whether widespread event-related brain potentials also show similar sensitivity. Importantly, such brain potentials and their underlying neural processes serve higher-level functions than peripheral receptors, and therefore their sensitivity to different environmental features is more complex and crucially depends on those functions (Ronga et al., 2013). For example, our group has previously found evidence that the VP reflects the unexpectedness of an abrupt environmental event (Iannetti et al., 2008; Valentini et al., 2011; Ronga et al., 2013; Moayedi et al., 2016; Novembre et al., 2018). Given that differential intensity reflects the degree of sensory change, and therefore largely contributes to unexpectedness and behavioural relevance, I expected it to strongly modulate the VP magnitude.

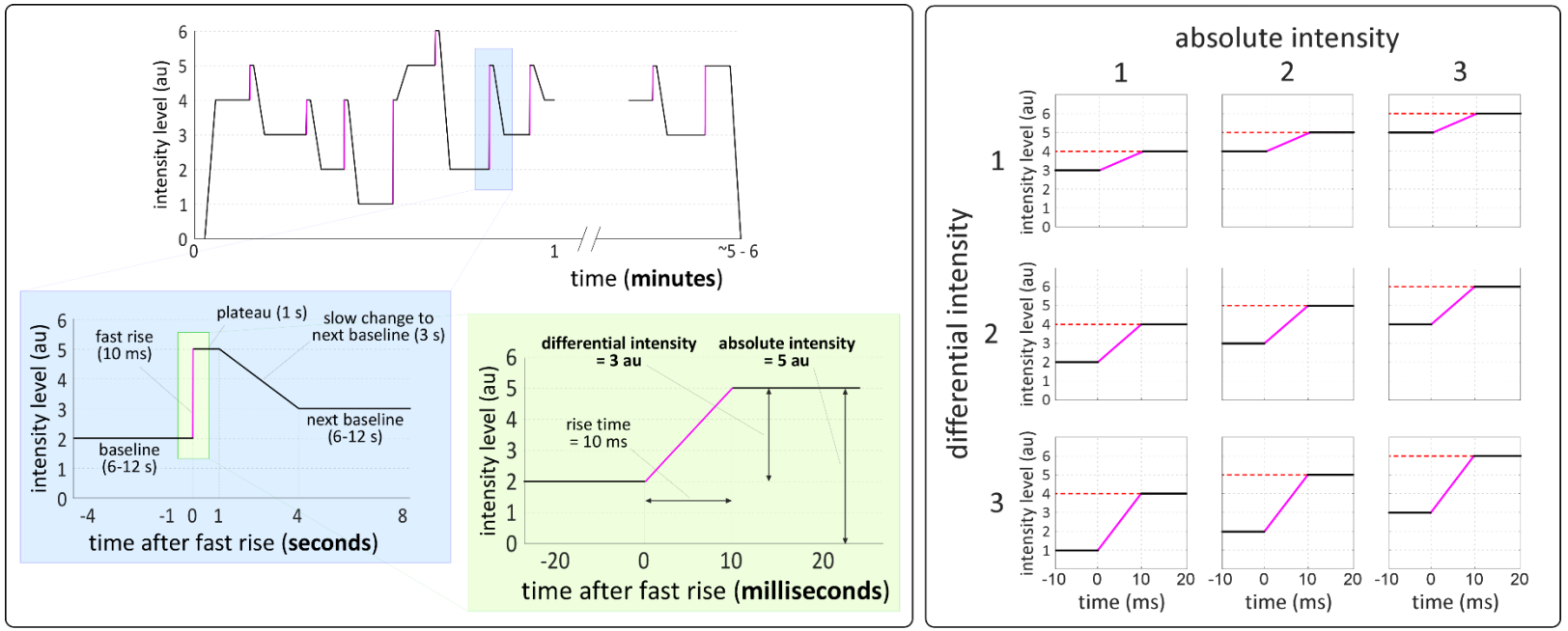

Figure 4.1. Stimulation profile and experimental design.

Left panel. Stimulation profile of a typical block of all three experiments. Stimulus intensity abruptly increased from a baseline level to a target level in 10 ms, plateaued for 1 s and then slowly increased or decreased to the next baseline in 3 s. *Right panel*. Differential and absolute intensity were modulated using a 3x3 factorial design. Each abrupt increase occurred between different baseline and target levels, thus yielding 9 conditions varying in their differential intensity (the difference between baseline and target) and absolute intensity (here defined as the target intensity reached by the increase).

4.2 Methods

Experiments 4.1 and 4.2

Human participants

A total of 36 healthy human participants took part in Experiments 4.1 and 4.2 (N = 18 unique participants in each experiment). In Experiment 4.1 (11 female, age range 21-46 yr, mean age 27 yr), EEG data were collected at UCL, London, UK. In Experiment 4.2 (10 female, age range 24-71 yr, mean age 34 yr), EEG data were collected at IIT, Rome, Italy. All participants gave written informed consent before taking part in the study. All procedures were approved by the respective local ethical committees.

Sensory stimuli

In Experiment 4.1, participants received tonic auditory stimuli, consisting of 600 Hz pure tones delivered binaurally through pneumatic insert-earphones (Etymotic ER-3C 10 Ohm). Auditory stimulation was controlled using Presentation® (Neurobehavioral Systems). In Experiment 4.2, participants received tonic vibrotactile stimuli. Vibrotactile stimuli were delivered through a stimulator attached to the participants' left index finger (Z7A-series DC motor, Jinlong Machinery & Electronics, China), while participants sat with the stimulated hand resting on their lap with the palm facing upwards. The vibrotactile stimulator was driven by a Texas Instruments DRV2605 haptic driver with a Real Time Playback (RTP) interface connected to an ATSAMD21 Cortex-M0 microcontroller and controlled by a PC via USB interface. Vibrotactile stimuli were controlled at high level using MATLAB (MathWorks) and the Psychophysics Toolbox (Brainard, 1997). In Experiment 4.2, white noise was continuously delivered through the same earphones used in Experiment 4.1, to prevent participants from hearing the vibrotactile stimulator. No participant reported hearing the vibrotactile stimulator while white noise was played.

Experimental design

In both experiments, abrupt (10 ms long) increases of stimulus intensity were embedded within tonic stimulation (Figure 4.1, *left panel*). These increases were of three levels of *differential* intensity and reached one of three levels of *absolute* intensity (Figure 4.1, *right panel*). This resulted in a 3x3 factorial design, with 9 conditions in total. The beginnings of the intensity increases were subsequently used for EEG time-lock analysis.

Each experiment consisted of 8 blocks, with 27 intensity increases per block (3 per condition), yielding 216 increases in total (24 of each condition). Figure 4.1 (*left panel*) shows the stimulation profile of a representative block: before the first stimulus, the baseline level was set by slowly rising the intensity level from zero (3 s). After each abrupt increase, stimulus intensity remained at the target level for 1 s. After this plateau, the intensity level slowly increased or decreased to reach the baseline of the next trial. The slow increase or decrease lasted 3 s, to avoid eliciting another VP. After the last stimulus of each block, the intensity slowly decreased to zero (3 s). The mean interval between two consecutive stimulus increases (i.e. between two trials) was 13 s (10-16 s). The nine conditions were presented in pseudorandom order, with the constraint that no more than 2 trials of the same condition were presented consecutively. Participants were allowed to rest for approximately 2 minutes between two consecutive blocks.

Preliminary definition of stimulus intensity levels

The stimulation paradigm entailed six equally spaced intensity levels[4]. These six levels were determined in a preliminary psychophysical experiment conducted in

[4] These levels were equally spaced with respect to *perceived* intensity, rather than *physical* intensity (stimulus energy).

five participants, separately for Experiments 4.1 and 4.2, using the following procedure. Participants were asked to manually adjust the intensity levels using a keyboard and a custom graphical interface. Levels were adjusted to ensure that all increases of intensity with a particular differential were *perceived* as being comparable, regardless of absolute intensity (e.g. to ensure that the perceived differential from level 2 to 4 and from level 3 to 5 was similar). At the beginning of this psychophysical experiment, the lowest level was set at the minimal clearly detectable intensity, and the highest level was set at the maximal comfortable intensity. The levels chosen by each participant to achieve a similar perception of differential intensity were finally averaged across participants. These average levels were used for all participants in subsequent EEG experiments. I also performed an additional control experiment with auditory stimuli, in which the preliminary psychophysical intensity level definition was performed separately by each participant before taking part in the main experiment. This control experiment examined whether inter-participant variability in the stimulus-perception relationship affected our results.

EEG recording and preprocessing

Brain activity was recorded using a 29-channel wireless EEG system (Quick-30, Cognionics, USA; 500 Hz sampling rate). During acquisition, participants were required to keep their gaze on a fixation cross (4 x 4 cm) placed centrally in front of them, at approximately 30° below eye-level. EEG signals were preprocessed and analysed using MATLAB (version 2018a, MathWorks) and Fieldtrip (Oostenveld et al., 2011). Continuous EEG data were first band-pass filtered between 0.5 and 30 Hz (Butterworth). Data were then segmented into epochs using a time-window of ±2 s from the beginning of the abrupt increase of stimulus intensity (epoch duration = 4 s). Artifacts due to eye blinks or eye movements were removed using a validated method based on independent component analysis (Jung et al., 2000). Within each epoch, any electrode with amplitude values exceeding ±100 μV was interpolated by averaging neighbouring electrodes; if more than three electrodes required interpolation, the epoch was

rejected. Remaining epochs were baseline corrected between 200 ms pre-stimulus and stimulus onset, and then visually inspected for remaining artifacts to be rejected. The average number of rejected epochs per participant was 22 ± 14 SD (i.e. approximately 10% of the total number of epochs) in Experiment 4.1 and 10 ± 8 (i.e. approximately 5% of the total number of epochs) in Experiment 4.2. The number of rejected epochs was not different across experimental conditions in Experiment 4.1 (one-way ANOVA: $p = 0.99$), Experiment 4.2 ($p = 0.29$) and Experiment 4.C ($p = 0.98$). Finally, epochs of the same condition were averaged, yielding 9 average waveforms for each participant. VP peaks were also extracted from the across-trial average of each participant and condition, using the following procedure. I first calculated the average response of each participant across all stimulus conditions. I then identified, on this average response, two time windows, each centred on the N and the P wave peaks. I used these time windows to extract separately, from each condition waveform and for each participant, the amplitude and latency of each peak. The mean peak latencies across conditions and participants were as follows. N wave: 113 ± 13 ms; P wave 212 ± 27 ms [Experiment 4.1; auditory stimulation]; N wave: 164 ± 24 ms; P wave: 261 ± 42 ms [Experiment 4.2; somatosensory stimulation].

Statistical analysis

Single-participant average waveforms of each condition were analysed using a linear mixed-effect (LME) model (MATLAB, Statistics and Machine Learning Toolbox) at each timepoint and electrode, with ‘differential intensity’ and ‘absolute intensity’ as fixed effects and ‘participant’ as a random effect. To correct for multiple comparisons, I used a cluster permutation test with 2000 permutations (Maris and Oostenveld, 2007; Phipson and Smyth, 2010) across all channels and timepoints within the time window -200 ms to +600 ms. In addition, to ascertain whether the LME results obtained using the point-by-point analysis were consequent to a modulation of response latencies, I analysed the peak latency values extracted from the average waveform of each participant and condition using an LME model with the same experimental factors described above. To test

for an interaction between the factors ‘differential intensity’ and ‘absolute intensity’, I also performed a two-way repeated measures ANOVA with false discovery rate (FDR) correction for all three EEG experiments.

Experiment 4.3

Animals & surgical procedure

The experiment was conducted on 5 adult male Sprague Dawley rats weighing 300-400 g at the Chinese Academy of Sciences, Beijing, China. Rats were fed ad libitum with water and food and were housed in separate cages under temperature- and humidity-controlled conditions. They were kept in a 12 h day/night cycle (lights on from 19:00-7:00). All experimental procedures adhered to local guidelines for animal experimentation and were approved by the local ethics committee. Surgical procedures and electrode positioning are detailed elsewhere (Xia et al., 2016; Jin et al., 2018; Zhang et al., 2019). Following surgery, rats were kept in individual cages for at least 7 days before the collection of ECoG data.

Sensory stimuli

Auditory stimulation was an 8000 Hz pure tone delivered from a loudspeaker placed below the cage (but not in contact with the cage floor). The difference in frequency of stimulation between the human and animal experiments reflects the between-species difference in auditory frequency sensitivity (Jamison, 1951; Hess, 2015). Stimuli were controlled using MATLAB (MathWorks) and the Psychophysics Toolbox (Brainard, 1997). As in the human experiments, auditory stimuli were delivered at six intensity levels, equally spaced in terms of perceived intensity. Unlike in the human experiment, these levels were defined using the rat power-law relationship between sound pressure level and perceived intensity (Pierrel-Sorrentino and Raslear, 1980; Raslear, 1989). A similar power-law relationship was observed when relating sound pressure levels and perceived

intensity reported by the human participants in the preliminary definition of stimulus intensity levels.

Experimental design

Experimental design was identical to Experiments 4.1 and 4.2, with the exception that the baseline periods had variable duration, given that abrupt increases of stimulus intensity had to be delivered manually by the experimenter when the animal was calm and not moving (after at least 6 s of baseline). As a result, the duration of the baseline period ranged between 11 and 131 s (median = 16.3 s). Each rat received 27 abrupt increases in each of 12 blocks, yielding 324 intensity increases in total (36 per condition).

ECoG recording & preprocessing

Cortical activity was recorded using a 14-channel wireless amplifier system (Multi Channel System MCS Gmbh, Germany; 2000 Hz sampling rate). During recording, rats were placed into a plastic chamber (length × width × height: 30 × 30 × 30 cm^3), within which they could move freely. Before the data collection, rats were placed in the same plastic cage for at least four slots of 2 hours each, to familiarise them with the recording environment. ECoG signals were processed using the EEGLAB toolbox in MATLAB (Delorme and Makeig, 2004). Raw ECoG data were downsampled to 1000 Hz, bandpass filtered from 1 Hz to 100 Hz, and finally segmented into epochs using a time-window ranging from -200 to +500 ms. Epochs with amplitudes exceeding ±500 μV were excluded from further analysis. The average number of rejected epochs per rat was 9 ± 5 SD (i.e. 3% of the total number of epochs). The number of rejected epochs was not different across experimental conditions (one-way ANOVA: $p = 0.31$).

Statistical analysis

Data collected in Experiment 4.3 were analysed using the same LME and cluster permutation testing approach used in Experiments 4.1 and 4.2. However, because the number of animals tested in Experiment 4.3 ($n = 5$) was lower than the number of humans tested in Experiment 4.1 and 4.2 ($n = 18$ each), I entered

single epochs into the model (instead of single-animal averages), to make statistical power comparable across distinct datasets.

4.3 Results

Experiment 4.1 - Auditory stimulation in humans

EEG waveform & topographies

In Experiment 4.1, I recorded the human EEG responses to abrupt increases of intensity of an ongoing auditory stimulus. Figure 4.2 (*top-left panel*) shows the grand average EEG response. Abrupt increases of stimulus intensity elicited a large negative-positive (N-P) complex, peaking at approximately 110 and 210 ms, respectively. Both the N and P waves had maximal amplitude at the vertex, but while the N topography extended more towards the temporal leads, the P topography decayed similarly in all directions away from the vertex (Figure 4.2, *top-left panel*). A smaller positive deflection peaking at approximately 330 ms followed the main P wave. This later positive peak had a more posterior topography with a maximum over Pz, possibly reflecting a P3b response (Polich, 2007; Figure 4.3, *top-left panel*). Overall, the waveform shape and topography of the N and P waves were very similar to the Vertex Potentials elicited by transient auditory impulse stimuli (Figure 4.2, *bottom-left panel*; Picton and Hillyard, 1974; Thomson et al., 2009; Valentini et al., 2011), confirming the similarity between change-evoked and impulse-evoked VPs found by Nishihara et al (2011), and supporting the working hypothesis that they reflect the same neural system.

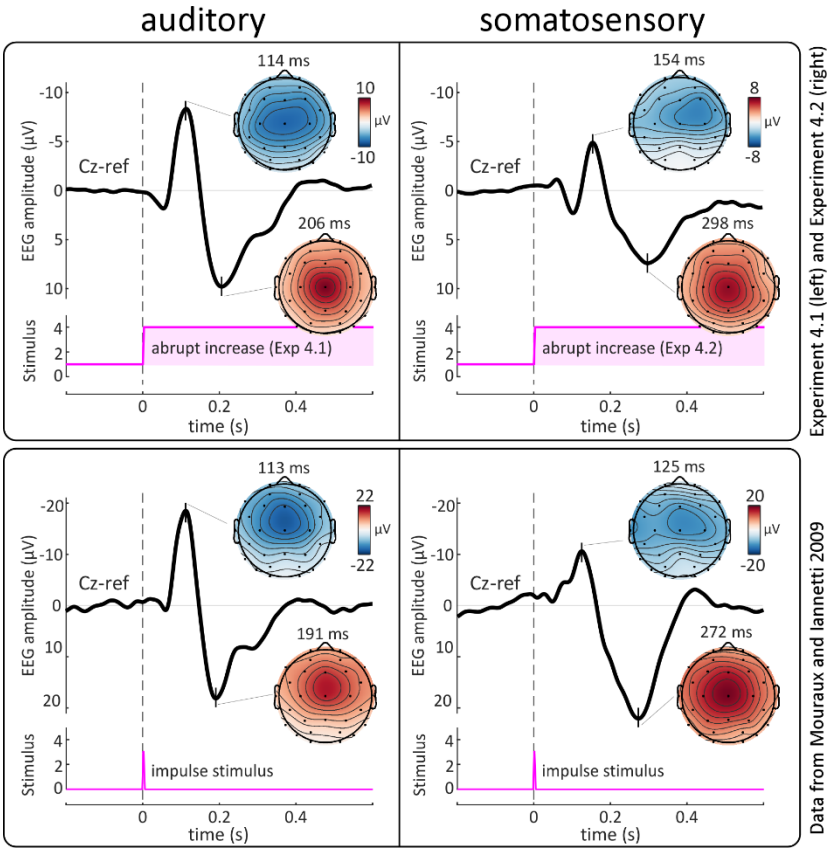

Figure 4.2. Experiments 4.1 and 4.2. Abrupt intensity increases embedded in ongoing stimuli elicit Vertex Potentials remarkably similar to those commonly evoked by impulse stimuli

Top panel. Grand average EEG responses elicited by abrupt increases of intensity of continuous auditory (*left*) and somatosensory (vibrotactile, *right*) stimulation. Data from Experiments 4.1 and 4.2. *Bottom panel.* Grand average EEG responses to auditory (*left*) and somatosensory (electrical, *right*) impulse stimuli. Data from Mouraux and Iannetti (2009). In both panels the EEG amplitude timecourse at Cz is shown in black. Vertical dashed lines indicate stimulus onset. Pink plots show stimulus profiles. Scalp topographies are shown at the peak latency of the negative and positive Vertex Potentials (VPs). Note how abrupt intensity increases embedded in ongoing stimuli (top panels) elicit VPs remarkably similar to those elicited by commonly-used impulse stimuli (bottom panels). Also note the longer latencies of the N and P waves elicited by vibrotactile stimuli (*top panel, right)* compared to electrical stimuli (*bottom panel, right*), given that electrical stimulation bypasses the mechanoreceptors and directly activates axons of Aβ afferents.

Effect of 'differential intensity'

Differential intensity strongly modulated the magnitude of both the N and P waves of the VP (Figure 4.3, *top-left panel*). The left column of Figure 4.4 shows the VP peak-to-peak amplitude extracted from each participant for the three levels of differential and absolute intensity. The modulation of VP magnitude by differential intensity was highly consistent across participants, with larger differentials eliciting larger responses. These observations were substantiated by LME modelling and cluster-permutation testing, which showed strong evidence that the factor 'differential intensity' affected the amplitude of the signal in two time windows across many electrodes: a negative cluster ($p = 0.0005$ at 2000 permutations[5]) at 70-130 ms, and a double-peaked positive cluster ($p = 0.0005$) at 140-370 ms. The two peaks of maximal modulations (at 88 and 190 ms respectively) had both latency and topography similar to the peaks of the VP (Figure 4.3, *top-left panel*). These modulations were large: LME estimated the amplitude of the negative/positive peaks to increase by -2.2/3.4 µV at each subsequent level of differential intensity (i.e. 26% and 34% of the respective grand average amplitudes). The differential intensity also modulated the EEG amplitude in a later time window, well after the end of the VP (at 460-540 ms; $p = 0.0015$; peak coefficient = 1.1 µV).

[5] Note that with permutation testing the p value is calculated according to the formula $p = b+1/m+1$, where *m* is the number of performed permutations, and *b* is the number of permutations giving a larger test statistic than the actual test statistic. Therefore, $p = 0.0005$ was the smallest possible p value, obtained when none of the 2000 permutations had a test statistic larger than the actual value (Phipson and Smyth, 2010).

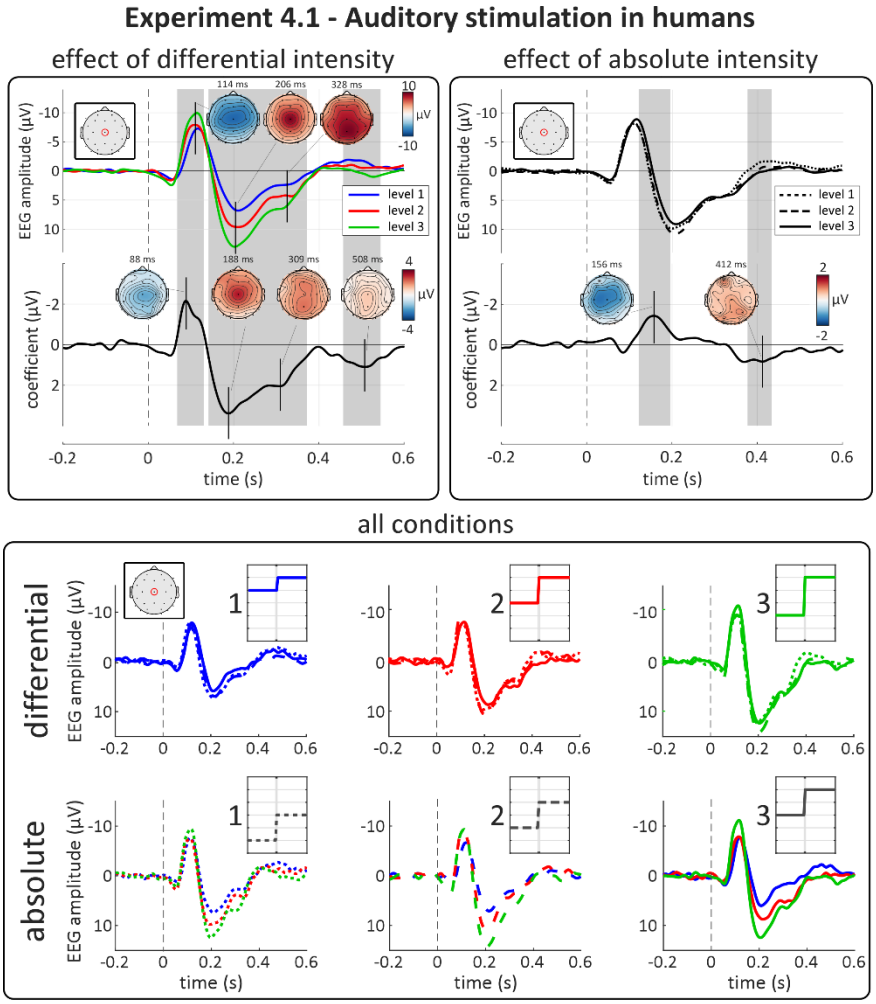

Figure 4.3. Experiment 4.1. Auditory-evoked Vertex Potentials are highly sensitive to differential, not absolute, intensity.

Top panels. Results of point-by-point LME analysis. Top plots show group-level average waveforms at Cz for each of the three levels of differential (*left panel*) and absolute intensity (*right panel*). Bottom plots show the LME model coefficient timecourse for each factor. Grey areas show significant clusters after permutation testing. Vertical dashed lines indicate stimulus onset. The amplitude of both negative and positive waves was strongly modulated by the factor 'differential intensity'. The peak topographies of these effects correspond well to those of the EEG response. The apparent amplitude modulation at the inflection point of the Vertex Potential by absolute intensity was consequent to a small latency shift (with higher absolute intensity resulting in longer-latency responses, see Results) rather than a modulation of magnitude *per se*.

Bottom panel. Group-level average waveforms at Cz, for each condition. Each row shows all 9 conditions of the experiment. Insets show schematic stimulus profiles, for each condition. Note the effect of differential, but not absolute intensity on both the negative and positive Vertex Potentials.

Effect of 'absolute intensity'

In contrast with the strong effects of differential intensity, there was no clear modulation of VP magnitude by absolute stimulus intensity (Figures 4.3 and 4.4). LME confirmed that the factor 'absolute intensity' did not affect the overall magnitude of the N and P waves (Figure 4.3, *top-right panel*), although there was an effect within a cluster around the inflection point between the N and P waves of the VP ($p = 0.0005$). This cluster most likely reflected a latency difference when the VP was elicited by stimuli of different absolute intensity – an interpretation supported by the LME analysis performed on the individually-extracted peak latencies, which showed evidence that 'absolute intensity' affected the latency of both the N ($p = 0.002$) and P ($p = 0.048$) waves. Finally, point-by-point LME revealed that 'absolute intensity' had a small effect in a late positive cluster well after the VP, at 370-430 ms ($p = 0.0015$; peak coefficient = 0.9 µV), with a slightly posterior and right-lateralised peak topography.

Experiment 4.2 - Somatosensory stimulation in humans

EEG waveform & topographies

In Experiment 4.2, abrupt increases of the intensity of the ongoing somatosensory stimulation elicited a large negative-positive (N-P) complex, peaking at approximately 150 and 300 ms (Figure 4.2, *top-right panel*). The scalp distribution of the P wave was clearly maximal at the vertex, whereas that of the N wave was slightly more frontal and contralateral to the stimulated hand, due to the overlap with smaller somatosensory-specific subcomponents (Treede et al., 1988; Valentini et al., 2012; Hu et al., 2014b). Overall, the shape and topography of the N and P waves were similar to the Vertex Potentials elicited by transient somatosensory impulse stimuli (Figure 4.2, *bottom-right panel*; Valentini et al., 2012). This result therefore generalises the observation that change-evoked and impulse-evoked VPs are highly similar (Nishihara et al., 2011) to the somatosensory modality.

Effect of 'differential intensity'

As in Experiment 4.1, differential intensity strongly modulated the magnitude of both the N and P waves (Figure 4.5, *top-left panel*). The right column of Figure 4.4 shows the VP peak-to-peak amplitude extracted from each participant for the three levels of differential and absolute intensity. Again, the modulation of VP magnitude by differential intensity was highly consistent across participants, with larger differentials eliciting larger responses. These observations were substantiated by LME modelling and cluster-permutation testing, which showed strong evidence that the factor 'differential intensity' affected the amplitude of the signal in two time windows across many electrodes: a negative cluster ($p = 0.0005$) at 130-180 ms, and a double-peaked positive cluster ($p = 0.0005$) at 210-380 ms. The two peaks of maximal modulation had centrally distributed topographies indicating that the effects were driven by the VP, rather than the modality-specific components that overlap with the N wave (Figure 4.5, *top-left panel*; Treede et al., 1988; Valentini et al., 2012; Hu et al., 2014b). As in Experiment 4.1, these modulations were large: LME estimated the amplitude of the negative/positive peaks to increase by -1.6/2.7 µV at each subsequent level of differential intensity (i.e. 33% and 36% of the respective grand average amplitudes).

Effect of 'absolute intensity'

As in Experiment 4.1, there was no clear modulation of VP magnitude by the absolute intensity (Figures 4.4 and 4.5). LME confirmed that the factor 'absolute intensity' did not affect the overall magnitude of the N and P waves (Figure 4.5, *top-right panel*), although there was an effect within a cluster around the inflection point between the N and P waves ($p = 0.0005$). As in Experiment 4.1, this cluster likely reflected a latency difference at different levels of absolute intensity (although in the opposite direction to Experiment 4.1) instead of a true modulation of the wave magnitude – an interpretation supported by the LME analysis performed on the individually-extracted peak latencies, which showed evidence that 'absolute intensity' affected the latency of both the N ($p = 5e\text{-}5$) and P ($p = 0.02$) waves. Finally, LME revealed that 'absolute intensity' had a small effect in a late positive cluster well after the VP, at 390-540 ms ($p = 0.0005$; peak coefficient = 1.3 µV), with a central and slightly posterior topography.

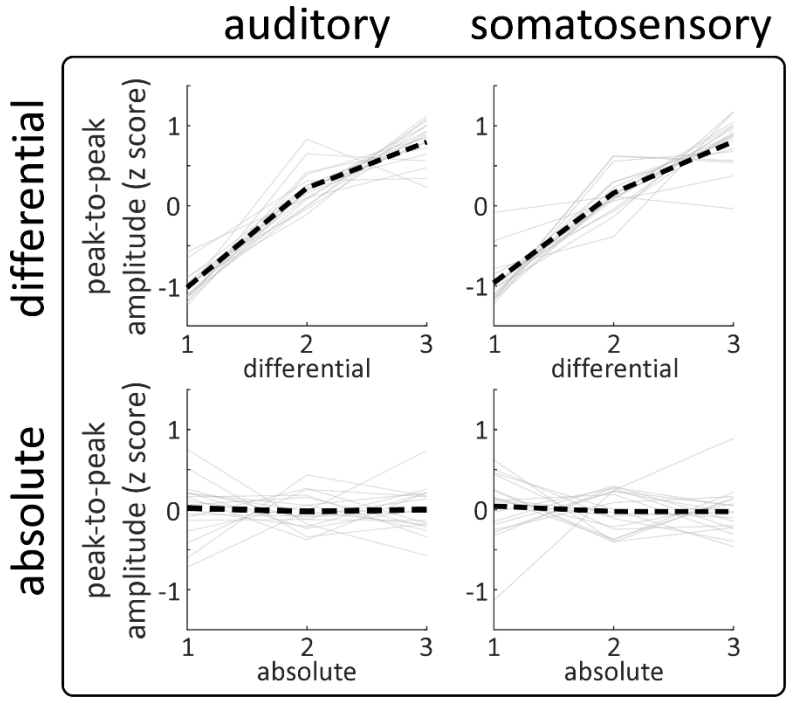

Figure 4.4. Experiments 4.1 and 4.2. The effects of differential and absolute intensity on the Vertex Potentials are consistent across modalities and participants.

Each graph shows the peak-to-peak amplitude of the Vertex Potentials for each participant (grey lines), together with the group-level average (black line) for each experimental factor (rows) and sensory modality (columns). Note the strong positive relationship between 'differential intensity' and response amplitude in both modalities, remarkably consistent across participants. There was no consistent effect of 'absolute intensity' on response amplitude.

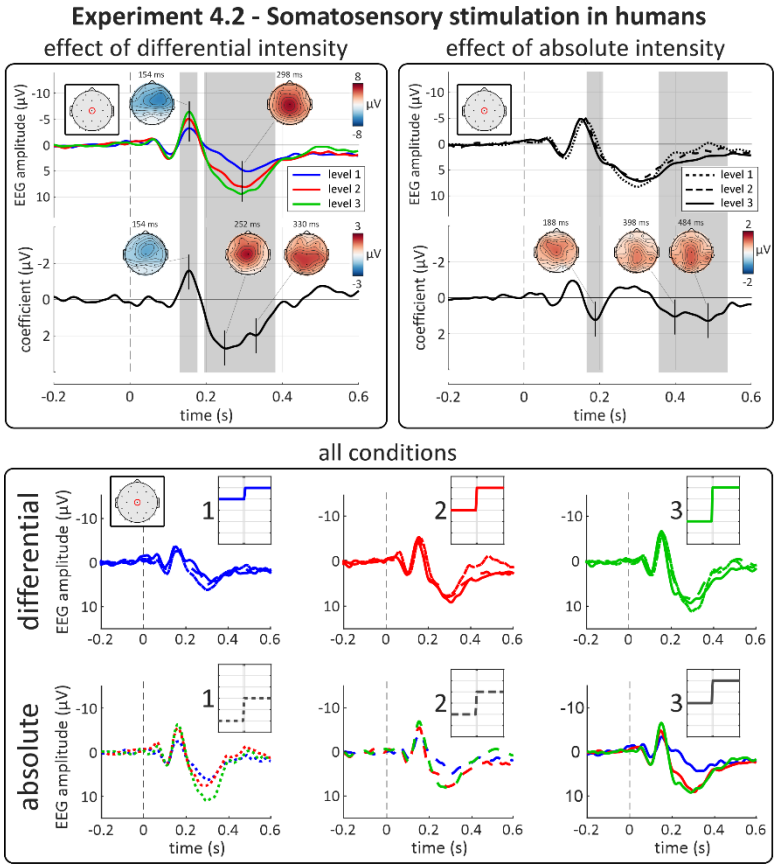

Figure 4.5. Experiment 4.2. Somatosensory-evoked Vertex Potentials are highly sensitive to differential, not absolute, intensity.
Top panels. Results of point-by-point LME analysis. Top plots show group-level average waveforms at Cz for each of the three levels of differential (*left panel*) and absolute intensity (*right panel*). Bottom plots show the LME model coefficient timecourse for each factor. Grey areas show significant clusters after permutation testing. Vertical dashed lines indicate stimulus onset. The amplitude of both negative and positive waves were strongly modulated by the factor 'differential intensity'. As expected, the peak topographies of these effects were maximal at the vertex, suggesting that the slightly unusual topography of the N wave in the EEG average reflects the superimposition of the VP and another component, perhaps generated by the primary somatosensory cortex contralateral to the stimulated hand (Valentini et al. 2012; Hu, Valentini, et al. 2014). The apparent amplitude modulation at the inflection point of the VP by absolute intensity was consequent to a small latency shift (with higher absolute intensity resulting in shorter-latency responses, see Results) rather than a modulation of magnitude *per se*. There was again a late positive cluster, well after the VP, modulated by 'absolute intensity'.

Bottom panel. Group-level average waveforms at Cz, for each condition. Each row shows all 9 conditions of the experiment. Insets show schematic stimulus profiles, for each condition. Note the effect of differential, but not absolute, intensity on both the negative and positive Vertex Potentials.

Experiment 4.3 - Auditory stimulation in rats

ECoG waveforms & topographies

In Experiment 4.3, my collaborator recorded ECoG from rats, while delivering auditory stimuli using the same procedure as in the human Experiment 4.1. Abrupt increases of stimulus intensity elicited large potentials in the time domain ECoG signal (Figure 4.6). These consisted of three potentials with expectedly shorter latencies than their human counterpart (Hu et al., 2015): (1) a fronto-lateral negativity peaking at 17 ms, (2) a fronto-lateral positivity peaking at 35 ms, and (3) a frontal negativity peaking at 85 ms. The shape and topography of these potentials correspond well to previously reported ECoG responses to transient auditory impulse stimuli (Knight et al., 1985; Hu et al., 2015; Guo et al., 2016).

Effect of 'differential intensity'

Similar to the human experiments, all main components of the electrocortical response were strongly modulated by differential intensity (Figure 4.6, *top-left panel*). LME showed strong evidence of three clusters in which the response magnitude was larger with larger differential intensity. These clusters had latencies similar to those of the ECoG response peaks: (1) a negative fronto-lateral cluster at 11-23 ms ($p = 0.0105$; peak coefficient = -15.8 µV)[6], (2) a positive fronto-lateral cluster at 27-44 ms ($p = 0.0130$; peak coefficient = 26.2 µV) and (3) a negative frontal cluster at 45-98 ms ($p = 0.0005$; peak coefficient = -46.9 µV). There was also an additional positive frontal cluster at 108-153 ms ($p = 0.0005$; peak coefficient = 20.1 µV), after the main three potentials.

[6] Note that these peak coefficients are calculated across all electrodes and are therefore not necessarily reflected in Figure 4.6, which shows the coefficients timecourses from four summary electrodes.

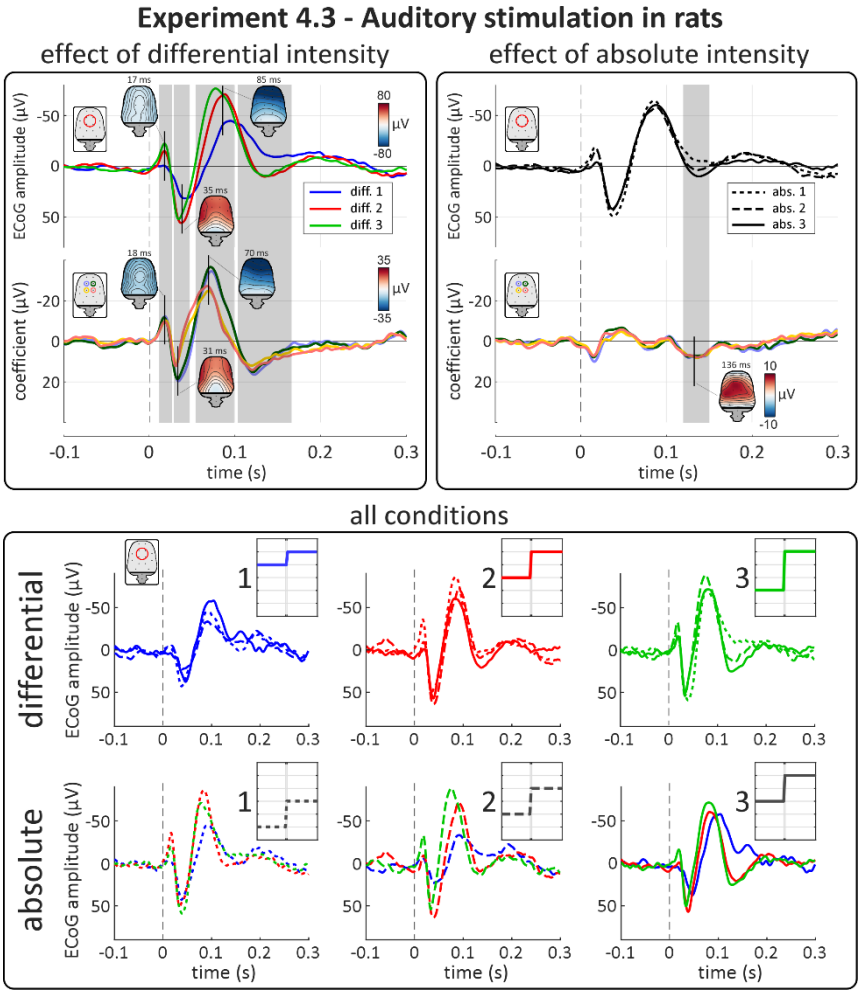

Figure 4.6. Experiment 4.3. Like humans ERPs, auditory ERPs in rats are highly sensitive to differential, not absolute, intensity.

Top panels. Results of point-by-point LME analysis. Top plots show group-level waveforms of the average of four summary electrodes for each of the three levels of differential (*left panel*) and absolute intensity (*right panel*). Bottom plots show the model coefficient timecourse for each factor, separately for each electrode used in the averages. Grey areas show significant clusters after permutation testing. Vertical dashed lines indicate stimulus onset. All three main components of the response were strongly modulated by the factor 'differential intensity', with effect topographies matching those of the peaks of the ECoG response. In contrast, the main three components were not modulated at all by 'absolute intensity'. There were some late effects of 'absolute intensity' and 'differential intensity' after the third component of the response, at ~121-136 ms.

Bottom panel. Group-level average waveforms of the average of four summary electrodes for each condition. Each row shows all 9 conditions of the experiment. Insets show schematic stimulus profiles for each condition. Note the effect of differential, but not absolute intensity on the main three components of the ECoG response.

Effect of 'absolute intensity'

As in the human experiments, there was no clear modulation of the amplitude of the three main potentials by absolute intensity (Figure 4.6, *top-right panel*). Thus, the rat ECoG responses equivalent to the human VP were also sensitive only to differential, and not absolute intensity. Again, LME revealed a late positive cluster at 121-150 ms ($p = 0.0005$; peak coefficient = 8.8 µV) whose amplitude was more positive for higher absolute intensity.

Experiment 4.C – Control experiment with individually defined intensity levels

Figure 4.7 shows the results of control experiment 4.C, in which the auditory intensity levels were determined separately for each participant prior to EEG data collection. These results were highly similar to those of Experiment 4.1: there was strong evidence for an effect of 'differential intensity' on the magnitude of the VP, and no evidence for an effect of 'absolute intensity'. This experiment demonstrates that inter-participant variability in the stimulus-perception relationship did not affect the results of Experiment 4.1.

Control analysis - ANOVA results from all human experiments

To test for interaction effects, I performed a two-way repeated measures ANOVA with FDR correction for all three EEG experiments (Experiments 4.1, 4.2 and 4.C). These tests showed highly similar main effects to the main LME analyses, and importantly showed no evidence of interaction effects (Figure 4.8).

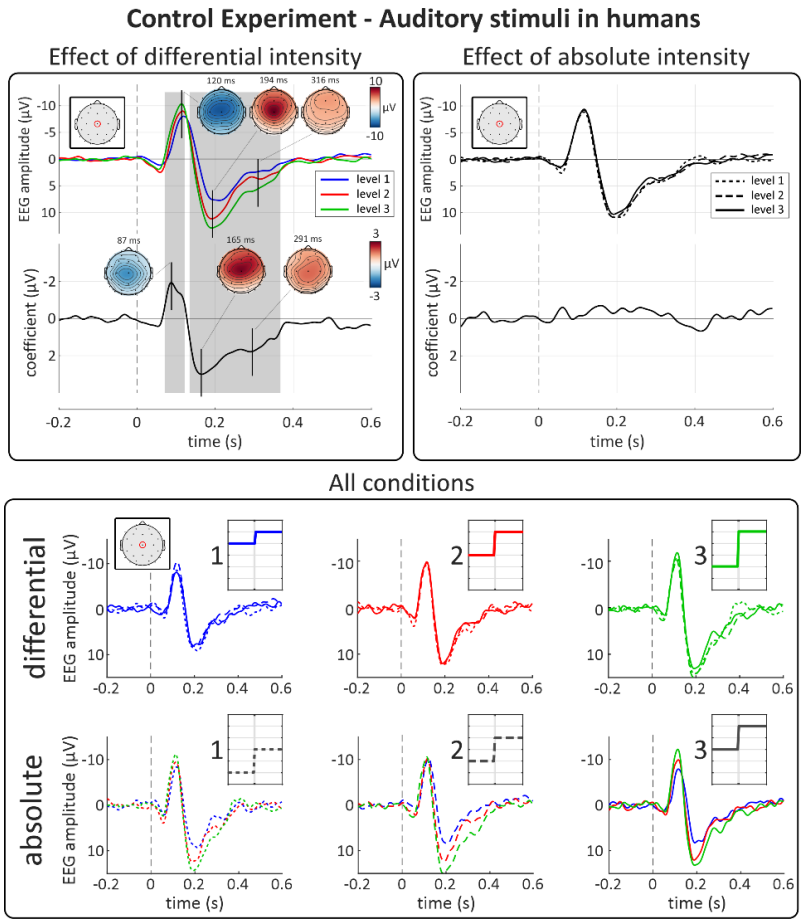

Figure 4.7. Control Experiment (4.C) results.
This additional experiment was performed in 8 participants (3 female, age range 25 – 45 yr, mean age 32 yr). *Top panels*. Results of point-by-point LME analysis. Top plots show group-level average waveforms at Cz for each of the three levels of differential (*left panel*) and absolute intensity (*right panel*). Bottom plots show the LME model coefficient timecourse for each factor. Grey areas show significant clusters from permutation testing. Vertical dashed lines indicate stimulus onset. Both negative and positive VPs were strongly modulated by the factor 'differential intensity'. The peak topographies of these effects correspond well to those of the EEG response. There was no evidence of a modulation of the EEG by the factor 'absolute intensity'. *Bottom panel*. Group-level average waveforms at Cz, for each condition. Each row shows all 9 conditions of the experiment. Insets show schematic stimulus profiles and colour-coding of the different conditions. Note the effect of differential, but not absolute intensity on both the negative and positive Vertex Potentials.

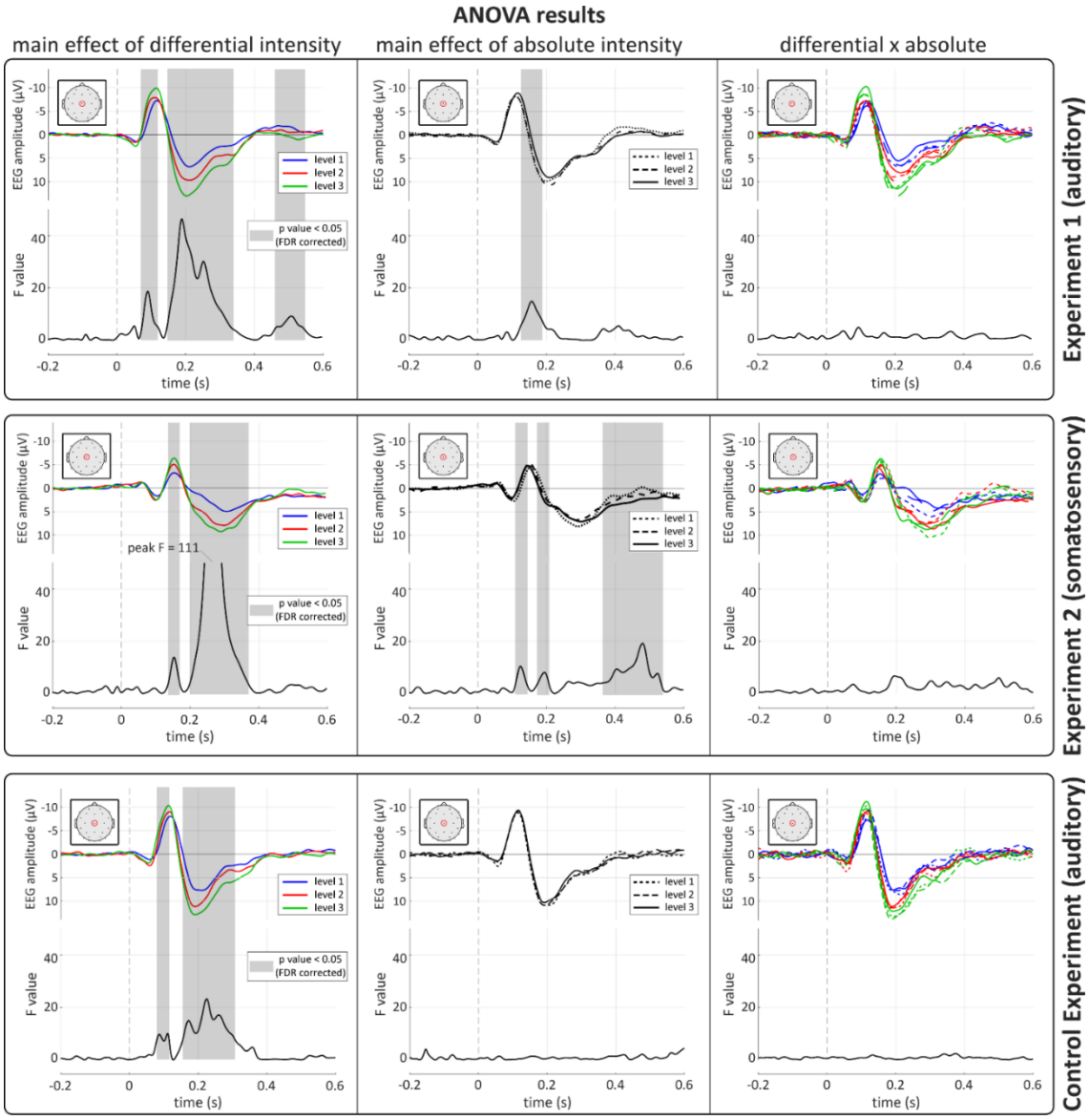

Figure 4.8. ANOVA results of Experiments 4.1, 4.2 and Control Experiment (4.C).

Each row shows the results of a two-way repeated-measures ANOVA conducted on the participant-level average waveforms. There was no evidence for an interaction of the factors ‘differential intensity’ and ‘absolute intensity’ in any of the three experiments, whereas the main effects of these two factors are highly similar to those found in the main analysis using linear mixed-effect modelling.

4.4 Discussion

In this chapter, I investigated the environmental features which determine the magnitude of electrocortical responses elicited in humans and rats by sudden sensory changes. Specifically, I exploited a novel paradigm that allows dissociating the effects of the *differential* and *absolute* components of stimulus intensity on response magnitude.

I obtained three main results. (1) The VP magnitude is largely determined by *differential* intensity, independently of *absolute* intensity. This finding indicates that the widely-known effects of intensity on impulse-evoked VPs are driven by differential intensity. (2) This result was observed in the responses elicited by both auditory and somatosensory stimuli, indicating that sensitivity to differential intensity is supramodal. (3) The same effect was observed in both rats and humans, suggesting that sensitivity to abrupt intensity differentials is phylogenetically well-conserved.

Vertex Potentials are sensitive to differential, but not absolute, stimulus intensity

In all three experiments, the magnitude of the VPs evoked by the abrupt intensity increases was largely determined by differential, not absolute intensity, indicating that the differential intensity underlies the well-established effect of impulse stimulus intensity on VP magnitude (e.g. Davis and Zerlin, 1966; Davis et al., 1968; Schweitzer and Tepas, 1974; Bromm and Treede, 1991; Beydoun et al., 1993; Iannetti et al., 2005, 2008; Huang et al., 2013; Hu et al., 2014). Thus, the VP is highly sensitive to the degree to which an abrupt change stands out from the recent sensory input (i.e. from the baseline intensity). As discussed in Chapter 3 (*General Introduction*), this contrast is a core component determining the unexpectedness of the sensory event. Many other factors which effectively modulate VP magnitude can be described in this way: for example, the degree to which an impulse stimulus stands out from the preceding sequence of stimuli. Indeed, the response habituation consequent to the repetition of the same

stimulus at short latencies (Ritter et al., 1968; Chapman et al., 1981; Iannetti et al., 2008; Wang et al., 2010; Herrmann et al., 2015) is reversed by behaviourally-relevant changes of stimulus modality (Valentini et al., 2011), intensity (Ronga et al., 2013), pitch (Herrmann et al., 2015), and location in egocentric coordinates (Moayedi et al., 2016). Altogether, these results indicate that the VP is sensitive to the unexpectedness of environmental changes at several hierarchical levels and timescales. I discuss later how this sensitivity allows organisms to detect and respond appropriately to salient events in the environment.

Sensitivity to differential intensity is consistent across sensory modalities

These results demonstrate that the sensitivity to differential intensity is present regardless of the sensory modality of the eliciting stimulus. This fits well with previous findings that VPs evoked by impulse stimuli of different modalities are similar in morphology, topography, and magnitude (provided that stimuli are saliency-matched; Mouraux and Iannetti 2009; Kilintari et al. 2018), that their habituation follows the same timecourse (Mancini et al., 2018), and that they share common supramodal generators (Mouraux and Iannetti, 2009). Therefore, the results observed here provide further evidence that the VP is a supramodal response that can be evoked by abrupt changes in the ongoing sensory input of *any sensory modality*. It is worth highlighting that this supramodal response is often incorrectly assumed to reflect the processing of specific sensory modalities. A striking example is the widely-used label “acoustic-change complex” (ACC) to refer to the EEG response elicited by changes in ongoing auditory stimuli (Martin and Boothroyd, 1999, 2000). Although broadly accepted in the clinical arena, the implication that this response reflects auditory-specific processing is not supported by either present results or previous findings (see Chapter 3, *General Introduction*). The widespread use of a label implying an auditory-specific interpretation (e.g. Friesen and Tremblay, 2006; Hoppe et al., 2010; He et al., 2015; Mathew et al., 2017) could obstruct understanding of audiological pathophysiology and therefore misinform future clinical decisions. Similar

misinterpretations affect the pain field, as our group has discussed elsewhere (Hu and Iannetti, 2016; Mouraux and Iannetti, 2018).

Sensitivity to differential intensity: lessons from the natural world

What is the advantage of a neural system sensitive to differential intensity? A viable hypothesis is that the sensitivity to larger, more unexpected differentials allows organisms to respond to environmental changes on the basis of their relevance to immediate behaviour. A large differential occurring in a short time acts as a sharper, more defined 'edge' in the temporal dimension, analogously to a spatial edge in the visual domain (Figure 4.9), and signals the occurrence of a new event or 'object' *with higher certainty* (Chait et al., 2008). Indeed, animals face a dynamic sensory environment in which a sudden sensory event could signal the arrival of a predator or a critical opportunity to catch prey. Such situations would demand immediate action to successfully escape that predator or catch that prey – and therefore survive. Given the physiological cost of eliciting a widespread brain response and any subsequent behavioural reaction, prioritising *more certain* environmental changes would allow the organism to minimise this cost as much as possible, without missing a potentially life-threatening event. The correct identification of a new object or event therefore has clear relevance to survival and wellbeing.

The striking similarity in sensitivity to differential intensity across humans and rats (Figures 4.3, 4.5 and 4.6) is interesting. Indeed, several aspects of sensory sensitivity differ dramatically across species: for example, the frequency of audible sounds in humans and rodents (Jamison, 1951; Hess, 2015) or the sampling rate of the visual system of humans and chickens (Zanker and Harris, 2002; Lisney et al., 2011). These differences reflect different statistical properties of behaviourally-relevant features in the habitats of the species (von Uexküll, 1909; Hughes, 2001). These results therefore suggest that the relevance of rapid increases of stimulus intensity is largely invariant in the habitats of both humans and rats and may be invariant across those of many other species. As a consequence, the neural system evolved to respond to these features is likely to be phylogenetically highly-conserved across species.

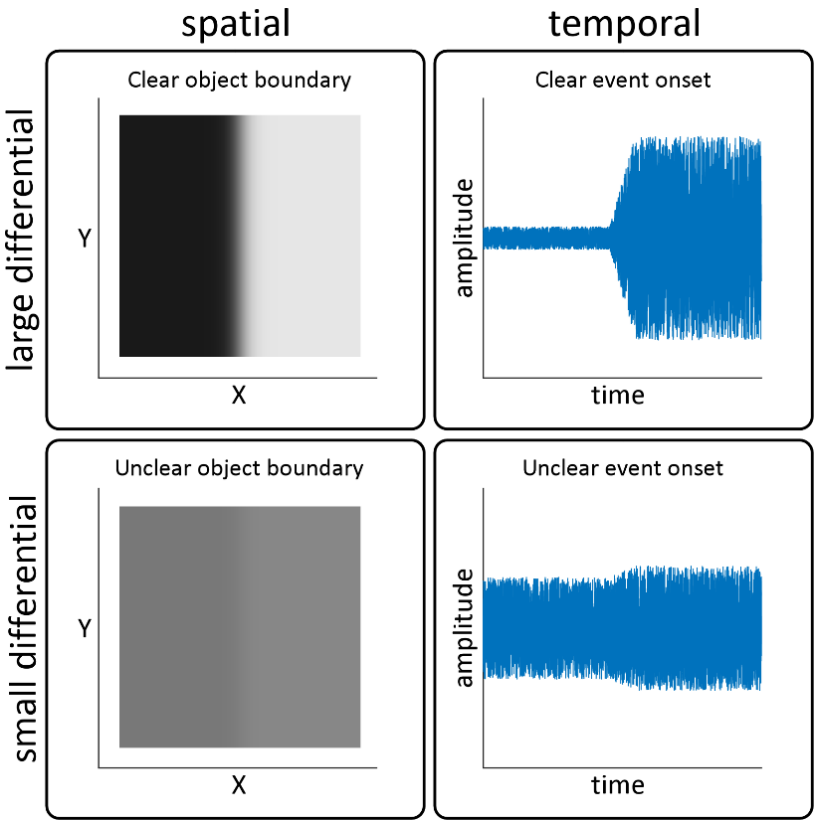

Figure 4.9. Abrupt increases of stimulus intensity are the temporal equivalent of spatial edges.

Left column. Representative plots of a spatial edge with large differential intensity (high contrast, *top*) and small differential intensity (low contrast, *bottom*). The large differential results in a sharper and more clearly defined edge, identifying an *object* with higher certainty.

Right column. Abrupt increases of auditory intensity with large (top) and small (bottom) differentials. As in the visual domain, a larger differential results in a sharper, more clearly defined edge, albeit in time rather than in space. A sharper temporal edge identifies the occurrence of an *event* with higher certainty.

5 Brain responses to sudden stimulus offsets: phenomenology and functional significance

5.1 Introduction

Abrupt and unexpected increases of sensory input (referred to as *onsets* from here onward) are likely to reflect the appearance of novel events or objects in the environment. These events have a clear importance to survival in the natural world, where they could signal situations requiring a rapid behavioural response when detected by an animal (such as the appearance of a threatening predator to be avoided). The results of Chapter 4 demonstrated that *onsets* elicit a brain response equivalent to the VP elicited by impulse stimuli. Consequently, we can assume that the vast body of work studying the response to impulse stimuli is also informative about the properties of the *onset* VP. For example, the sensitivity to the surprise content of the eliciting stimulus (reviewed in Chapter 3; Iannetti et al., 2008; Wang et al., 2010; Valentini et al., 2011; Ronga et al., 2013).

In contrast, the brain responses to abrupt and unexpected *decreases* of sensory input (referred to as *offsets* from here onward) have been investigated far less. The imbalance between studies of neural responses to *onsets* and *offsets* is surprising, given that *offsets* can also reflect events demanding swift and potentially life-saving behavioural responses: for example, the sudden dimming of light intensity can reflect a predating hawk, and thus triggers freezing behaviour in chicks (Hébert et al., 2019). Accordingly, one might hypothesise that the brain responses to both *onsets* and *offsets* reflect the functioning of a common neural system devoted to the detection of, and appropriate reaction to, abrupt intensity changes *of any kind* (i.e. regardless of their direction or the sensory modality in which they occur).

Unsurprisingly, a few studies have indeed shown that abrupt *offsets* of both auditory and somatosensory stimuli elicit a negative-positive EEG potential, maximal at scalp vertex and qualitatively similar to that elicited by *onsets*,

although typically smaller in magnitude (Davis and Zerlin, 1966; Onishi and Davis, 1968; Schweitzer and Tepas, 1974; Schweitzer, 1977; Parker et al., 1982; Jones, 1992; Yamashiro et al., 2008; Baltzell and Billings, 2014). All these studies, however, present several fundamental issues related to their experimental design, data analysis, and result interpretation.

First, experimental designs were often unsuitable to obtain a fair comparison of *onset*- and *offset*-evoked VPs, as *onset* stimuli generally occurred at relatively long or more variable time after the previous *offset* stimulus (e.g. 10-12 s; Yamashiro et al., 2008), whereas *offset* stimuli often followed more predictably and/or sooner after the preceding *onset* (typically by less than 3 s; e.g. Yamashiro et al., 2008). Given the well-known dependence of the VP amplitude on the temporal predictability of the eliciting stimulus (e.g., Iannetti et al., 2008), it is not surprising that these designs resulted in habituated *offset* VPs of smaller amplitude than *onset* VPs (Onishi and Davis, 1968; Spychala et al., 1969; Schweitzer and Tepas, 1974; Schweitzer, 1977; Parker et al., 1982; Spackman et al., 2006; Yamashiro et al., 2008). This unfair comparison may be the cause of the common observation that the *offset* VP amplitude is smaller than that of the *onset* VP. In addition, and even more important for the objectives of the current investigation, is the fact that the habituation consequent to imperfect experimental paradigms prevents an adequate comparison of several other response features. For example, the habituation of some response subcomponents (but not others) could alter the overall scalp distribution, and thereby prevent adequate spatial comparison of the *onset* and *offset* VPs. Additionally, this same habituation could obscure possible behavioural consequences of the *offset* VP, such as the modulations of motor output observed with impulse stimuli (Novembre et al., 2018).

Second, a proper quantitative comparison of the evolution of the scalp distributions of *onset* and *offset* responses across time was missing. This is largely due to the historical use of low-density EEG systems unable to adequately

capture the response scalp distribution (Onishi and Davis, 1968; Spychala et al., 1969; Schweitzer and Tepas, 1974; Elfner et al., 1976; Schweitzer, 1977; Hillyard and Picton, 1978; Parker et al., 1982; Jones, 1992; Yamashiro et al., 2008), and also to the habit, widely accepted until the 90s, to only measure the peak amplitude of the main VP waves (Davis and Zerlin, 1966; Onishi and Davis, 1968; Spychala et al., 1969; Schweitzer and Tepas, 1974; Schweitzer, 1977; Hillyard and Picton, 1978; Parker et al., 1982; Jones, 1992; Spackman et al., 2006; Yamashiro et al., 2008; Baltzell and Billings, 2014).

Third, several authors have too quickly assumed that *offset* VPs reflect modality-specific sensory systems[7] (Spychala et al., 1969; Jones, 1992; Spackman et al., 2006; Baltzell and Billings, 2014). For example, VPs elicited by auditory *offset* are often explicitly interpreted as reflecting the functioning of the auditory system (e.g. for sound perception), without considering the possibility that the responses are instead supramodal (Jones, 1992; Baltzell and Billings, 2014). Even when not stated explicitly, this interpretation is implied due to the focus on one sensory modality (Schweitzer and Tepas, 1974; Elfner et al., 1976; Schweitzer, 1977). As such, the functional properties of *offset* VPs have usually not been interpreted beyond the realm of perception of single sensory modalities.

Consequently, whether the VPs elicited by abrupt *offsets* reflect the activity of the same supramodal neural system activated by *onsets* remains an unanswered question. Without such basic knowledge, our understanding of the functional significance of these large brain responses remains incomplete. In this chapter, I tackled this question by recording brain activity with 64-channel EEG (i.e. at higher density than previous studies), using stimulation paradigms specifically

[7] Notably, the literature describing evoked potentials to impulse or *onset* stimuli is not devoid of this fundamental problem either. For a review on the topic, see Chapter 3 (*General Introduction)* or Mouraux and Iannetti (2018).

designed to allow a fair comparison of both the phenomenological and functional properties of *onset* and *offset* responses. Should *onset* and *offset* responses reflect the functioning of the same neural system, I predicted that they would (1) have quantitatively highly-similar temporal evolution of their scalp distributions, and (2) be largely composed of similar, supramodal subcomponents. I also predicted that, like their *onset*-evoked counterpart, *offset*-evoked VPs would be (3) highly sensitive to the unexpectedness of the eliciting stimulus (Wang et al., 2010; Valentini et al., 2011; Liberati et al., 2018), and (4) similarly related to the activation of the motor system (Novembre et al., 2018, 2019). In four experiments conducted on 44 healthy human participants I thoroughly tested these four predictions.

5.2 Methods

Participants

A total of 34 unique healthy human participants (5 female, age range 19 - 72 yr, mean ± SD age, 31 ± 10 yr) took part in one or more out of four experiments (N = 14, 10, 14 and 20; Exp 5.1, 5.2, 5.3 and 5.4 respectively). All participants gave written informed consent before taking part in the study. All procedures were approved by the local ethical committee.

Sensory stimulation

In all four experiments, participants received either auditory or tactile tonic stimuli. In Experiments 5.1, 5.3 and 5.4, participants received auditory stimuli, consisting of 600 Hz pure tones delivered binaurally through pneumatic insert-earphones (Etymotic ER-3C 10 Ohm). In Experiment 5.2, participants received the same auditory stimuli, but delivered through a loudspeaker (Q Acoustics 3020), as well as tonic mechanical stimulation on the right-hand dorsum. Mechanical stimulation was delivered manually by the experimenter using a cylindrical stainless-steel wire with a flat tip (diameter = 0.25 mm), mounted on a plastic rod with a weight, which was free to move inside a handheld stainless-steel tube (Iannetti et al., 2013). Consequently, when the rod was applied perpendicularly to the skin, it exerted a constant force of ~128 mN. Precise timing of pinprick stimulation was measured by connecting a 1.5 V battery to the stimulator and stimulation site to create an electric circuit upon contact with the skin; the resulting potential difference was measured between two electrodes, one placed on the hand near the stimulation site and the other placed on the upper arm. Auditory stimulation was controlled using MATLAB (Mathworks) and the Psychophysics toolbox (Brainard, 1997) in all experiments. Correct timing of somatosensory stimulation in Experiment 5.2 was ensured by playing through headphones the same auditory stimuli to the experimenter delivering the mechanical stimuli.

Experimental design

All experiments were conducted in a dim, silent, temperature-controlled room. During recording blocks, participants were required to keep their gaze on a fixation cross (4 x 4 cm) placed centrally in front of them, at approximately 30° below eye-level. Between recording blocks, participants were allowed to relax for up to 2 minutes.

In Experiment 5.1, abrupt *onsets* and *offsets* of stimulus intensity (rise/fall time = 10 ms) were delivered in separate blocks (Figure 5.1). In each *onset* or *offset* the difference between baseline and target intensity (i.e. the differential intensity) was identical. Figure 5.1 shows the stimulation profiles of representative blocks of *onsets* and *offsets*: before each abrupt change, the baseline intensity level was reached by slowly changing the intensity from the target level of the previous change (4 s). After each abrupt change, stimulus intensity remained at target level for 1 s. The mean interval between two consecutive changes (i.e. between two trials) was 14 s (11 – 17 s; uniform distribution). Each participant received 12 blocks of stimuli, each lasting ~2.5 mins and containing 12 abrupt changes, yielding 144 changes in total (72 *onsets* and 72 *offsets*). *Onset* and *offset* blocks were delivered in pseudorandom order, with the constraint that no block of the same type was repeated more than twice in a row.

In Experiment 5.2, participants received tonic auditory and somatosensory stimuli in separate blocks, with abrupt *onsets* and *offsets* of stimulus intensity (auditory rise/fall time = 10 ms) embedded in the stimulation profile. Participants sat in front of a table with their stimulated (right) hand resting on the table surface, while the experimenter sat on the opposite side, facing the participant. A curtain prevented the participants from seeing both the stimulated hand and experimenter. The loudspeaker delivering the auditory stimuli was placed near this hand. During the EEG recording blocks, the intensity of the ongoing stimulus would abruptly increase (*onset*), remain at a peak intensity level for 8 – 14 s (uniform distribution), and then abruptly decrease (*offset*) and remain at zero intensity for

8 – 14 s before the next *onset*. Thus, *onsets* and *offsets* were delivered in a continuous stream, and were preceded and followed by the next *onset* or *offset* after a variable and unpredictable interval. The peak intensity level of auditory and somatosensory stimuli was carefully matched for each participant, in a preliminary session. Auditory and somatosensory stimuli were delivered in 8 alternating blocks (balanced across participants). Each block lasted ~2.2 mins and contained 12 abrupt changes, yielding 96 changes in the entire experiment (24 *onsets* and *offsets* for each sensory modality).

In Experiment 5.3, three consecutive auditory changes (rise/fall time = 10 ms) of identical differential intensity were repeated at a frequency of 1 Hz (a triplet: S1-S2-S3; Iannetti et al. 2008). *Onsets* and *offsets* were never intermixed within the same triplet. Before each triplet, the baseline level preceding the first change (S1) was reached by slowly changing the intensity level (duration: 4 s) from the target level of the last change (S3) of the previous triplet. The mean interval between two consecutive triplets (e.g. from the S1 of a given triplet to the S1 of the following triplet) was 16 s (13 – 19 s; uniform distribution). Each participant received 4 blocks of stimulation. Each block lasted ~3 minutes and contained 12 triplets, yielding 48 triplets in the entire experiment (24 triplets for each of the two conditions).

In Experiment 5.4, participants were required to perform a simple isometric motor task, in which they exerted a constant force (~1.5 N) on an isometric force transducer held between their index finger and thumb (Novembre et al., 2018, 2019). At the beginning of each block, participants were instructed to exert a gradually increasing force while receiving verbal feedback about the force applied: once a force level between 1.25 and 1.75 N was reached, participants were instructed to keep the force applied as constant as possible, and at that point the recording started. Throughout the recording block, while performing the motor task, participants received task-irrelevant auditory stimuli with embedded abrupt changes (rise/fall time = 5 ms). The stimulation profile was similar to

Experiment 5.1, except for the following three differences: (1) *onsets* and *offsets* were intermixed within each block (pseudorandomised with the constraint that no more than 3 consecutive intensity changes could have the same direction); (2) the plateau following each change lasted 3 s instead of 1 s, to allow optimal sampling of the stimulus-induced force modulation, which can last up to 3 s (Novembre et al., 2018, 2019); and (3) stimulus intensity always increased to and decreased from the same peak intensity (as in Experiment 5.2), which was set before the experiment to the highest intensity the participant could tolerate. Each participant received 6 blocks. Each block lasted ~2.5 mins and contained 10 abrupt changes, yielding 60 changes in the entire experiment (30 *onsets* and 30 *offsets*).

EEG recording and preprocessing

In all experiments, EEG was recorded using 64 active electrodes placed on the scalp according to the International 10-10 system and referenced to the nose. EEG signals were amplified and digitised using a sampling rate of 2048 Hz (Biosemi Active-2 system), then preprocessed and analysed using MATLAB (version 2018a, MathWorks), Letswave (Mouraux and Iannetti, 2008), and Fieldtrip (Oostenveld et al., 2011). Continuous EEG data were first band-pass filtered between 0.5 and 30 Hz (Butterworth). Data were then segmented into 4-s long epochs (-2 to +2 s relative to the beginning of each abrupt intensity change). Artifacts due to eye blinks or eye movements were removed using a validated method based on independent component analysis (Jung et al., 2000). Within each epoch, any electrode with amplitude values exceeding ±100 µV was interpolated by averaging the signal sampled from its neighbouring electrodes; if more than three electrodes needed interpolation, the epoch was rejected. Remaining epochs were baseline corrected (reference interval -0.2 s to 0 s). The average percentage of rejected epochs per participant was (mean ± std): 3.5 ± 3.4% [Experiment 5.1], 5.4 ± 4.9% [Experiment 5.2], 3.6 ± 4.6% [Experiment 5.3], and 3.6 ± 5.4% [Experiment 5.4]. Finally, average ERP waveforms were computed for each participant and condition.

Force recordings & preprocessing

The force applied by participants in Experiment 5.4 was sampled at 1000 Hz using a force-torque transducer (ATI nano17, Industrial Automation) using a custom software written in LabVIEW (National Instruments). At the start of each recording session, the force value was set to zero to mitigate the effects of sensor drifts. To facilitate the two-finger grip, the transducer was mounted between two cylindrical plastic extensions. Continuous data were segmented using a time-window from -0.4 to 3 s relative to the beginning of each abrupt intensity change (epoch duration = 3.4 s). Epochs contaminated by artifacts (deviating, at any timepoint, more than 3 SDs from the participant's mean exerted force across all trials) were excluded from further analysis. The corresponding EEG epochs were also excluded. Consequently, the percentage of rejected epochs was the same as the EEG data: 3.6 ± 5.4%. Finally, epochs were baseline corrected using the -0.05 to 0 s prestimulus interval, and high-pass filtered to isolate the transient force modulations (Novembre et al., 2018).

Statistical analysis

In Experiment 5.1, I compared the scalp distribution of the ERPs elicited by *onsets* and *offsets* by calculating the spatial correlation (i.e. the correlation across channels) between the average waveforms for each condition, for each timepoint and each participant (Murray et al., 2008). The across-participant consistency of spatial correlation timecourses was statistically assessed by performing a point-by-point one-sample t-test (against zero) of the spatial correlation values (Fisher's z-transformed) for each participant, with cluster permutation testing (1000 permutations; Maris and Oostenveld, 2007).

In Experiment 5.2, I explored the selectivity of the constituent subcomponents of the ERPs elicited by abrupt *onsets* and *offsets* of both auditory and somatosensory stimuli. First, the participant-level average waveforms for each of the four conditions were cropped between -0.5 and +1.5 s and concatenated. These waveforms were then decomposed into a set of independent components

(ICs) of fixed scalp topography using probabilistic independent component analysis (pICA; Beckmann and Smith, 2004; Mouraux and Iannetti, 2008, 2009). pICA uses an estimate of the intrinsic dimensionality of the data to approximate the true number of independent sources contributing to the signal. As a result, each IC is more likely to reflect a single physiological source of activity compared to a traditional unconstrained ICA (Mouraux and Iannetti, 2008). I then computed, for each IC, the proportion of signal variance explained at each timepoint by dividing their global field power by the total global field power across all ICs. These proportions were subsequently averaged across the post-stimulus interval (0 to +0.5 s) separately for each condition, yielding four values for each IC reflecting the mean explained variance for each condition. To quantify how selective the ICs were for each of the four conditions, I then calculated the correlation (Pearson, r) between these explained variance values for each pair of conditions across all ICs (i.e. at group-level). As a summary value of the selectivity of each IC, I computed a selectivity ratio which was equal to the largest explained variance value divided by the mean explained variance across the rest of the conditions – this value therefore reflected how selectively the IC explained variance for one condition. I then correlated (Spearman's rank, r_S) these selectivity ratios with the mean variance explained in all conditions, across all ICs.

In Experiment 5.3, I compared the ERPs elicited by each of the three stimuli composing the triplet (S1-S2-S3), separately for *onset* and *offset* triplets. Participant-level averages for each condition were analysed using a point-by-point, two-way repeated-measures ANOVA in the time-window -0.2 to 0.6 in each channel, with factors: 'change direction' (two levels: onset and offset) and 'stimulus repetition' (three levels: S1, S2 and S3). Cluster permutation testing was used to correct for multiple comparisons (1000 permutations).

In Experiment 5.4, I analysed single-participant average force waveforms using point-by-point, one-sampled t-tests against zero (i.e. against the mean baseline amplitude), to determine the response consistency across participants. Cluster permutation testing was used to correct for multiple comparisons (1000 permutations).

5.3 Results

Experiment 5.1 - Auditory onsets and offsets elicit highly similar Vertex Potentials (Prediction 1)

In Experiment 5.1, I compared the morphology and spatial distribution of the brain responses elicited by increases (*onsets*) and decreases (*offsets*) of stimulus intensity with equal differential intensity (see Chapter 4) and equal rise or decay time, embedded within an ongoing auditory stimulus (Figure 5.1). For more detail on the experimental design see Methods (5.4). Figures 5.1 and 5.2 show the single-participant and group-level average waveforms elicited by *onsets* and *offsets*. Morphology and topography of the responses were qualitatively similar: both *onsets* and *offsets* elicited a large, widespread negative-positive (N-P) complex, maximal at the scalp vertex (Cz) and peaking at approximately 124 and 127 ms (N wave, *onset* and *offset* condition respectively) and 193 and 213 ms (P wave, *onset* and *offset* condition respectively) (group-level average waveforms, Figures 5.1 and 5.2).

To quantitatively compare the temporal evolution of the two responses across the scalp, I computed the spatial correlation between the participant-level average *onset* and *offset* waveforms, for each condition at each timepoint (Figure 5.2; Murray et al., 2008). I observed strong evidence that the spatial distributions of *onset* and *offset* responses were very similar in a large post-stimulus interval (84 - 330 ms; cluster $p < 0.01$). Spatial correlations were strong and maximal at approximately 130 and 220 ms, i.e. around the peak latencies of the N and P waves in the grand average waveform (mean $r = 0.85$ and 0.77 for N and P waves, respectively).

Figure 5.1. Experiment 5.1. Stimulation profile and experimental design. *Left.* Stimulation profile of typical *onset* (*top*) and *offset* (*bottom*) blocks in Experiment 5.1. Stimulus intensity abruptly increased (*onset*; pink segments) or decreased (*offset*; blue segments) from a baseline level to a target level in 10 ms (coloured segments), plateaued from 1 s and then slowly increased or decreased to the next baseline level in 4 s. All abrupt intensity changes had the same differential intensity (1/4 of the intensity range). *Right.* Grand averages (black) and participant-level averages (grey) elicited by *onsets* (top) and *offsets* (bottom).

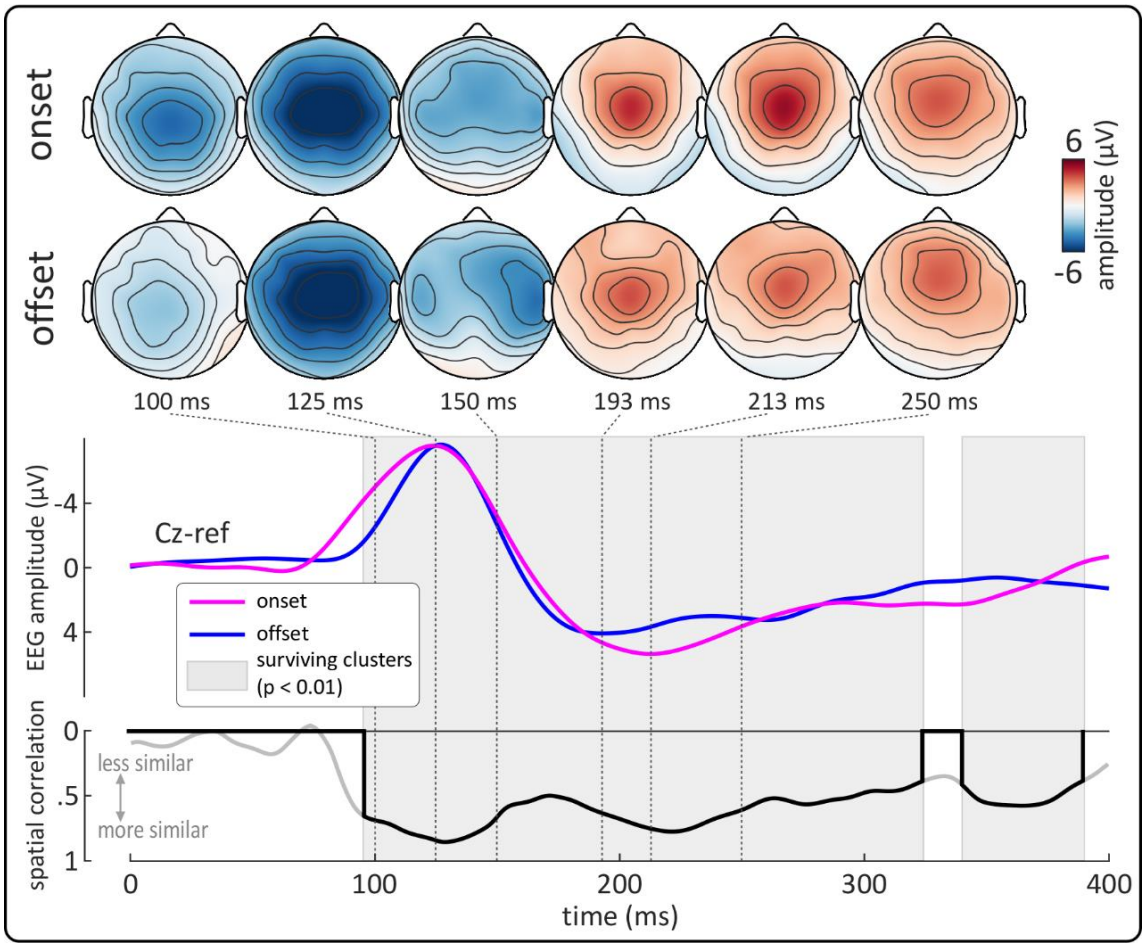

Figure 5.2. Experiment 5.1. Abrupt *onsets* and *offsets* of auditory stimuli elicit highly-similar Vertex Potentials.

Topographies show the evolution of the scalp distribution of the *onset* and *offset* ERPs over time. Top plot shows the grand-average waveforms (Cz) elicited by abrupt *onsets* and *offsets* of auditory stimuli. Bottom plot shows the timecourse of the mean spatial correlation between the two waveforms. Grey area shows clusters in which spatial correlation was statistically significant at group-level. Both responses were highly similar throughout their timecourse. The similarity was strongest at the peak latencies, where both responses were dominated by widespread negative and positive waves, maximal at scalp vertex (Vertex Potentials).

Experiment 5.2 - Offset-evoked Vertex Potentials are highly supramodal (Prediction 2)

In Experiment 5.2, I employed a novel 2x2 experimental design to compare the VPs elicited by *onsets* and *offsets* in two sensory modalities: somatosensation and audition. This design not only allowed me to test Prediction 2 (that, like *onset*-evoked VPs, *offset*-evoked VPs would largely reflect supramodal neural activity), but also provided further evidence to confirm Prediction 1 in a different group of participants and across two modalities. Figure 5.3 shows the group-level average waveforms of Experiment 5.2. As in Experiment 5.1, both *onsets* and *offsets* elicited highly similar negative-positive complexes maximal at scalp vertex, although the N wave elicited by somatosensory *offsets* had a less central scalp distribution, likely because the left-lateralised subcomponent (presumably reflecting the primary somatosensory cortex contralateral to the stimulated hand; Valentini et al., 2012) was more visible given the smaller overlapping N wave of the *offset* Vertex Potential.

To quantitatively determine the condition-wise selectivity of the neural activity underlying these responses (and thereby test Prediction 2), I first concatenated the participant-level averages across the four experimental conditions (auditory *onset*, auditory *offsets*, somatosensory *onsets*, somatosensory *offsets*). I then decomposed these waveforms into their underlying subcomponents using probabilistic independent component analysis (pICA). In contrast to standard ICA, where the number of independent components (ICs) is either equal to the number of recording channels or has to be defined manually *a priori*, pICA estimates the true number of ICs from the data (Beckmann and Smith, 2004; Mouraux and Iannetti, 2009; see Methods). This approach is outlined in Figure 5.4, using results from an example participant.

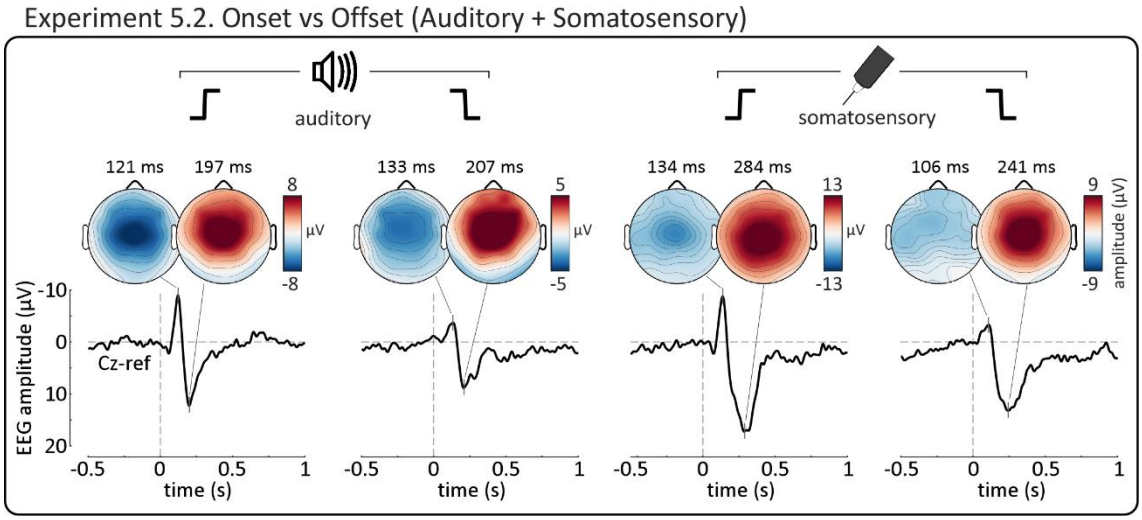

Figure 5.3. Experiment 5.2. Both onset- and offset-evoked Vertex Potentials are highly supramodal

Plots show the grand-average waveforms (Cz) elicited by abrupt auditory *onsets* (*far-left*), auditory *offsets* (*middle-left*), somatosensory *onsets* (*middle-right*) and somatosensory *offsets* (*far-right*). Scalp distributions are shown for the N and P wave of each condition. All four waveforms were dominated by highly similar Vertex Potentials, although the N wave of the somatosensory *offset* VP overlapped with a left-lateralised component, presumably reflecting the primary somatosensory cortex contralateral to the stimulated hand (Valentini et al., 2012).

Figure 5.4. Experiment 5.2. Probabilistic independent component analysis (pICA) applied to the average waveforms from an example participant

The concatenated participant-level averages (*left panel*) were decomposed, using pICA, into a set of temporally independent and spatially fixed independent components (ICs) best reflecting the dimensionality of the data (*right panel*). Four example ICs are shown along with their spatial distributions. Scatterplot shows how selective each component was for a particular condition, compared with how much variance it explained on average. Colour opacity shows selectivity for a particular condition (auditory onset: blue; offset: green; somatosensory onset: pink; offset: yellow). The three most selective components (IC 5, 6 and 10) were somewhat selective for auditory offset (green), onset (blue) and offset respectively. Note that the largest component (IC 2) was very unselective, while the most selective components did not contribute greatly to the overall variance of the waveforms.

To quantify the degree of selectivity of the resulting ICs for each of the four conditions, I first computed the mean variance explained by each IC for each condition (0 to +0.5 s post-stimulus), and then calculated their correlations in all possible pairs of experimental conditions and across all ICs (i.e. at group-level). All correlations (Figure 5.5, *left panel*; see Table 5.1 for r & p values) were strong and positive, indicating that ICs explaining a certain degree of variance in one condition were very likely to explain a similar degree of variance in the other conditions. In other words, there were no or few ICs explaining a large degree of variance in only one condition.

As a summary value of the selectivity of each IC, I computed the ratios of explained variance across conditions (see Chapter 5.4, *Methods* for details) – the larger the ratio the more selective the IC. The key result is that the selectivity ratio was highly negatively correlated with the mean explained variance across all conditions (r_s = -0.31, p = 0.009; Figure 5.5, *right panel*). This indicates that supramodal and non-selective ICs (i.e. ICs explaining both *onset* and *offset* responses, in both somatosensory and auditory conditions) reflected more of the neural activity underlying the responses than the more selective ICs. Altogether, these results show that the brain responses observed in each of the four conditions were dominated by similar neural activity, which was highly supramodal and non-specific for either *onsets* or *offsets*.

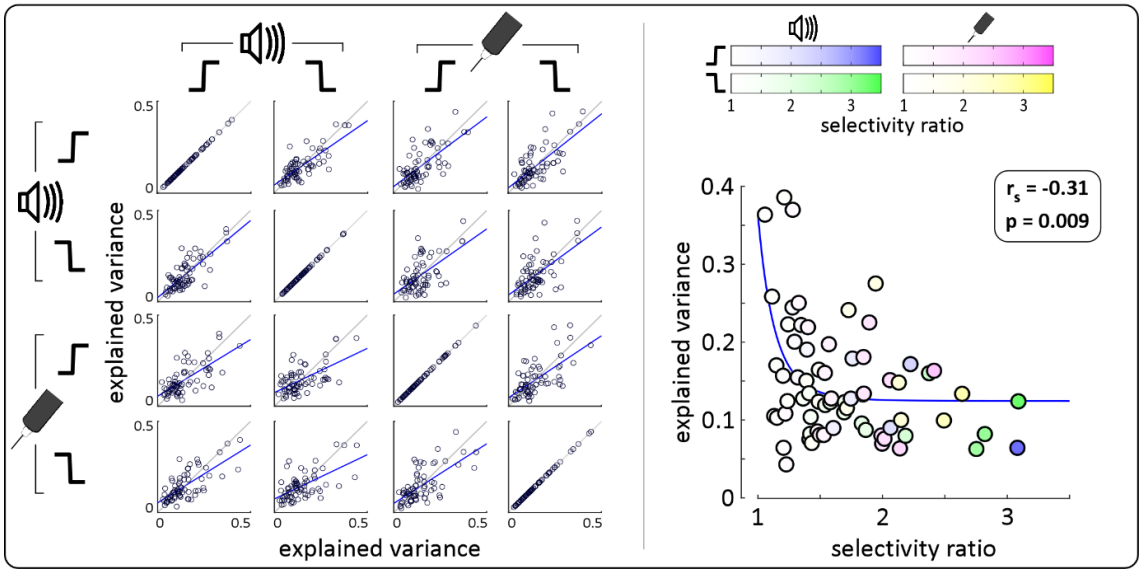

Figure 5.5. Experiment 5.2. Group-level pICA results. Supramodal, non-specific components explained the most variance.

Left. Scatterplots show, for each component, the mean explained variance in each pair of conditions, at group-level (i.e. circles show components from each participant). Blue lines show linear regression. Grey lines are identity lines. Strong positive correlations can be seen in all scatterplots, showing that components explaining a certain amount of variance in one condition were likely to explain a similar amount of variance in other conditions.

Right. Scatterplot shows how selective these same components were for a particular condition, compared with how much variance it explained on average. Colour opacity shows selectivity for a particular condition (auditory *onset*: blue; *offset*: green; somatosensory *onset*: pink; *offset*: yellow). Blue line shows non-linear regression (power law). The strong negative correlation shows that components explaining the most variance were also the least selective, while the most selective components explained the least variance.

Table 5.1. Correlations of explained variance between each condition, across components (Experiment 5.2).

r values		**auditory**		**somatosensory**	
		onset	*offset*	*onset*	*offset*
auditory	*onset*	n/a	**0.77**	**0.69**	**0.72**
	offset	**0.77**	n/a	**0.59**	**0.60**
somatosensory	*onset*	**0.69**	**0.59**	n/a	**0.67**
	offset	**0.72**	**0.60**	**0.67**	n/a

p values		**auditory**		**somatosensory**	
		onset	*offset*	*onset*	*offset*
auditory	*onset*	n/a	**9.3e-15**	**6.4e-11**	**4.7e-12**
	offset	**9.3e-15**	n/a	**1.0e-07**	**4.6e-08**
somatosensory	*onset*	**6.4e-11**	**1.0e-07**	n/a	**4.0e-10**
	offset	**4.7e-12**	**4.6e-08**	**4.0e-10**	n/a

Experiment 5.3 - Both onset- and offset-evoked Vertex Potentials are highly sensitive to the surprise content of the stimulus (Prediction 3)

The results of Experiments 5.1 and 5.2 show substantial phenomenological and compositional similarity between the responses elicited by *onsets* and *offsets*, regardless of whether the eliciting stimulus was auditory or somatosensory. In Experiment 5.3, I expanded on these findings by exploring the sensitivity of the responses to the surprise content of the eliciting stimulus. It is well-established that impulse-evoked VPs (and therefore *onset*-evoked VPs also) are highly sensitive to the surprise of the eliciting stimulus, with more surprising (i.e. less expected) stimuli producing a VP of larger amplitude (Wang et al., 2010; Valentini et al., 2011; Torta et al., 2012; Ronga et al., 2013). Should the VPs elicited by abrupt *offsets* reflect the same neural system subserving *onset*-evoked VPs, it follows that *offset* responses should also be highly sensitive to this factor.

To test this, I exploited an established paradigm that effectively dissociates the magnitude of the afferent sensory barrage from its surprise content, by modulating temporal predictability: participants received trains of three consecutive changes (i.e. a triplet: S1, S2, S3) of either *onsets* or *offsets* with identical differential intensity (see Chapter 4), at 1 Hz (Figure 5.6). In this paradigm, S2 and S3 are more temporally predictable than S1, and are therefore less surprising (Iannetti et al., 2008).

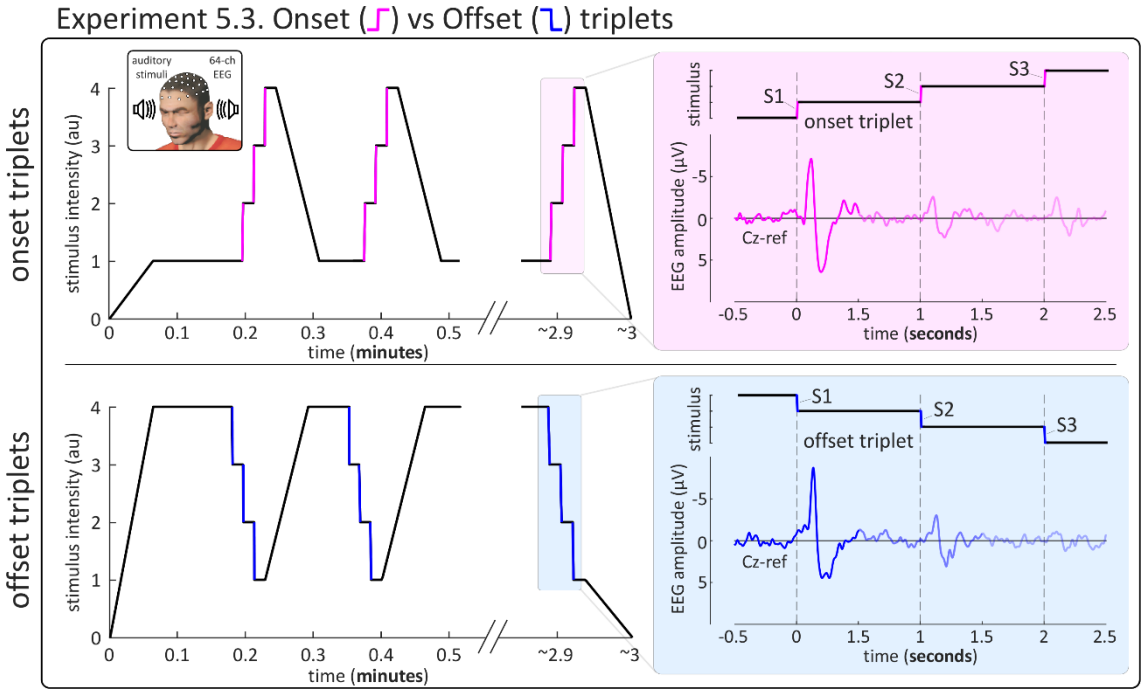

Figure 5.6. Experiment 5.3. Stimulation profile and experimental design. *Left.* Stimulation profile of typical *onset* (top) and *offset* (bottom) blocks in Experiment 5.3. From baseline, stimulus intensity abruptly increased (*onset*) or decreased (*offset*) three times in a row (S1-S2-S3) with 1 s interval between each change (i.e. a triplet at 1 Hz). Before each triplet, the baseline level preceding the first change (S1) was reached by slowly changing the intensity level from the previous triplet in 4 s.

Right. Grand averages for the Vertex Potentials (VPs) elicited by the three stimuli in the triplet. Repetition of the abrupt change reduced the magnitude of subsequent VPs, for both *onsets* and *offsets*.

In both *onset* and *offset* triplets, stimulus repetition resulted in a clear reduction of VP amplitude such that VP amplitude was lower for S2 and S3 than for S1 (Figure 5.6; *right*). These observations, which dovetail previous findings using impulse stimuli (Ritter et al., 1968; Iannetti et al., 2008; Wang et al., 2010; Valentini et al., 2011; Liberati et al., 2018), were substantiated by a two-way ANOVA with factors: 'change direction' (two levels: onset and offset), and 'stimulus repetition' (three levels: S1, S2 and S3). Figure 5.7 shows the results of this ANOVA. There was strong evidence of a main effect of 'stimulus repetition' between ~89 – 150 ms and ~168 – 297 ms (cluster p = 0.006, in both intervals[8]), i.e. around the peak latency of the main vertex waves. Importantly, the scalp distribution of these main effects was widespread (Figure 5.7), and there was no evidence of a 'change direction' x 'stimulus repetition' interaction. These two results indicate that the spatial distribution of the surprise-dependent habituation of the VP was similar across the *onset* and *offset* conditions. Finally, there was no evidence of a main effect of 'change direction' until well after the VP latency (at ~390 ms). Overall, these three results suggest that similar constituent subcomponents were habituated by stimulus repetition, thus providing further evidence that the VPs elicited by *onsets* and *offsets* reflect a common underlying network sensitive to stimulus surprise.

[8] Note that identical cluster p values are fairly common with permutation testing, due to the formula used to calculate these values (Phipson and Smyth, 2010).

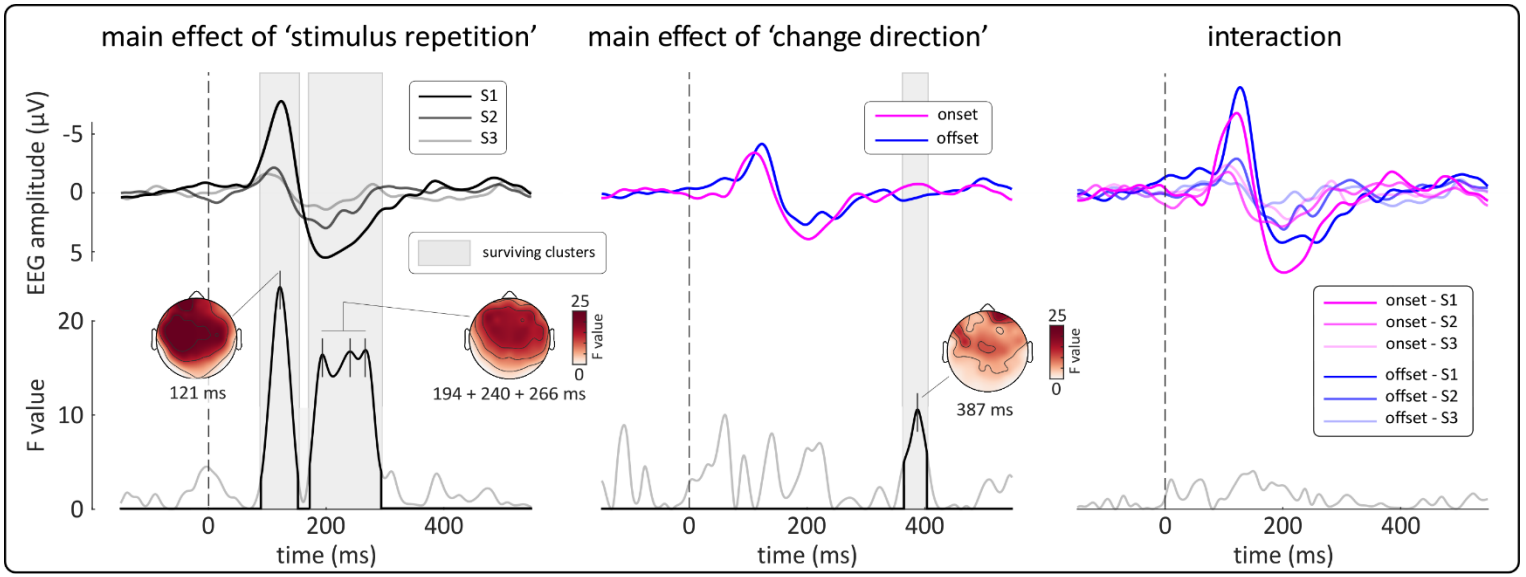

Figure 5.7. Experiment 5.3. Onset and offset Vertex Potentials were similarly habituated by predictable repetition at 1 Hz.

Top row. Group-level average waveforms (Cz) for each level of 'repetition' (left), 'change direction' (middle) and for each individual condition (right).

Bottom row. F value timecourse for each factor (Cz). Grey areas show significant clusters after permutation testing. The N and P waves were both significantly modulated by factor 'stimulus repetition', reflecting the habituation of the Vertex Potentials (VPs) after the first abrupt change (S1). Importantly, these effects were widespread across the scalp and there was no evidence of an interaction, indicating that the *onset* and *offset* VPs habituated similarly across the scalp. There were no significant effects associated with the factor 'change direction' during the timecourse of the VP. These results show that that similar underlying neural generators were modulated by stimulus repetition and provide further evidence that the *onset* and *offset* VPs reflect a common brain network.

Experiment 5.4 – Onsets and offset Vertex Potentials are similarly related to activation of the motor system (Prediction 4)

The results of Experiments 5.1-5.3 provide strong evidence that the VPs evoked by *onsets* and *offsets* reflect the functioning of a common neural system. A final important aspect to investigate is whether *onsets* and *offsets* are similarly related to behaviour. Our group has recently demonstrated that VPs elicited by impulse stimuli are tightly coupled with a modulation of muscular output during an isometric force task (Novembre et al., 2018, 2019).

In Experiment 5.4, I tested whether stimulus *onsets* and *offsets* also have similar motor consequences. I used a highly-sensitive force transducer to record fine variations in the isometric force exerted by participants. Both *onsets* and *offsets* elicited a transient and multipolar force modulation, similar to that previously observed in response to impulse stimuli (Figure 5.8, *middle*). *Onsets* elicited an initial force decrease at ~110 ms, followed by a force increase at ~270 ms and a further decrease at ~370 ms (Figure 5.8; Novembre et al., 2018). *Offsets* elicited a similar increase and decrease of force at ~280 and ~410 ms, respectively, although with no initial decrease (perhaps related to the lack of a clear early deflection in the corresponding EEG response; Figure 5.8). These observations were substantiated with point-by-point t-tests against zero (Figure 5.8, *bottom*).

I finally note that before applying the high-pass filter necessary to highlight the transient force modulations (Novembre et al., 2018), a long-latency and long-lasting force modulation was present for both *onsets* and *offsets* (Figure 5.8, *grey waveforms*). Interestingly, the polarity of this force modulation was opposite in the two conditions: positive when elicited by *onsets* and negative when elicited by *offsets* – a finding possibly hinting towards a differential effect of change direction on delayed behaviour, clearly deserving further investigation.

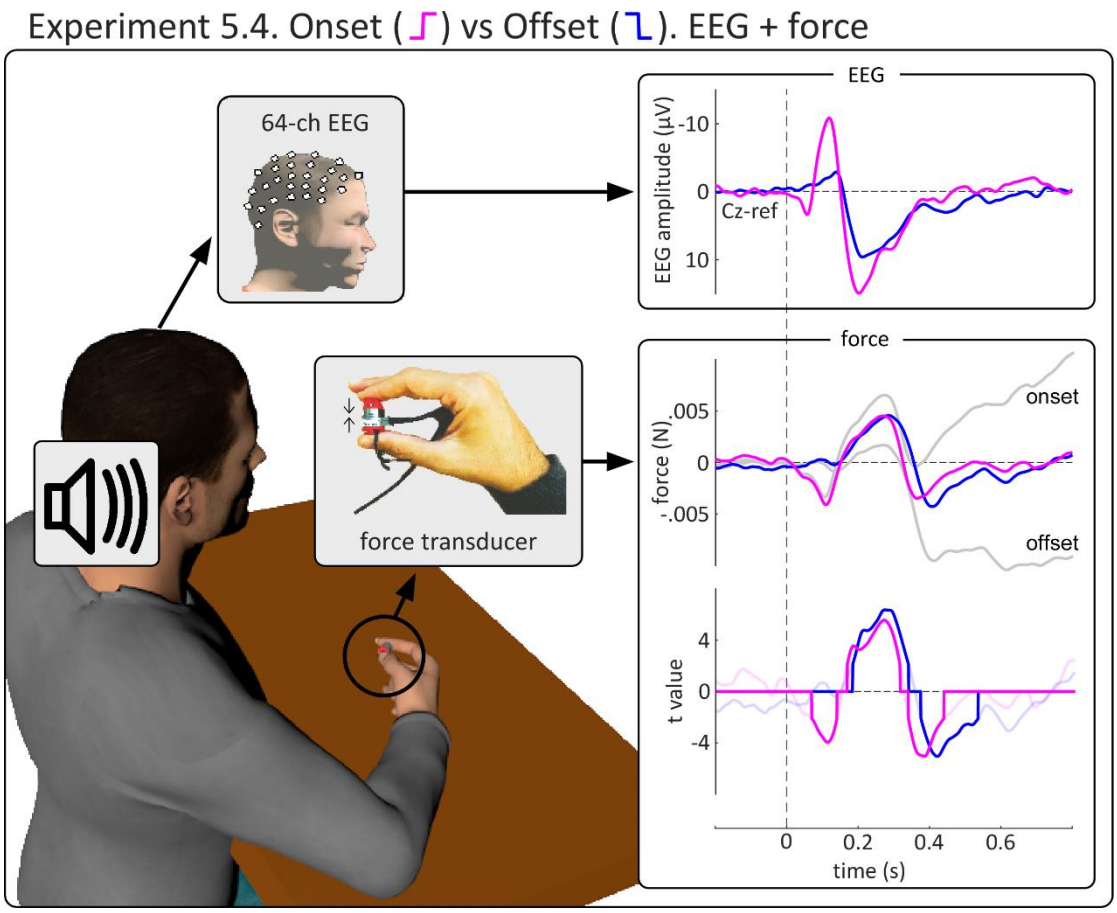

Figure 5.8. Experiment 5.4. Abrupt *onsets* and *offsets* elicit similar modulations of motor output during an isometric force task.
Left. The experimental setup used in Experiment 5.4. Participants sat at a table applying a constant force (measured by a force transducer), while receiving abrupt *onsets* and *offsets* of auditory stimulation. *Right.* Top row shows the grand-average EEG responses elicited by *onsets* (pink) and *offsets* (blue). Middle row shows the grand-average force modulations. Coloured plots show the high-pass filtered signals; grey plots show the unfiltered signals. Bottom row shows the t-value timecourse from the t-tests against zero across all participants. Bold lines show significant clusters.

Onsets and *offsets* both elicited a similar transient increase of force at ~280 ms, followed by a decrease at ~400 ms. *Onsets*, but not *offsets*, elicited an initial decrease of force at ~100 ms. These results indicate that both *onsets* and *offsets* elicited a largely similar multiphasic pattern of force modulations. Unfiltered force plots show that both *onsets* and *offsets* both elicited a late force modulation, albeit in the opposite direction.

5.4 Discussion

In this chapter, I compared the EEG responses elicited by abrupt and unexpected stimulus *offset* with the well-characterised Vertex Potentials elicited by stimulus *onsets.* Chapter 4 and previous studies have highlighted the importance of *onset*-evoked VPs, showing that they reflect a neural system highly sensitive to unexpected, and therefore behaviourally-relevant environmental changes (Iannetti et al., 2008; Wang et al., 2010; Valentini et al., 2011; Torta et al., 2012; Ronga et al., 2013), regardless of the sensory modality in which those changes occur (Mouraux and Iannetti, 2009; Liang et al., 2010). In contrast, far less is known about the brain responses elicited by abrupt and unexpected stimulus *offsets*. Consequently, whether *onset* and *offset* EEG responses reflect the functioning of the same neural system is unknown, limiting our understanding of the functional importance of a large and fundamental phenomenon of the mammalian brain (Bancaud et al., 1953; Knight et al., 1985; Beydoun et al., 1997).

I addressed this problem in four experiments in which I recorded the brain activity from 44 participants while delivering abrupt *onsets* and *offsets*. Importantly, *onsets* and *offsets* were carefully matched with respect to all stimulus features (i.e. abruptness, differential intensity, and unexpectedness) except the direction of the change in intensity. I predicted that if *onsets* and *offsets* elicit Vertex Potentials (VPs) reflecting the same neural system, then they (1) would have quantitatively highly-similar temporal evolution of their scalp distributions, and (2) would be largely comprised of similar, supramodal subcomponents. Additionally, I predicted that, like the *onset* VP, the *offset* VP would be (3) comparably sensitive to the unexpectedness of the stimulus, and (4) related to a similar activation of the motor system. Overall, there was a remarkable degree of phenomenological and functional similarity between the brain responses elicited by abrupt *onsets* and *offsets* of auditory and somatosensory stimuli. This result suggests that these electrocortical responses mostly reflect the activation of a common, supramodal

neural network, consequent to the detection of behaviourally-relevant environmental changes.

Abrupt onsets and offsets activate a common, supramodal brain network

Experiments 5.1 and 5.2 demonstrate that *onsets* and *offsets* of both auditory and somatosensory stimuli elicit highly similar EEG responses in the time domain, dominated by the large negative-positive waves composing the VP. In Experiment 5.1, I employed a point-by-point spatial correlation to compare the spatial distributions of the *onset* and *offset* responses throughout their timecourse, at much higher spatial and temporal resolution than previous studies. The evolution over time of the response scalp distributions was highly similar across *onset* and *offset*-evoked responses, expanding on a previous study which found similar correlations but restricted their analysis to the response peaks and used a low-density 15-channel EEG system (Yamashiro et al., 2008).

In Experiment 5.2, I adapted an established method for classifying ERP independent components (IC) according to their selectivity for particular conditions (Mouraux and Iannetti, 2009; Liang et al., 2010), but improved upon the previously-used binary classification with a less-arbitrary and more quantitative analysis of the selectivity of each IC (Figures 5.4 and 5.5). This approach demonstrated that the *onset* and *offset* responses elicited in the auditory and somatosensory modalities are largely comprised of similar neural activity which is supramodal and non-specific to either *onsets* or *offsets*, extending the previous finding to multiple sensory modalities. This clearly does not imply that the neural activity elicited by onsets and offsets is identical, but given the limited spatial resolution of EEG, the differences between the neural activity underlying *onset* vs *offset* responses are likely to be fine-grained in both the auditory and somatosensory modalities. Indeed, I did find some smaller ICs which were more selective for one sensory modality (as in previous work: Mouraux and Iannetti, 2009; Liang et al., 2010) or for a particular direction of intensity change. However, not only did these ICs reflect the smallest proportions

of response variance (Figure 5.5), but they were also only marginally selective, with no IC having a selectivity ratio larger than ~3 (see Methods), and were therefore far from being *"specific*" for any particular condition. Thus, these results demonstrate that most of the variance of the auditory and somatosensory *onset*- and *offset*-evoked VPs (i.e. the bulk of the recorded response) was supramodal and non-specific for the direction of the intensity change. This finding contradicts some common interpretations that *onset* and *offset* responses reflect the detection of intensity changes solely within a particular sensory modality (e.g. Martin and Boothroyd, 1999, 2000; Weise et al., 2012, 2018). For example, the VP elicited by changes in auditory intensity has been interpreted by some authors in a modality-specific fashion, and the response consequently labelled as the "auditory change complex" (ACC; Martin and Boothroyd, 1999, 2000), an interpretation still pervasive in the clinical literature (Friesen and Tremblay, 2006; Hoppe et al., 2010; He et al., 2015; Mathew et al., 2017).

In addition to the phenomenological results of Experiments 5.1 and 5.2, the results of Experiments 5.3 and 5.4 provide functional evidence that a common network subserves onset and offset brain responses. Experiment 5.3 demonstrates that *onsets* and *offsets* are similarly sensitive to the temporal predictability of the eliciting stimulus, with more predictable (and therefore less surprising) stimuli eliciting a smaller brain response (Figure 5.7) – a finding consistent with the observation that *offsets* following shortly after the preceding *onset* elicit a smaller-amplitude VP (Davis and Zerlin, 1966). The scalp distribution of the response habituation was also similar across *onsets* and *offsets*. This similarity implies that the neural generators sensitive to stimulus surprise were the same in both *onset* and *offset* responses, therefore providing even stronger evidence for a shared neural substrate. Experiment 5.4 additionally provides evidence that the *onsets* and *offsets* similarly modulate the muscular output, clearly pointing towards a similar functional significance of these responses – as discussed in more detail in the following section. Altogether, these

findings suggest that abrupt *onsets* and *offsets* activate a common, supramodal brain network.

Offset-evoked Vertex Potentials do not merely encode changes of sensory intensity, but rather the behavioural relevance of those changes

As mentioned in previous paragraphs, *offset*-evoked VPs have often been interpreted in terms of modality-specific perception. A naïve explanation of the VPs elicited by *onsets* and *offsets* might be that they merely encode the cortical representation of the beginning and end of a sensory event. However, the results of Experiment 5.3 demonstrate that the magnitude of the *offset* response does not faithfully represent the intensity drop, but rather its unexpectedness or *surprise* content, which I define here as the degree to which the stimulus violates expectations. This is a function of both (1) the particular predictions of the system and (2) the amount which the stimulus stands out from recent sensory input. Notably, this is also the case for the more investigated *onset* brain response (Iannetti et al., 2008; Wang et al., 2010; Valentini et al., 2011; Ronga et al., 2013).

What then is the functional significance of these *offset* responses? The sensitivity of an ERP to unexpected sensory events can be explained as the encoding of prediction error associated with a violation of expectations (Friston, 2005). In such a 'free-energy' framework, the system underlying the VP may have a number of priors (derived from either from evolution experience, or both), such as that no intensity change will occur, but that when an intensity change occurs repeatedly at constant interval, it will continue to repeat. Thus, these repeated stimuli are more expected and result in a smaller surprise signal (i.e. in a VP of smaller amplitude; Iannetti et al., 2008). The occurrence of changes in specific stimulus features within the sequence of repeated stimuli (e.g. changes in stimulus intensity, modality, or spatial location) can violate this prediction, resulting in another increase of the surprise signal and thereby reversing the habituation of the Vertex Potential (i.e. *dis*habituation; Valentini et al., 2011; Ronga et al., 2013; Moayedi et al., 2016). These priors (or rules) can be studied to determine the

function of the system. Indeed, previous studies of the *onset*-evoked VP have revealed that not all types of sensory changes are equally capable of eliciting a surprise signal. For example, the habituation due to the repetition of identical stimuli can be reversed only by changes of particular stimulus properties, such as changes of sensory modality (Valentini et al., 2011), changes of stimulus location in egocentric, but not somatotopic, coordinates (Torta et al., 2012; Moayedi et al., 2016) and successive increases, but not decreases, of stimulus intensity in a sequence of abrupt stimuli (Ronga et al., 2013).

The predictions of this system seem to be tuned such that the most surprising sensory changes are those which have more relevance for *urgent and immediate* behaviour. For example, the importance of stimuli moving towards the core of the body, but not away from the core of the body (Torta et al., 2012; Moayedi et al., 2016), or the importance of stimuli becoming sequentially more intense (Ronga et al., 2013) have a clear relevance to survival in a natural environment: they could represent a threat to the body which demands immediate attention and behavioural reaction. Several other lines of evidence link VPs to immediate behavioural reaction: in Experiment 5.4, both *onsets* and *offsets* were capable of eliciting a specific modulation of muscle activity, possibly to prepare the individual for swift reactions to current of future environmental events (Novembre et al., 2018); furthermore, the amplitude of VPs has been shown to reliably predict the speed of subsequent speeded reactions (Moayedi et al., 2015; Kilintari et al., 2018; Tiemann et al., 2018). Importantly, this relationship is even stronger when the behaviour has a more ethological urgency, such as a defensive limb withdrawal rather than an equivalent non-defensive movement (Moayedi et al., 2015). It therefore seems likely that, rather than purely reflecting the sensory-cortical encoding of sudden drops of sensory input, the *offset*- (and *onset*-) evoked VPs instead reflect a predictive model which is geared towards the detection of behaviourally-relevant environmental changes, and the preparation for appropriate motoric response to those changes.

6 Vertex Potentials are tightly correlated with the defensive hand-blink reflex

6.1 Introduction

In ecological settings, sudden sensory events can indicate threats and the need for immediate behavioural response to avoid danger. Consequently, these events can often trigger rapid defensive reflexes. For example, the withdrawal reflex to painful heat stimuli (Creed et al., 1932). But subcortical reflexes can also be flexible, undergoing top-down modulation from cortical systems which process behaviourally-relevant, higher-level information about the eliciting stimulus, reflecting the usefulness of the action in question (Sambo et al., 2012b; Bufacchi and Iannetti, 2018). If the VP also reflects the behavioural-relevance of the eliciting stimulus, its amplitude may vary depending on the magnitude of a defensive reflex triggered by that stimulus.

In this chapter I test this possibility with a well-studied behavioural model: the defensive hand blink reflex (HBR) elicited by abrupt and intense stimulation of the hand (Miwa et al., 1998; Leó N et al., 2011). The HBR magnitude is known to vary depending on stimulus properties which affect the usefulness of the action. For example, it is modulated by factors which affect the probability that a threat will collide with the face, e.g. the spatial proximity of the stimulated hand to the face (Sambo et al., 2012a, 2012b; Wallwork et al., 2016; Bisio et al., 2017), movement of the stimulated hand (Wallwork et al., 2016; Bisio et al., 2017; Bufacchi, 2017), gravitational context (Bufacchi and Iannetti, 2016), probability of stimulus occurrence (Sambo et al., 2012a), the presence of a protective screen (Sambo et al., 2012a) and the use of a learned protective posture (Biggio et al., 2019), as well as more general properties, such as stimulus energy and inter-stimulus interval (Miwa et al., 1998; Sambo et al., 2012b, 2012a).

In this experiment, I exploited a previously-used paradigm to study the relationship between the HBR and the VP, in which the magnitude of the reflex is modulated by the proximity of the eliciting stimulus to the face (Sambo et al., 2012a).

6.2 Methods

Participants

39 healthy volunteers (11 women; age range 18-30 yr, mean ± SD 22 + 3.1) participated in the study and gave written informed consent before taking part. Experimental procedures were approved by the University College London ethics committee. All experiments were performed in accordance with the Declaration of Helsinki, as well as local guidelines and regulations

Somatosensory stimulation

Somatosensory stimuli consisted of constant-current, 200-μs long square pulses generated by an electrical stimulator (DS7A, Digitimer). Stimuli were delivered using a surface bipolar electrode placed on the median nerve at the wrist on the left or right hand, depending on the experimental condition (see *Experimental design* below). Stimulus intensity was adjusted for each participant at the beginning of each recording block, to elicit a clear HBR in three consecutive trials (Miwa et al., 1998; Sambo et al., 2012b). The mean stimulus intensity across participants was 30.2 mA.

Experimental design

The experiment design was based on a previous study (Sambo et al., 2012a), and consisted of four blocks, each comprising 20 stimuli delivered every ~30 s. Between each stimulus, a short tone instructed the participant to alternate the right arm between two different positions: “Far” and “Near”. In the “Far” position, both forearms rested flat on a table, with elbow angles of ~150 degrees. In the “Near” position, the right forearm was held at ~75 degrees with respect to the arm, such that the right hand was held ~4 cm in front of the ipsilateral side of the face, while the left hand remained on the table. In half of the blocks, the right hand

was stimulated (i.e. the *moving* hand), while in the other half the left hand was stimulated (i.e. the *stationary* hand). The order of the blocks was counterbalanced across participants. This design resulted in four experimental conditions: 'Moving Hand - Near', 'Moving Hand - Far', 'Stationary Hand - Near' and 'Stationary Hand - Far', with 20 trials each in total.

EEG & EMG recording

EEG activity was recorded from 26 electrodes placed on the scalp according to the international 10-20 system and referenced to the nose. EMG activity was recorded from the orbicularis oculi muscle, bilaterally, using pairs of surface electrodes with the active electrode placed over the mid-lower eyelid and the reference electrode a few centimetres laterally to the outer canthus. All signals were amplified and digitised at a sampling rate of 1024 Hz (SD 32, Micromed).

EEG preprocessing

EEG signals were preprocessed and analysed using EEGLAB, as well as custom-written scripts in Matlab. The data were first band-pass filter from 0.5 to 100 Hz and notch filtered from 48 to 52 Hz. Data were then segmented into epochs using a time-window of ±2 s from stimulus onset (epoch duration = 4 s). Artifacts due to eye blinks or eye movements were removed using a validated method based on independent component analysis (Jung et al., 2000).

EMG preprocessing

EMG signals were first band-pass filtered between 0.5 and 100 Hz, notch filtered from 48 to 52 Hz, and full-wave rectified. HBR responses were averaged between eyes (as in refs Sambo and Iannetti, 2013; Bufacchi et al., 2016; Wallwork et al., 2016; Bisio et al., 2017; Fossataro et al., 2018). HBR magnitude was calculated for each trial as the area under the curve (AUC; Sambo et al., 2012a). For each participant, AUC values were transformed into Z scores, both within-subject and

within-condition (in separate analysis pipelines). Normalised AUC values were finally averaged across trials for each experimental condition.

Statistical analysis

To replicate the results of Sambo et al (Sambo et al., 2012a), I performed a two-way repeated-measures ANOVA on the group-level normalised HBR values for each condition, with factors 'Hand Position' (two-levels: 'Near' and 'Far') and 'Stimulated Hand' (two-levels: 'Moving Hand' and 'Stationary Hand').

To test for similar modulations of the EEG, I performed a point-by-point two-way repeated-measures ANOVA on the group-level averages for each condition, with the same factors as above. The resulting F values were false discovery rate (FDR) adjusted for multiple comparisons.

To explore the relationship between the spontaneous trial-by-trial variability of the HBR and VP, I performed a point-by-point correlation between the single-trial HBR values (normalised within-condition) and EEG across all channels, in a time-window from -0.5 s to 1 s. These correlations were performed twice, once after regressing out the effect of trial number within block from both the EEG and HBR respectively, and once without this step. This was done to assess how much correlation between the two responses was driven by the expected habituation of each response within each block. To correct for multiple comparisons, I performed cluster permutation testing with 2000 permutations for each of the time-course correlations (Maris and Oostenveld, 2007). I also isolated the N1 response contralateral to the stimulated hand (likely reflecting the primary somatosensory cortex; Valentini et al., 2012) using an adaptive spatial filter (Bufacchi et al., 2021) and correlated the peak amplitude of this response with the HBR magnitude across trials.

6.3 Results

Results of ANOVA on HBR magnitude

Figure 6.1 shows the group-level average HBR magnitudes for each condition. The ANOVA showed very strong evidence for effects of 'Hand Position' ($F = 32$, $p = 8.1e\text{-}6$), 'Stimulated Hand' ($F = 10$, $p = 3.4e\text{-}3$) and the interaction between these factors ($F = 26$, $p = 2.8e\text{-}5$). Post-hoc t tests revealed that the source of the interaction was (1) a larger HBR in the 'Near' hand position compared to the 'Far' position when the moving hand was stimulated ($t = -6.2$, $p = 1.9e\text{-}6$), but not when the stationary hand was stimulated ($t = -2.0$, $p = 0.060$), and (2) a larger HBR when the moving hand was stimulated compared to the stationary hand, in the 'Near' position ($t = -5.2$, $p = 2.3e\text{-}5$) but not in the 'Far' position ($t = -1.1$, $p = 0.29$). The results of all post-hoc t tests are shown in Table 6.1. These results indicate that proximity of the stimulated hand to the face enhanced the HBR magnitude.

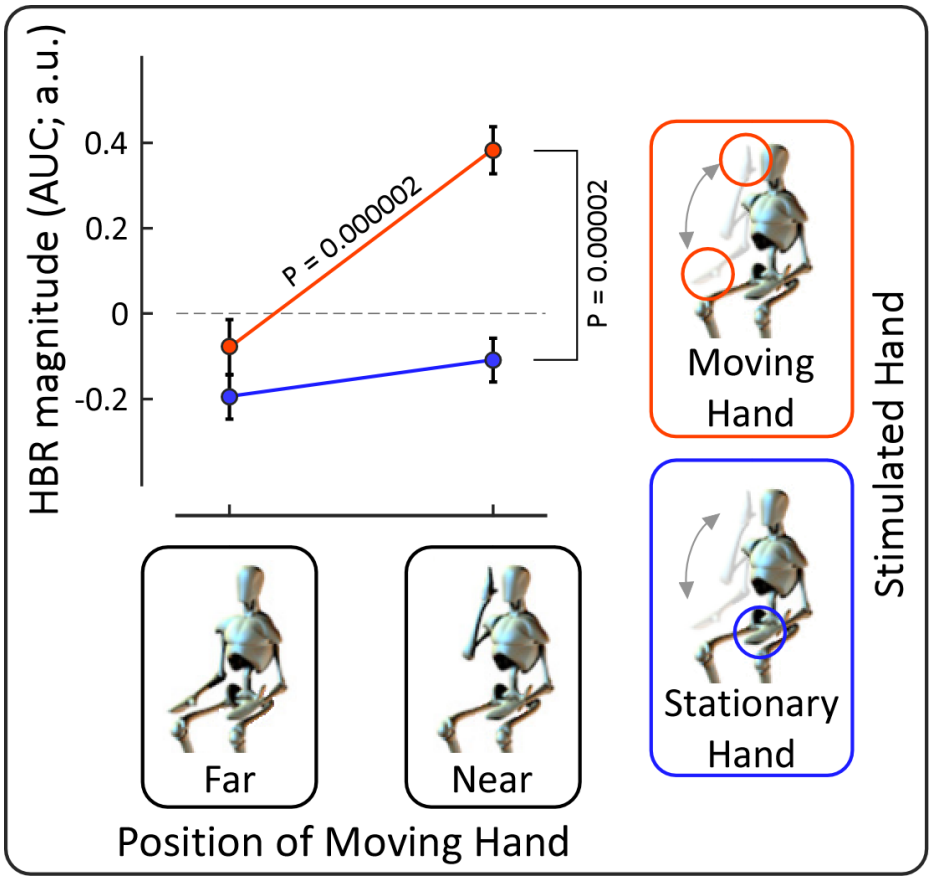

Figure 6.1. Proximity of the stimulated hand to the face enhances the hand-blink reflex.

Electrical stimuli were delivered to the median nerve of either the left or right wrist (depending on the block) to elicit the hand-blink reflex (HBR). The right hand alternated between two positions: near to and far from the face. Plot shows group-level, normalised HBR magnitude (z-score) in each of the four conditions. P values show significant comparisons between conditions (post-hoc t tests). Error bars show SEM for each condition. Proximity of the moving hand to the face enhanced HBR magnitude only when the stimulus was delivered to this hand.

Table 6.1. Post-hoc t tests of HBR magnitude.

t values		**Moving**		**Stationary**	
		Near	Far	Near	Far
Moving	Near	n/a			
	Far	**-6.17**	n/a		
Stationary	Near	**-5.20**	-0.27	n/a	
	Far	**-5.71**	-1.08	-1.97	n/a

p values		**Moving**		**Stationary**	
		Near	Far	Near	Far
Moving	Near	n/a			
	Far	**1.86e-6**	n/a		
Stationary	Near	**2.25e-5**	0.79	n/a	
	Far	**5.95e-6**	0.29	6.02e-2	n/a

Results of ANOVA on EEG amplitude

Figure 6.2 shows the group-level average waveforms recorded at the scalp vertex (top row), as well as the F value timecourse for the two factors and the interaction (bottom row). There was weak evidence of a main effect of 'Stimulated Hand' between 0.11–0.13 s ($p = 0.04$) and 0.37–0.39 s ($p = 0.03$). Both of these effects were lateralised (Figure 6.2), suggesting they may be driven by lateralised somatosensory-specific subcomponents of the ERP (see Discussion). There was also evidence of a small, short-lasting interaction between 0.22-0.26 s with vertex-maximal topography (corresponding to the P wave peak; max $p = 0.01$). There was no evidence of a main effect of 'Hand Position'. These results indicate that the VP was largely unaffected by proximity of the eliciting stimulus to the face.

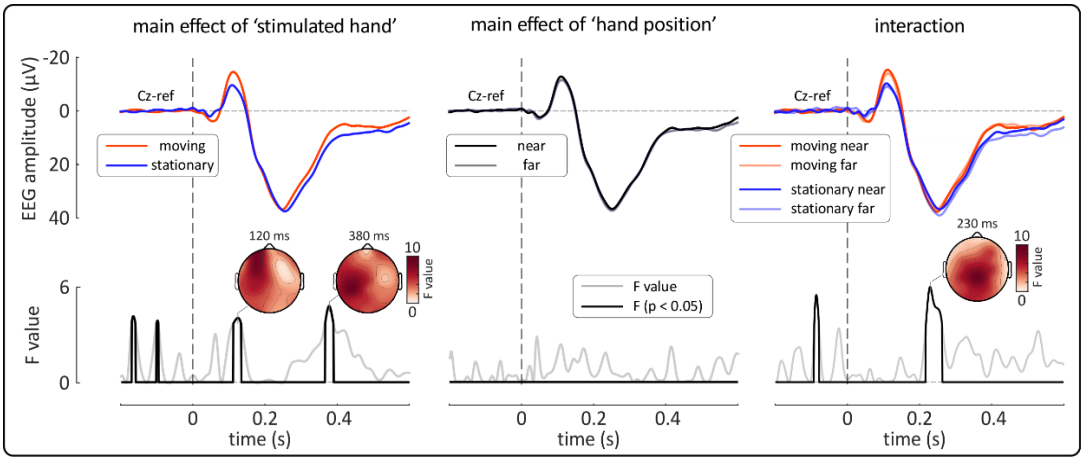

Figure 6.2. Vertex Potential magnitude was largely unaffected by position of the stimulated hand.

Top row. Group-level average waveforms at Cz for each level of the factor 'Stimulated Hand (left), 'Hand Position (middle) and for every individual condition (right). *Bottom row.* F values from the two-way ANOVA. Black plots indicate significant time windows. Weak lateralised effects of the factor 'Stimulated Hand' were observed in the early and latest part of the response, probably reflecting the activation of either left or right primary somatosensory cortex depending on the hand stimulated. No main effects of 'Hand Position' were found, and only a small, short-lived interaction effect was found at the P wave peak.

Trial by trial correlations between EEG and HBR magnitude

Figure 6.3 (*top panel*) shows the results of trial-by-trial correlations between the EEG and HBR magnitudes. Practically the entire VP was highly correlated with the HBR magnitude across trials, and this relationship was still present (although attenuated somewhat) when the effect of trial order was regressed out of both the EEG and HBR magnitudes. There was clear evidence that the EEG signal was correlated with HBR magnitude in clusters from ~95 – 160 ms, ~180 – 330 ms and ~400 – 960 ms (cluster p = 5e-4, 5e-4 and 5e-4 at 2000 permutations). The first two clusters corresponded to the N and P waves, peaking at 120 and 250 ms respectively with central scalp distributions like those of the grand average peaks (although the cluster corresponding to the P wave was slightly more frontally distributed). Peak r values were -0.17 and 0.13 (first and second cluster respectively), indicating larger VP magnitude with larger HBR magnitudes. The third cluster appeared to correspond to a third wave, also centrally distributed, following the first two VP peaks, which was not clearly visible on the grand average waveform and was negatively correlated with the HBR magnitude (r = -0.12). Similar results were found after regressing out the effect of trial order: the adjusted EEG signal and HBR magnitude correlated in clusters from ~96 – 141 ms, ~200 – 260 ms and ~400 – 820 ms (cluster p = 5e-4, 5e-4, and 3e-3). The scalp distributions of each peak were even more similar to those of the EEG grand average than before the trial-order regression was performed. The r values were weaker but still strong (r = -0.12, 0.075 and -0.10), indicating that a lot of the correlation between the EEG and HBR was not simply driven by a similar habituation timecourse within each block. Figure 6.3 (*bottom panel*) shows the results of the trial-by-trial correlation between the isolated N1 subcomponent and the HBR magnitude. No relationship was found between the magnitude of the local N1 subcomponent and the magnitude of the HBR, either before (r = -0.04, P = 0.06) or after (r = -0.002, P = 0.94) regressing trial-order effects out.

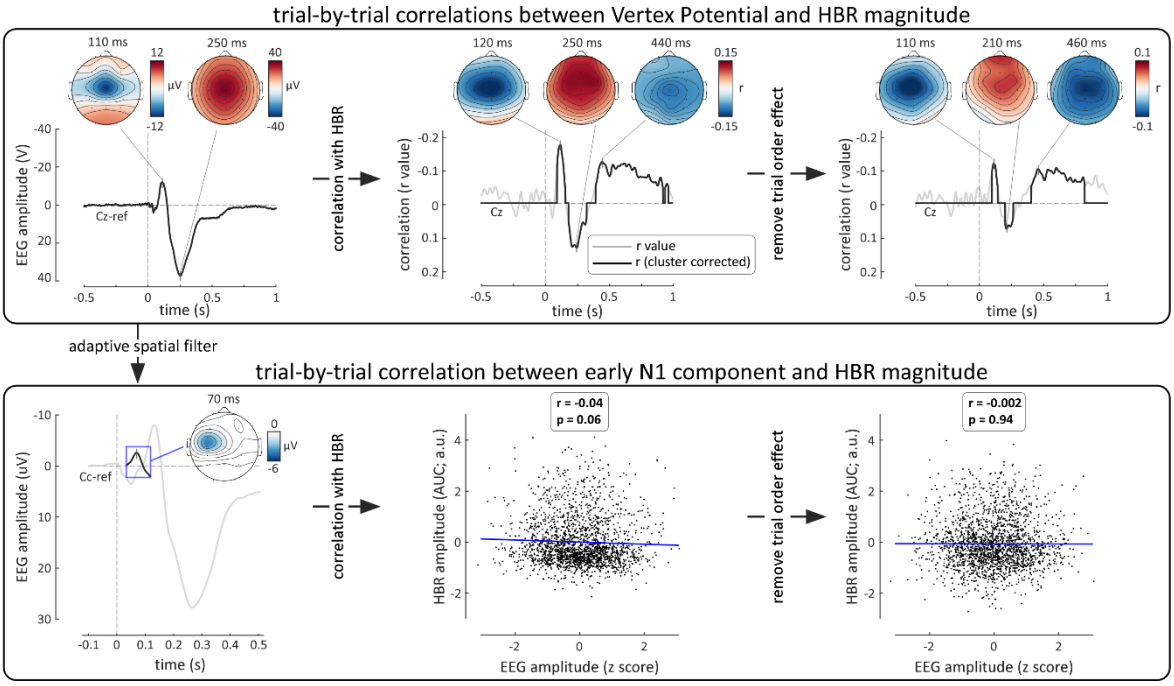

Figure 6.3. Trial-by-trial correlations between EEG and hand-blink reflex magnitude.

Top. Results of trial-by-trial correlations between Vertex Potential (VP) and hand-blink reflex (HBR) magnitude. Left plot shows grand average waveform at Cz. Middle plot shows the correlation (r value) timecourse at Cz. Right plot shows correlations after regressing out effects of trial order from EEG and HBR. Bold lines show significant clusters (i.e. cluster $p < 0.05$). Topographies show scalp distributions at peaks of all waveforms. Practically the entire VP timecourse was highly correlated with the HBR magnitude. A lot of this correlation was still present after removing the effect of trial order, indicating that the responses were correlated independently of their similar habituation timecourse.

Bottom. Left plots shows the isolated, early N1 response at Cc (i.e. C3/C4, contralateral to stimulated hand). Middle and right scatterplots show trial-by-trial correlation between N1 peak amplitude and HBR magnitude, before and after regressing out the trial order effect respectively. The early N1 subcomponent was uncorrelated with the HBR, indicating that the correlations observed with the later VP response were not simply driven by variability in the afferent sensory inputs.

6.4 Discussion

Proximity of stimulated hand affected HBR magnitude, but not the VP amplitude

These results replicate the well-known, large enhancement of the HBR magnitude by the proximity of the stimulated hand to the face (Sambo et al., 2012b, 2012a; Wallwork et al., 2016). Conversely, there was little evidence of modulations of the VP by the same experimental factors. The small lateralised effects of the factor 'Stimulated Hand' were probably driven by early and late ERP subcomponents reflecting primary somatosensory cortex contralateral to the stimulated hand (Valentini et al., 2012; Hu et al., 2014b). Additionally, there was no evidence of a main effect of 'Hand Position' and evidence of a small, short-lasting interaction only at the P peak, which seemed to reflect a smaller P wave when the moving hand was near to the face and the stationary hand was stimulated. These results indicate that there was a relationship between the HBR magnitude and stimulus proximity, but no similar relationship between the EEG amplitude and proximity.

The HBR and VP were highly correlated on a trial-by-trial basis

Despite the lack of a similar relationship with the experimental factors between the HBR and VP, the two responses were highly correlated *within condition* (i.e. their spontaneous trial-by-trial variability was similar). These correlations show that when the HBR was larger, so was the VP response in the EEG. The correlations were largely preserved when the effect of trial number was regressed out of each response, indicating that the relationship was not purely driven by similar response habituation throughout the experiment. Importantly, the correlation was also not simply driven by variability in the afferent volley (e.g. due to trial-by-trial variations in the electrical stimulation of Aβ fibres) as the HBR magnitude did *not* correlate with the earlier N1 response. This relationship therefore appears to reflect either (1) an overlap between the supramodal neural generators of the VP and the neurones responsible for the top-down modulation of the HBR trial-by-trial, or (2) a common upstream neural system, affecting both

the HBR and VP magnitudes, which must be located after the supramodal and modality-specific systems split (i.e. between the periphery and the cortex). The entire VP seemed to be correlated with the HBR magnitude (shown by the widespread, central topography of the correlations; Figure 6.3), which might suggest a common upstream system is more likely, but there is no direct evidence for either possibility. Although it is not clear which of the two interpretations is true at present, either possibility demonstrates a tight link between behaviour and the supramodal network underlying the VP, but not between behaviour and the somatosensory-specific processing reflected by the N1 response (Mouraux and Iannetti, 2009; Valentini et al., 2012; Hu et al., 2014b). This is consistent with previously observed correlations between the VP and reaction time (Moayedi et al., 2015; Tiemann et al., 2018). The results of Moayedi et al are particularly relevant, as they found a stronger relationship between the VP reaction time for *defensive* movements. Interestingly, I did not find any evidence of correlation with the early N1 response and behaviour, unlike the publications cited above. This discrepancy could be explained by the use of an adaptive spatial filter to better isolate the N1 response from the overlapping VP (Bufacchi et al., 2021), rather than simple re-referencing used in previous work (e.g. Moayedi et al., 2015).

7 Movement of environmental threats modifies the relevance of the defensive eye-blink in a spatially-tuned manner.

(This chapter has been published as Somervail et al. in *Scientific Reports*, 2019)

7.1 Introduction

In previous chapters I discussed how the brain response to sudden sensory events reflects a widespread cortical activation, which may allow the organism to produce more effective rapid behavioural responses to potential threats. In Chapter 6, I showed that the Vertex Potential amplitude correlates with the hand-blink reflex (HBR), suggesting either (1) an overlap between the supramodal neural generators of the VP and the neurones responsible for the top-down modulation of the HBR trial-by-trial, or (2) a common upstream neural system affecting both the HBR and VP magnitude. In this chapter I focus on the behavioural response itself. In particular, I study how sensitivity to certain environmental features allows the nervous system to maximise the behavioural utility of that response, via top-down cortical modulation.

While subcortical reflex circuits allow the rapid execution of simple motor responses to sudden and potentially threatening events, stereotyped responses are not always optimal to ensure survival. Top-down cortical modulation of those circuits therefore allows reflexes to be “primed” so that the most appropriate response can be immediately triggered with minimal delay[9]. These modulations have been described for several reflexes, and can take into account many

[9] I.e. without the substantial delay associated with multi-synaptic cortical processing.

stimulus-related factors (Grillon et al., 1991; Sandrini et al., 2005; Hess et al., 2007; Janssens et al., 2014; Wang and Munoz, 2015).

The HBR, for example, is top-down modulated by several stimulus-related factors, including the spatial proximity of the stimulated hand to the face (shown in the previous chapter; Sambo et al., 2012a, 2012b; Wallwork et al., 2016; Bisio et al., 2017), as well as movement of the stimulated hand (Wallwork et al., 2016; Bisio et al., 2017; Bufacchi, 2017), probability of stimulus occurrence (Sambo et al., 2012a), stimulus energy and inter-stimulus interval (Miwa et al., 1998; Sambo et al., 2012b, 2012a). Due to the interaction between the spatial proximity of the stimulus and several other stimulus properties, the HBR has come to be interpreted as a measure of "peri-personal space" (PPS; e.g. Sambo et al., 2012b; Sambo and Iannetti, 2013; Bisio et al., 2017; Biggio et al., 2019; Fossataro et al., 2019), a hypothetical zone around the body receiving special processing for the purpose of defence or interaction with the environment (De Vignemont and Iannetti, 2015). However, this framework is flawed for a number of reasons, such as the implication of a strict boundary between "near" and "far" spaces with distinct neural representations (for a review see: Bufacchi and Iannetti, 2018). Instead, I will use the better concept of an *action relevance field,* which reflects the relevance of an action depending on stimulus location and other factors (Bufacchi et al., 2016; Bufacchi and Iannetti, 2018).

In contrast to the well-characterised effects of stimulus-dependent properties, the effects of stimulus-*independent* environmental factors on the HBR *action relevance field* are less explored; to the best of my knowledge, only two such factors have been tested: gravitational cues (Bufacchi and Iannetti, 2016) and physical barriers between the hand and face (Sambo et al., 2012a). Importantly, both factors are static, and the effect of moving, environmental objects that are separate to the stimulus triggering the reflex remains unexplored. Here I explored whether dynamic, *stimulus-independent* environmental features unrelated to the stimulus eliciting the reflex can top-down modulate the HBR. Specifically, I tested

whether the neural system modulating the HBR is sensitive to the presence and movement of threatening objects in the environment.

To address this question, I performed two experiments in 40 healthy human volunteers. I recorded the HBR elicited by electrical somatosensory stimuli delivered at different hand positions while participants were immersed in virtual reality (VR) environments and exposed to fast-moving virtual arrows originating from several locations. In Experiment 7.1, I observed that the occurrence of arrows flying towards the participant altered the shape of the HBR proximity-response function, suggesting a more gradual fall-off of the *action relevance field*. In Experiment 7.2, the arrows originated from spatially distinct sources and I observed that the effect was directionally-tuned towards the source of the arrows.

7.2 Methods

Participants

40 healthy volunteers participated in the study and gave written informed consent before taking part. Experimental procedures were approved by the University College London ethics committee. All experiments were performed in accordance with the Declaration of Helsinki, as well as local guidelines and regulations. Experiment 7.1 included 20 participants (11 women; age range 19–41 yr, mean ± SD 24.9 ± 6.0). Experiment 7.2 included 20 participants (12 women; age range 18–25 yr, mean ± SD 20.8 ± 2.1).

Somatosensory stimulation

Somatosensory stimuli consisted of constant-current, 200-μs long square pulses generated by an electrical stimulator (DS7A, Digitimer). Stimuli were delivered using a surface bipolar electrode placed on the median nerve at the wrist. In Experiment 7.1, stimuli were delivered to the right hand; In Experiment 7.2 stimuli were delivered to either hand. At the beginning of each recording block, stimulus intensity was adjusted to elicit a clear HBR in three consecutive trials (Miwa et al., 1998; Sambo et al., 2012b). Participants who refused an increase in stimulus

intensity before three clear HBR responses were observed, or who had a clear HBR in less than 50% of trials were considered non-responders and did not take part in the experiment (Sambo et al., 2012a). In HBR responders the mean stimulus intensity across participants (± SD) was 39.4 ± 15.0 mA [experiment 7.1], and 46.8 ± 21.3 mA [experiment 7.2]). In Experiment 7.1, participants were recruited from a group of previously screened HBR responders (Sambo et al., 2012b; Bufacchi and Iannetti, 2016). In Experiment 7.2, 20 out of 64 participants tested (i.e. 31%) were classified as HBR-responders and took part in the rest of the experiment. This 31% response rate is lower than commonly reported (~60%; Miwa et al., 1998; Sambo et al., 2012b, 2012a; Sambo and Iannetti, 2013), including in a more recent study using a similar VR system (61%; Fossataro et al., 2020). This discrepancy may have been due to the VR headset acting as a physical barrier protecting the face (Sambo et al., 2012a), or because I did not use a full-body avatar to embody the participants in the virtual environment (see *Virtual Reality* below for further details; Fossataro et al., 2020).

EMG recording

EMG activity was recorded from the orbicularis oculi muscle, bilaterally, using pairs of surface electrodes with the active electrode placed over the mid-lower eyelid and the reference electrode a few centimetres laterally to the outer canthus. Signals were amplified and digitised at a sampling rate of 2048 Hz (SD 32, Micromed).

Virtual Reality

In both experiments, participants were immersed in virtual reality environments programmed in-house. In Experiment 7.1, the VR environment was programmed in Unity, and was presented to the participants in the CAVE system at the UCL Computer Science Department (https://vr.cs.ucl.ac.uk). This system offers the advantage of allowing participants to see their entire body within the virtual environments (Figure 7.1, *Experiment 7.1*). In Experiment 7.2, the VR environment was programmed in Unreal Engine 4 and was presented to the

participants through the HTC Vive head-mounted display. In both experiments participants remained seated during the data collection but were permitted to explore the virtual environment between blocks. Given that the VR head-mounted display prevented participants from seeing their own body, in Experiment 7.2 the position of each hand was tracked with a motion controller that allowed the projection of a virtual hand at the same position of the participant's own hand (Figure 7.1, *Experiment 7.2*). Between each block of Experiment 7.2, participants played a simple game requiring them to hit target balloons with their virtual hand, since the simultaneous movement of virtual and real body parts has been shown to enhance embodiment (Banakou et al., 2013; Peck et al., 2013).

Experimental design

In Experiment 7.1, participants sat facing a virtual tower (Figure 7.1, *Experiment 7.1*). They were instructed to keep their gaze fixed on the top of the tower, with the forearms resting on their legs. Somatosensory stimuli were delivered to the right hand, with an inter-stimulus interval of approximately 30 s. Approximately 10 s before stimulus onset participants were verbally instructed to place and hold their hand in one of the following three positions. In the 'Near' position, the forearm was at ~75 degrees with respect to the arm (with the wrist ~ 4 cm from the face, on the midline). In the 'Middle' position, the forearm was at ~90 degrees with respect to the arm. In the 'Far' position, the forearm was extended at ~180 degrees with respect to the arm. In all positions, the hand was aligned between the eyes and the top of the tower. After each stimulus, participants returned to the resting position, with the forearm resting on the thigh. 72 somatosensory stimuli were delivered in three separate blocks. Thus, 8 stimuli were delivered at each hand position in each block. In half of the trials, a cluster of arrows was launched towards the participant's face from the tower in front of them. In the remaining half of the trials, somatosensory stimuli were delivered without arrows. The order of hand positions and the presence of arrows were pseudorandomised so that no condition occurred more than twice in a row.

In Experiment 7.2, participants faced three equidistant virtual towers: one on the midline and the other two on the right and left sides, at approximately 33 degrees from the midline. Twenty-four somatosensory stimuli were delivered to each hand, in 8 separate blocks; in half of the blocks, somatosensory stimuli were delivered to the left hand and in the other half they were delivered to the right hand. Each trial started with a visual instruction to keep the gaze on the middle tower. In a third of trials, no arrows were launched (condition 'No Arrows'). In the remaining two-thirds of the trials, a cluster of arrows was launched towards the participant's face: in half of *these* trials, arrows were launched from the tower ipsilateral to the stimulated hand (condition 'Congruent'); in the remaining half, arrows were launched from the tower *contralateral* to the stimulated hand (condition 'Incongruent'). The order of these three conditions was pseudorandomised, with the constraint that no condition occurred more than twice in a row. In each trial with arrows, participants were informed of the source of the arrows by a visual cue displayed above the corresponding tower. In contrast to Experiment 7.1, the stimulated hand was always kept in the same position: the left hand was aligned between the eyes and the left tower, and the right hand was aligned between the eyes and the right tower. The forearm was kept between ~100 and 130 degrees with respect to the arm. The hand position was adjusted for each individual participant to make sure that (1) the arrows presented in the congruent condition made contact with the hand, while (2) the arrows presented in the incongruent condition did not.

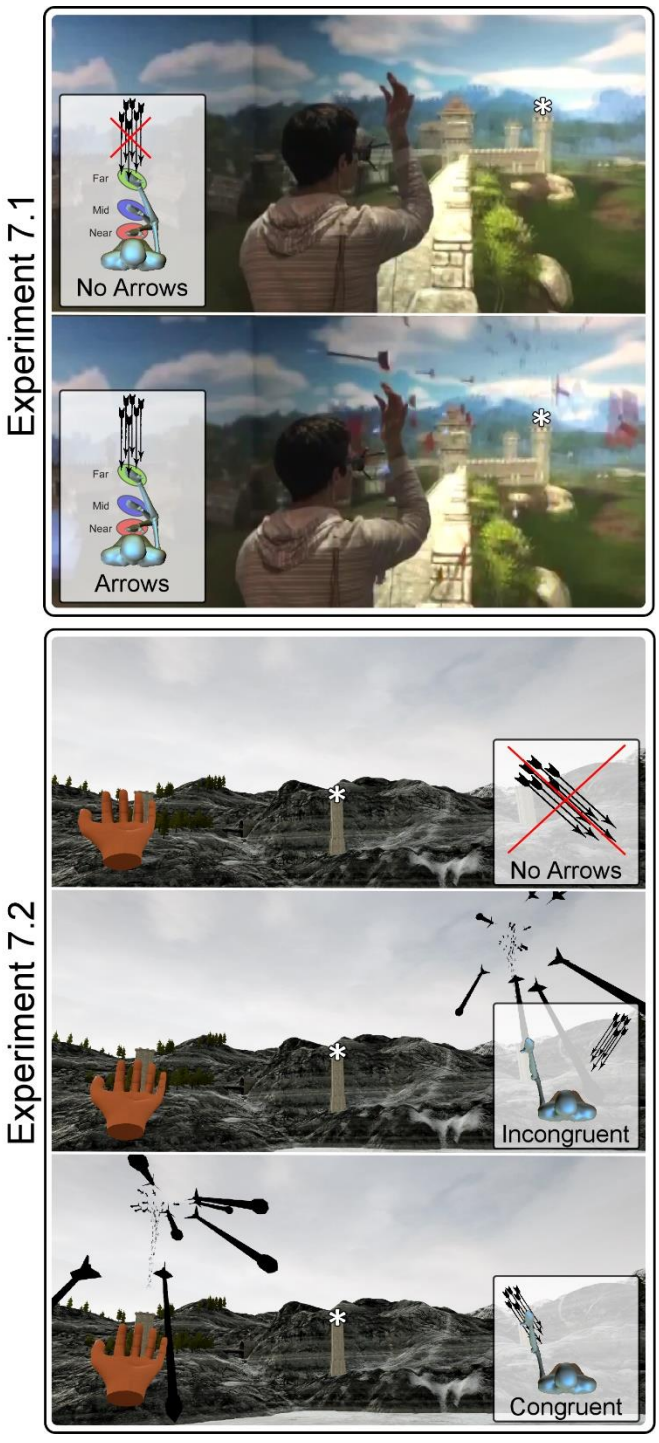

Figure 7.1. Virtual Reality environments and experimental conditions for Experiment 7.1 and Experiment 7.2.

Each image shows the virtual environment during one experimental condition. Asterisks indicate the fixation points. Insets show top-down schematic views of the experimental conditions.

Experiment 7.1. The CAVE virtual reality system is shown with a participant holding their hand in the Middle hand position with either no arrows (top image) or arrows present (bottom image).

Experiment 7.2. The display of the HTC Vive headset is shown in three conditions for a block in which the left hand was stimulated. The top image shows the condition with no arrows. The middle image shows the condition with arrows that were launched from the tower on the opposite side to the stimulated hand (spatially incongruent). The bottom image shows the condition in which arrows were launched on the side of the stimulated hand (spatially congruent).

EMG preprocessing and statistical analysis

EMG signals were pre-processed using Letswave 6 (www.letswave.org; Mouraux and Iannetti, 2008). EMG signals were first band-pass filtered between 55 and 395 Hz, notch filtered (width = 2 Hz) at each harmonic of 50 Hz from 100 Hz to 350 Hz, and full-wave rectified. Given the lack of previously-reported interactions between the factor 'eye side' (contralateral and ipsilateral to the stimulated hand) and a number of experimental manipulations (Sambo et al., 2012b), HBR responses were averaged between eyes (as in refs Sambo and Iannetti, 2013; Bufacchi et al., 2016; Wallwork et al., 2016; Bisio et al., 2017; Fossataro et al., 2018). HBR magnitude was calculated for each trial as the area under the curve (AUC; Sambo et al., 2012b). For each participant, AUC values were transformed into Z scores. These normalised AUC values were finally averaged across trials for each experimental condition. In Experiment 7.1, this procedure yielded 6 AUC average values for each participant: (1) Hand Far, No Arrows; (2) Hand Far, Arrows; (3) Hand Middle, No Arrows; (4) Hand Middle, Arrows; (5) Hand Near, No Arrows; (6) Hand Near, Arrows. In Experiment 7.2, this procedure yielded 3 AUC average values for each participant: (1) Arrows, Congruent; (2) Arrows, Incongruent; (3) No Arrows. Given that HBR responses elicited by left and right hand stimulation are no different, in Experiment 7.2 I merged the results from both hands together (as in Sambo et al., 2012b).

In Experiment 7.1, I performed a two-way, repeated-measures ANOVA with the within-subject experimental factors '*Hand Position'* (three levels: Near, Middle, Far) and '*Arrows'* (two levels: Yes, No). In Experiment 7.2, I performed a one-way, repeated-measures ANOVA with the within-subject experimental factor '*Arrows'* (three levels: No Arrows, Arrows-Incongruent, Arrows-Congruent). P values were corrected for violations of the sphericity assumption (Greenhouse-

Geisser correction; P_{GG}). Significant main effects and interactions were followed up with *post-hoc* t tests. Effect sizes were calculated as Cohen's d (Cohen, 1988).

Geometric modelling

I also performed a geometric modelling analysis, which assumed that when a shock occurs at the wrist, the brain makes an assessment of the probability that the possible threat represented by the shock might interact with - and thus damage - the face (Bufacchi et al., 2016). This probability, i.e. the estimated hit-probability of the *stimulus* eliciting the HBR (not of the arrows) is affected by the estimated directions in which the threat might move: if the threat is more likely to move towards the face, the HBR in response to that threat will be stronger. I postulated two nested models. In the first model, the possible directions in which the threat represented by the somatosensory stimulus might move were *not* affected by the movement of the arrows. In the second model, the possible directions of the threat *were* affected by the arrows: the movement bias of the threat represented by the shock on the wrist was altered in the same direction as the arrows were moving. The strength of the bias postulated by the second model was varied in order to find the best fit between the model and the HBR magnitude (Bufacchi et al., 2016; Bufacchi and Iannetti, 2016). A small baseline bias towards the face, regardless of the presence and the trajectory of the arrows, was also assumed in both models.

Goodness of fit testing allowed me to assess whether each geometric model fit the data or had to be rejected. For this analysis, the data must be normally distributed and have equal variance. To satisfy these conditions, I calculated the Z-scores of the power-transformed AUCs, as described in more detail elsewhere (Bufacchi et al., 2016). After these transformations, data from Experiment 7.1 was normally distributed ($p = 0.207$; Anderson-Darling test) and had equal variance across all conditions ($p = 0.313$; Bartlett's test). However, data from Experiment 7.2 did not have equal variance ($p = 0.0314$; Bartlett's test), and thus goodness of fit testing could not be performed on that data. As such, the parameter fitting

and initial assessment of model validity had to be performed on Experiment 7.1 first. Because the model was found to fit the data of Experiment 7.1 well (see results), I then used that fitted model to calculate the probability that the threat represented by the somatosensory stimulus hits the face for Experiment 7.2. Subsequently, I performed a linear mixed effects model to test whether these probabilities were significant predictors of the HBR magnitudes in Experiment 7.2. Thus, the linear mixed effects model predicted the trial-by-trial HBR magnitude with a fixed effect of hit probability and a random effect of participant number.

7.3 Results

Experiment 7.1 – Fast-moving and threatening objects modulate the proximity-dependent enhancement of the hand-blink reflex

Results are shown on Figure 7.2 (*top-left panel*). To investigate the possible effect of the fast-moving arrows on the proximity-dependent modulation of the HBR, I performed a two-way, repeated-measures ANOVA with the within-subject experimental factors '*Hand Position'* (three levels: Near, Middle, Far) and '*Arrows'* (two levels: Yes, No). There was strong evidence for a main effect of the factor '*Hand Position'* on HBR magnitude ($F = 7.69$; $P_{GG} = 0.00194$), and no evidence for a main effect of the factor '*Arrows'* ($F = 2.17$; $P_{GG} = 0.157$). Importantly, there was evidence for an interaction between the two factors ($F = 6.02$; $P_{GG} = 0.00813$; all ANOVA results are summarised in Table 7.1). Post-hoc t tests revealed that the source of the interaction was (1) a larger HBR in the 'Middle' position when arrows were fired than when no arrows were fired, while this was not the case in the 'Near' and 'Far' positions, and (2) the lack of an effect of hand-position when arrows were fired, while there was a strong effect of hand-position when no arrows were fired (results of post-hoc tests are detailed in Table 7.2). These results indicate that the shape of the proximity-response function of the HBR changed, suggesting a more gradual fall-off of the *action relevance field* when arrows were fired.

Table 7.1 - Experiments 7.1 & 7.2 - Summary of ANOVA results

	F	P_{GG}
Experiment 7.1		
Main effect of 'Hand Position'	**7.69**	**0.00194**
Main effect of 'Arrows'	2.17	0.15700
Interaction	**6.02**	**0.00813**
Experiment 7.2		
Effect of 'Arrows'	**4.91**	**0.02370**

Table 7.2 - Experiment 7.1 - Summary of post-hoc tests

p values

		No Arrows			**Arrows**		
		near	mid	far	near	mid	far
No Arrows	near	N/A					
	mid	**7.2e-5**	N/A				
	far	**0.001**	0.750	N/A			
Arrows	near	0.759	**0.005**	**0.012**	N/A		
	mid	0.977	**0.040**	0.063	0.512	N/A	
	far	0.774	0.078	0.112	0.120	0.528	N/A

t values

		No Arrows			**Arrows**		
		near	mid	far	near	mid	far
No Arrows	near	N/A					
	mid	**-5.045**	N/A				
	far	**-3.727**	0.324	N/A			
Arrows	near	0.311	**3.193**	**2.775**	N/A		
	mid	-0.029	**2.199**	1.975	-0.668	N/A	
	far	-0.291	1.864	1.665	-1.629	-0.642	N/A

d values

		No Arrows			**Arrows**		
		near	mid	far	near	mid	far
No Arrows	near	N/A					
	mid	**-1.128**	N/A				
	far	**-0.833**	N/A	N/A			
Arrows	near	N/A	**0.714**	**0.621**	N/A		
	mid	N/A	**0.492**	N/A	N/A	N/A	
	far	N/A	N/A	N/A	N/A	N/A	N/A

Experiment 7.2 – The effect of fast-moving objects on the hand-blink reflex is spatially tuned towards the source of the objects

Results are shown on Figure 7.2 (*top-right panel*). To investigate whether the change in shape of the HBR proximity response function observed in Experiment 7.1 was sensitive to the trajectory of the arrows, I performed a one-way, repeated-measures ANOVA with the experimental factor '*Arrows'* (three levels: No Arrows, Arrows-Incongruent, Arrows-Congruent). This analysis showed evidence of a difference between experimental conditions ($F = 4.91$, $P_{GG} = 0.0237$; Table 7.1). Post-hoc t tests revealed that the source of this difference was a larger HBR in trials with arrows that were spatially congruent to the stimulated hand, compared to (1) trials with no arrows and (2) trials with arrows that were spatially incongruent. By comparison, there was no difference between trials with spatially incongruent arrows and trials without arrows. Results of post-hoc tests are detailed in Table 7.3.

Table 7.3 - Experiment 7.2 - Summary of post-hoc tests

			t values	*p values*	*d values*
Arrows Congruent	vs	No Arrows	**2.27**	**0.0352**	**0.507**
Arrows Congruent	vs	Arrows Incongruent	**3.36**	**0.0033**	**0.751**
Arrows Incongruent	vs	No Arrows	0.377	0.7110	N/A

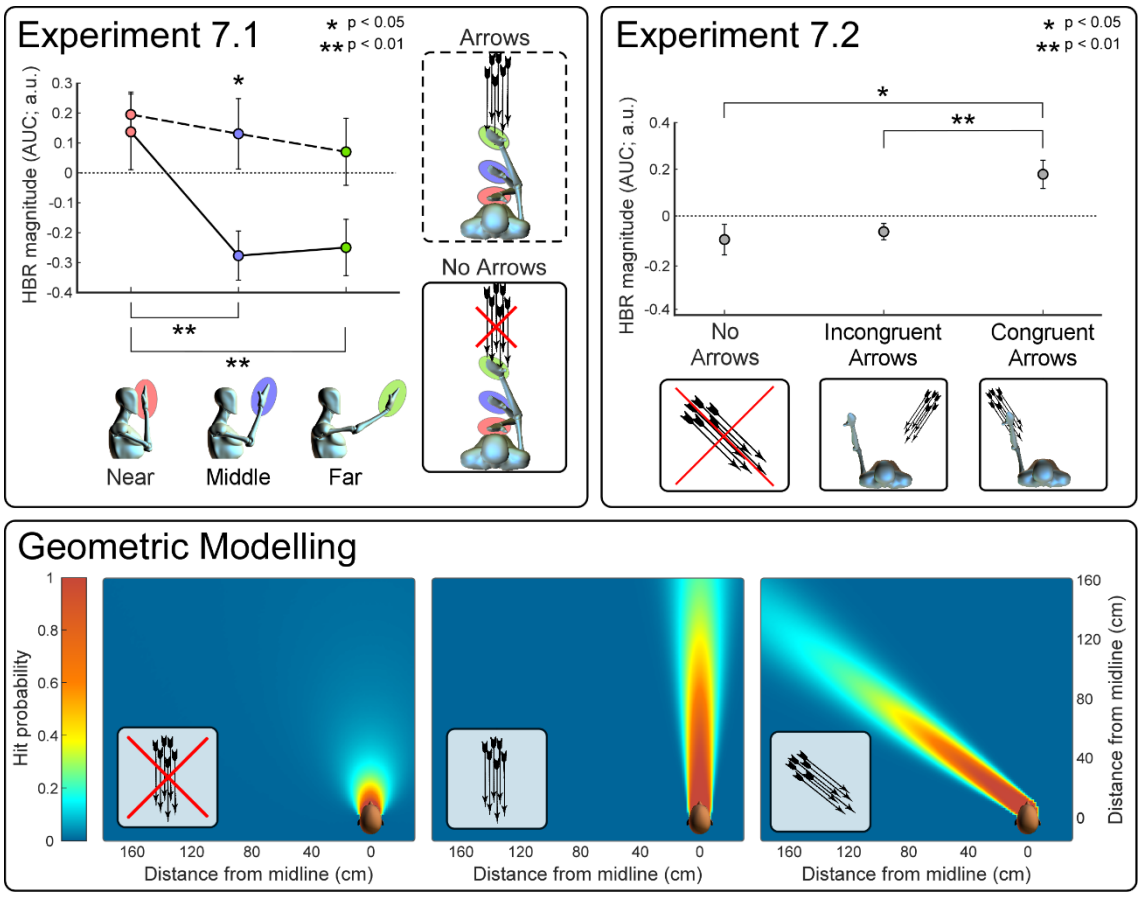

Figure 7.2. Experimental results and model-fitting.
Asterisks show significant comparisons between conditions (post-hoc t tests). Error bars show SEM for each condition. *Top-left panel: Experiment 7.1.* Mean HBR magnitude (area under the curve; AUC) across all participants for each condition of Experiment 7.1. The solid line shows the proximity response function with no arrows present, while the dashed line shows the response function with arrows present. The shape of this function changed when arrows were fired, suggesting a more gradual fall-off. The HBR was larger when arrows were fired in the Middle hand position than when no arrows were fired. Differences between hand positions were found only when arrows were not fired. *Top-right panel: Experiment 7.2*. Mean HBR magnitude (AUC) across all participants for each condition of Experiment 7.2. The HBR was larger when spatially congruent arrows were present compared to when there were incongruent arrows or no arrows. There was no difference between the HBR magnitude when incongruent arrows were fired and when no arrows were fired. *Bottom panel: The best-fitting geometric model.* Hit probability predicted by the best fitting model is shown in three conditions: with no arrows present (left), with arrows flying from the forward direction, as in Experiment 7.1 (middle) and with arrows flying from the forward-left direction, as in Experiment 7.2 (right). When arrows are present, the area of high hit probability expands in a direction corresponding to the trajectory of the arrows.

Geometric modelling

The geometric model of the HBR *action relevance field* assumed that when a shock occurs at the wrist, the brain assesses the probability that the possible threat - represented by this shock - might contact and thus damage the face. This probability is affected by the estimated directions in which the threat might move. The model in which these estimated directions were *not* affected by the movement of the arrows was clearly rejected by the goodness of fit testing on the data from Experiment 7.1 (GoF $p = 0.00195$[10]). In contrast, the model in which these directions *were* affected by movement of the arrows fit the data from Experiment 7.1 well (GoF $p = 0.382$[11]).

The linear mixed effects model on the data from Experiment 7.2 showed that that the geometric model that fit the data well in Experiment 7.1 was also a significant predictor of HBR magnitude in Experiment 7.2 ($p = 0.00216$[12]). Thus, these modelling results provide support for the notion that movements of environmental objects (separate from those eliciting the defensive reflex) can affect the brain's assessment of the relevance of defensive actions, by influencing the predicted probability of contact with the face.

[10] Note that for this type of test, $p < 0.05$ indicates that the model is rejected.

[11] Note that $p > 0.05$ indicates that the model is accepted.

[12] Note that p values for this type of test should be interpreted the usual way.

7.4 Discussion

In Experiment 7.1 I found that when arrows were being fired towards the participant, the stimulus proximity-response function of the HBR changed such that the region within which HBR magnitude was enhanced expanded (Figure 7.2). Importantly, the differences in HBR amplitude between the '*Arrows'* and '*No Arrows'* conditions were not equal at each of the three hand positions and were maximal in the Middle position. Thus, the effect was not a simple overall increase in HBR magnitude when arrows were fired, but a specific distance-dependent modulation. This can be interpreted as a spatially-tuned alteration of the *action relevance field* due to the environmental context (Figure 7.2, *Geometric Modelling*).

Movement of environmental objects unrelated to the stimulus modulate the defensive blink reflex

This observation is, to the best of my knowledge, the only instance of an *action relevance field* being modulated by movement of environmental objects separate from the stimulus eliciting the behavioural response[13]. Considering the results of Noel et al. (Noel et al., 2015) is relevant: they first characterised the spatial properties of an *action relevance field*[14] for rapid reactions to somatosensory stimuli while auditory stimuli moved towards participants (measured by reaction time[15]). They then observed that this field was modulated by walking: the proximity-dependent fall-off of reaction times was more gradual when participants

[13] Note that I refer here also to the PPS literature.

[14] Note that Noel et al used the PPS framework to interpret their results.

[15] In this paradigm, reaction times in response to the somatosensory stimuli are enhanced by proximity of the auditory stimuli.

were walking forward while they were exposed to the optic flow consistent with their forward motion, suggesting an expansion of the zone in which the reaction times were enhanced. However, this finding was not due to the visual stimulation, as in a crucial control experiment they observed a similar expansion when participants were walking on a treadmill but without the optic flow consistent with their forward motion (Noel et al., 2015). Thus, the present result seems to be the first evidence that the movement of environmental *visual* stimuli separate to the stimulus is capable of modulating an *action relevance field*.

The modulation of defensive blink reflex is spatially-tuned in the direction of the threatening environmental object

From Experiment 7.1 alone it is unclear whether the modulation of the *action relevance field* is stereotyped, or sensitive to the trajectory of the moving objects; Experiment 7.1 could not distinguish between omnidirectional expansion[16] (i.e. occurring in all directions), stereotyped unidirectional expansion (e.g. occurring only in front of the participant), or an expansion occurring only in the direction of the stimulus (i.e. only towards the source of the arrows). Therefore, in Experiment 7.2 I compared the effect of arrows with different trajectories. I observed that the HBR magnitude was increased only when the arrows' trajectory was congruent to the stimulated hand, while the HBR magnitude was not modulated at all when the arrows' trajectory was incongruent to the hand (Figure 7.2, *Experiment 7.2*). These results provide strong evidence that the modulation of the *action relevance field* of the HBR was tuned to the direction of the source of the arrows.

[16] I.e. expansion of the zone in which the HBR magnitude was enhanced.

Thus, the present result shows that the nervous system can intelligently respond to the specific dynamics of moving environmental objects. This is another example of a high-level factor, presumably occurring at neocortical level, modulating the HBR circuitry at brainstem level. Other examples include the probability of occurrence of the reflex-eliciting stimulus, the estimated protective value of objects, and the effects of gravity (Sambo et al., 2012a; Bufacchi and Iannetti, 2016). In all, these factors point towards a remarkably sophisticated mechanism which continuously adjusts the strength of motor defensive responses according to their relevance in context (Bufacchi and Iannetti, 2018), using information from multiple sensory modalities: proprioceptive (eye-hand proximity; Sambo et al., 2012b), vestibular (gravitational cues; Bufacchi and Iannetti, 2016) and visual (moving arrows).

These modulations can be explained by a geometric model of hit-probability

Our group has previously supplied evidence that this mechanism involves estimating the probability that threats will interact with, and thus damage, the face. In several studies, we have shown that HBR results fit such a geometric model well, under a variety of hand positions and postural manipulations (Bufacchi et al., 2016; Bufacchi and Iannetti, 2016). Here, I confirm that this model is sufficient to explain the observed changes in the *action relevance field* of the HBR, and add that it can also explain its directionally-tuned modulation (Figure 7.2, *Geometric Modelling*). Indeed, in the model that fit the data of both Experiments 7.1 and 7.2, the presence of environmental moving objects (i.e. the arrows) biased the probability that the threat would hit the face. This model can therefore explain both the change in shape of the proximity-dependent function observed in Experiment 7.1, as well as the spatial congruence effect observed in Experiment 7.2. In Experiment 7.1, the increased bias towards the face altered the hit probability differently depending on the position of the hand, and hence increased the relevance of the HBR differently. In Experiment 7.2, when arrows

were congruent to the stimulated hand, an increased bias in the direction of the arrows' trajectory (i.e. towards the face) increased the estimates of hit probability, and hence increased the relevance of the HBR (Figure 7.2, *Geometric Modelling*). However, when the arrows' direction was incongruent the bias did not point towards the face, and thus did not increase the estimates of hit probability.

Kinematics or semantic value?

The present results reflect a clear directionally-tuned effect of arrows on the shape of the *action relevance field* of the HBR (Figure 7.2, *Geometric Modelling*). But is this effect due to the fact that arrows are inherently threatening objects? Other *action relevance fields* are clearly affected by the semantic content of stimuli (Taffou and Viaud-Delmon, 2014; Ferri et al., 2015). Alternatively, is the present effect caused by the arrows' speed? Or by their size and shape? Indeed, we already know that non-movement related factors such as trigeminal neuralgia (a condition in which innocuous trigeminal stimulation triggers paroxysmal facial pain) can affect HBR response fields (Bufacchi et al., 2017). As I was interested specifically in the effect of the *trajectory* of environmental objects, this experiment was not designed to investigate the contribution of other object features such as their semantics, speed, size and shape. I therefore have no relevant data to directly address this point. However, the congruence effect observed in Experiment 7.2 did show that the movement trajectory of environmental objects was crucial to the expansion. Particularly, there was no such expansion in trials in which the arrows followed a trajectory that did not pass through the stimulated hand when compared to the trials without arrows (Figure 7.2, *Geometric Modelling*). Thus, it is unlikely that the shape or semantic information *alone* could have caused the observed effect; at most they were necessary but not sufficient causes. For example, it may be the case that arrows need to fly at a minimum speed to produce this effect, or that the looming object must be perceived as threatening (as in de Haan et al., 2016). Therefore, whether the effect I observed was only consequent to the movement trajectory, and that any object being fired

towards the participants would modulate the HBR *action relevance field* in the same fashion remains an open question to be addressed in future studies.

Neural substrates

Several cortical areas in the primate brain have response profiles that could underlie the previously-described proximity-response relationship of the HBR (Sambo et al., 2012b; Bufacchi et al., 2016; Bufacchi, 2017), as well as the additional directionally-sensitive modulation I report here. These include the ventral intraparietal area (VIP) and the polysensory zone of F4, which both contain bimodal neurons that respond to (1) tactile stimuli within a tactile receptive field, and (2) visual stimuli presented in a receptive field anchored to the tactile receptive field. Furthermore, many of these neurons are sensitive to combinations of joint angles and manipulations (Hyvarinen and Poranen, 1974; Colby et al., 1993; Fogassi et al., 1996; Graziano et al., 1997; Duhamel et al., 1998). Additionally, neurons in these areas are sensitive to stimulus motion: for example, VIP neurons have a high degree of selectivity for the direction of stimulus movement and are also selective for stimulus speed (Colby et al., 1993), while many neurons in F4 have a visual receptive field that expands with the velocity of approaching stimuli (Fogassi et al., 1996). These areas also receive inputs from the superior colliculus and pulvinar (Makin et al., 2012), both of which respond to looming stimuli and are involved in time-to-impact judgements (Billington et al., 1998). We could therefore imagine a population of neurons with tactile receptive fields on the face, and visual receptive fields extending away from the face. The visual receptive field properties of such neurons could enact the movement sensitivity of the brainstem circuit subserving the HBR, while the joint-angle sensitivity of these neurons could enact the hand-position dependent manipulation of HBR magnitude. In contrast, the fact that the HBR modulation due to arrows is not equal at all hand positions (Figure 7.2, *Experiment 7.1*) rules out the possibility that it was enacted by a multisensory neuron with a tactile receptive field on the wrist and a visual receptive field surrounding it: if this were

the case, the HBR modulation should have been equal at all hand positions. In Chapter 6, the correlations between HBR and VP suggested there may be an overlap between the neurones top-down modulating the HBR and neural generators of the VP; the frontal/parietal cortical regions mentioned above could contain these neurones.

Conclusion

In conclusion, the *action relevance field* derived from the HBR magnitude is sensitive to the ongoing movement and trajectory of other objects in the environment. This result, in conjunction with previous findings that this field is affected by gravitational cues (Bufacchi and Iannetti, 2016) and physical barriers in the environment (Sambo et al., 2012a), shows that the HBR relevance is not only determined by properties of the stimulus triggering the HBR, but also to the environmental context. These results support a view that the proximity response function derived from a certain behavioural response reflects the contextual relevance of that action (Bufacchi and Iannetti, 2018). This relevance, which is partially determined by the probability that an object will make contact with the body, is therefore informed not only by the properties of the triggering stimulus, but also by the features of the environmental context which are relevant to impact prediction.

8 General Discussion

8.1 Summary of results

In this thesis, I presented a series of experiments investigating sudden sensory events, the EEG responses they elicit, and their relationship to behaviour.

In Chapter 4, I showed that, in both humans and rats, the VP elicited by abrupt increases of sensory intensity embedded within an ongoing sensory stimulus (i.e. stimulus *onsets*) is highly sensitive to the magnitude of those increases of intensity (i.e. differential intensity), but insensitive to the absolute level of stimulus intensity. This result was found for the VPs elicited by both auditory and somatosensory stimuli, showing the supramodal nature of this sensitivity to large sensory differentials. These results demonstrate that the VP is sensitive to environmental changes which are more surprising, at several hierarchical levels and timescales. I also showed that these *onsets* elicit the same supramodal Vertex Potential (VP) as the more commonly used impulse stimuli.

In Chapter 5, I showed that abrupt decreases of sensory intensity embedded within an ongoing sensory stimulus (i.e. stimulus *offsets*) also elicit VPs sharing a great deal of morphological and functional properties with the VPs elicited by stimulus *onsets* and impulse stimuli: besides having similar scalp distribution, they are largely comprised of supramodal neural activity, whose magnitude rapidly habituates when those *offsets* are repeated at short and predictable latency (i.e. when the surprise or *behavioural-relevance* of those *offsets* is reduced). Additionally, *offsets* elicited a similar modulation of motor output as the stimulus *onsets* and impulse stimuli, providing more evidence of a link between the VP and behaviour.

In Chapter 6, I studied this link with behaviour more directly, by recording both the VP and hand-blink reflex (HBR) elicited by sudden and intense stimulation of the wrist. I showed that the HBR was highly correlated with the VP, but (importantly) was not correlated with the earlier and somatosensory-specific N1 wave, indicating a tight link between the supramodal component of the cortical response to sudden stimuli, and a clearly defensive behaviour.

In Chapter 7, I showed that the subcortical circuits generating this defensive behaviour (the HBR) are top-down modulated by cortical activity which reflects the dynamics of environmental objects. Specifically, I found that HBR magnitude is sensitive to the movement of threatening environmental objects which affect the behavioural-relevance of the stimulus eliciting the reflex

This thesis therefore supports and expands upon previous work by showing that (1) both the brain responses and behaviours elicited by sudden sensory events are sensitive to several environmental features which determine the behavioural-relevance of those events (Chapters 4, 5 and 7) and (2) the Vertex Potential is selectively related to an urgent and defensive behaviour elicited by sudden sensory events (i.e. the HBR; Chapter 6), Altogether, these findings demonstrate that sudden changes of sensory input activate a widespread, supramodal brain network, functioning in parallel with the sensory-specific systems. This supramodal network is highly sensitive to the surprise content, and therefore the behavioural-relevance, of the sudden environmental changes which activate it, and has a tight relationship with the motor system and behaviour.

In the following sections I first outline a promising account of the underlying neural basis of the Vertex Potential. I then explore the functional implications of this perspective. Finally, I detail a future research direction which I plan to undertake following the PhD to build on this work.

8.2 The extralemniscal system: a likely neural substrate for the Vertex Potential

As discussed in the Chapter 3 (*General Introduction*), researchers recording the VP often assume that it reflects sensory processing specific to the modality used to elicit the response (e.g. Hegerl et al., 1994; Martin and Boothroyd, 1999, 2000; Shahin et al., 2003; Baumann et al., 2008; Valeriani et al., 2008; Carpenter and Shahin, 2013; Baltzell and Billings, 2014; Krahé et al., 2014; Staikou et al., 2016; Wagner et al., 2016; Paloyelis et al., 2016; Uglem et al., 2017; Squintani et al., 2018; Hird et al., 2018; Zhang et al., 2021). However, this account is not tenable when considering evidence from this thesis or from previous work. Here, I discuss this evidence and propose a promising alternative account of the neural basis of the VP. To do so, it is necessary to first detail some background information about sensory pathways in the brain.

In virtually all sensory modalities, information about the environment is relayed by two main sensory pathways. *Lemniscal* pathways convey high-fidelity information in a given sensory modality to the corresponding sensory cortex via *core* cells found in *modality-specific* thalamic nuclei, such as the dorsal lateral geniculate nucleus in the visual modality (Jones, 1998, 2001; Hu, 2003; Clascá et al., 2012; Bellesi et al., 2014). Conversely, *extralemniscal* pathways convey low-fidelity information from multiple sensory modalities to diffuse cortical targets, via *matrix* cells found throughout the thalamus, although most prominently in the nuclei traditionally labelled *non-specific*[17], such as the nuclei of the intralaminar group (Jones, 1998, 2001; Hu, 2003; Clascá et al., 2012; Bellesi et al., 2014).

[17] Note that the term “non-specific” has gone out of fashion recently, due to the implication that all of these nuclei are homogenous and have the same “non-specific” function (Bentivoglio et al., 1991). However, I use the term here to distinguish these nuclei from the *modality*-specific relay nuclei.

This distinction appears to be neglected when researchers assume that the VP reflects modality-specific processing: in effect they only consider the lemniscal system. An alternative perspective is that the VP reflects the cortical consequences of the activation of the extralemniscal system. Although this was once a popular view (e.g. Jasper, 1960; Lindsley, 1969; Fruhstorfer, 1971; reviewed in Näätänen and Picton, 1987), it has since been mostly forgotten and replaced with a solely lemniscal interpretation (e.g. in the refs listed at the start of this section). However, several lines of evidence from this thesis and the more recent literature support the extralemniscal account:

1) Sensitivity to sudden environmental changes

Several results suggest that, like the VP, the extralemniscal system is sensitive to sudden environmental changes. Firstly, non-specific thalamic responses can only be elicited by sufficiently sudden stimuli, while specific responses can be activated by a range of stimuli, including stimuli which are not sudden (Albe-Fessard and Kruger, 1962; Albe-Fessard and Besson, 1973; Peschanski et al., 1981). For example, neurones in the (non-specific) Centromedian–Parafascicular Complex (CM-Pf) are activated by sharply applied pinprick on the skin, but not by slowly applied pressure, light touch or hair bending (Albe-Fessard and Kruger, 1962; Peschanski et al., 1981). Similarly, the sensitivity of the VP to differential (but not absolute) intensity found in Chapter 4, together with the well-established importance of stimulus rise-time (Onishi and Davis, 1968), indicate that the VP is primarily sensitive to the *rate of intensity change* (i.e. the first derivative of intensity over time) or, in other words, the *suddenness* of the change. Indeed, personal experience suggests that only sufficiently sudden stimuli will effectively elicit a VP. Secondly, the extralemniscal system is less sensitive to repetitive and unchanging stimulation: non-specific responses will rapidly habituate when identical stimuli are repeated at short-latency (Peschanski et al., 1981; Calford and Aitkin, 1983; Bordi and LeDoux, 1994; Edeline et al., 1999; Anderson et al., 2009), similar to the habituation of the VP seen in Experiment 5.3 and previous work (Ritter et al., 1968; Chapman et al., 1981; Woods et al., 1984; Treede et al.,

2003; Iannetti et al., 2008; Wang et al., 2010; Herrmann et al., 2015). Conversely, the lemniscal system is more resistant to stimulus repetition, and neurones in specific thalamic nuclei can reliably respond to stimuli which are repeated as fast as 10 Hz (Albe-Fessard and Besson, 1973). Thirdly, when a change is introduced in the sequence of stimuli, the habituation of non-specific responses can be reversed; for example, if the stimulus location (Peschanski et al., 1981; Calford and Aitkin, 1983) or auditory tone frequency (Kraus et al., 1994) are changed. The habituation of the VP can also be reversed by changing certain stimulus features, for example by displacing the stimulus in body-centric coordinates (Moayedi et al., 2016), changing the auditory tone frequency (Herrmann et al., 2015), or changing the stimulus modality (Valentini et al., 2011).

2) Supramodality

An important property of the extralemniscal system is supramodality (Albe-Fessard and Besson, 1973; Jones, 1998, 2001; Bellesi et al., 2014): electrophysiological responses from non-specific thalamic neurones can be elicited by stimuli of several modalities (Guilbaud, 1968; Albe-Fessard and Besson, 1973; Peschanski et al., 1981; Komura et al., 2005). Unlike their lemniscal counterparts, which project only to middle layers of modality-specific cortical areas (such as primary sensory cortices), these non-specific neurones project widely across the cortex, to superficial layers of areas such as anterior cingulate cortex (Hsu and Shyu, 1997), superior frontal gyrus (Amassian, 1954), inferior parietal lobule (Geschwind, 1965), secondary somatosensory cortex (S2), insular cortex, medial premotor cortex and primary motor cortex (reviewed in Albe-Fessard and Besson, 1973). Considering the above we would expect activation of these two systems to elicit distinct cortical responses: (1) a large widespread response corresponding to the diffuse projections of the non-specific system (which would be the same regardless of modality) and (2) a smaller localised response reflecting activation of the sensory cortex specific to the eliciting sensory modality. Accordingly, the responses elicited by stimuli of different modalities are dominated by the same widespread, supramodal Vertex

Potential, with local modality-specific subcomponents contributing much less to the response (Chapter 5; see also Chapter 3; Mouraux and Iannetti, 2009; Liang et al., 2010; Valentini et al., 2012). Interestingly, the latencies of the modality-specific subcomponents (e.g. the somatosensory N1 and P4 waves) correlate with each other (trial-by-trial), but not with the vertex N and P waves (and vice versa; Hu et al., 2014b), providing further evidence that the two subcomponents reflect distinct, parallel systems. Source modelling of the supramodal subcomponent identifies regions which overlap somewhat with the non-specific cortical regions, including S2, anterior cingulate and insular cortex (Garcia-Larrea et al., 2003; Mouraux and Iannetti, 2009), although given the difficulty associated with source analysis of widespread EEG responses (Grech et al., 2008), these results should be taken lightly.

3) Direct and interventional evidence from pharmacological and anatomical lesions

The similarities outlined so far suggest that the widespread cortical activation of the VP is consequent to the activation of non-specific thalamic neurones with diffuse cortical projections. However, the most compelling and direct evidence for this hypothesis comes from the use of general anaesthetics: unlike the lemniscal system, responses of the extralemniscal system are selectively abolished by most general anaesthetics (Albe-Fessard and Besson, 1973). This property makes these drugs a powerful tool to dissociate the activity of the two systems. Indeed, a crucial interventional study recording the electrocortical activity in rats demonstrated that the VP elicited by abrupt auditory stimuli was abolished by the general anaesthetic pentobarbital, but was largely unaffected by a bilateral ablation of the primary auditory cortex, while the modality-specific lateralised response was abolished by this lesion but mostly unaffected by the anaesthetic (Simpson and Knight, 1993). These results indicate that the extralemniscal pathways, but not the traditional lemniscal pathways, are necessary for the generation of the VP response. Some similar results have been found in humans, with VPs being abolished by propofol (Simpson et al., 2002), midazolam

(Zaslansky et al., 1996) and nitrous oxide (Jessop et al., 1991), but mostly unaffected when elicited by auditory stimuli in patients with lesions of auditory cortex (Woods et al., 1984, 1987), while the VP *was* abolished in two patients whose lesions extended upward to the inferior parietal lobule (Woods et al., 1987), which receives input from non-specific thalamic nuclei (Geschwind, 1965). However, other studies gave contradictory results (reviewed in Naatanen et al., 1987), and due to the uncertainty of the extent of damage in brain-damaged patients, results from such studies should be taken somewhat lightly.

8.3 The extralemniscal system: functional implications

If this hypothesis is true, what are the implications for the functions of the neural activity underlying the VP? Traditionally, the extralemniscal pathways have been described as a non-specific activating system, capable of producing global arousal of the brain (Van Der Werf et al., 2002). Several lines of evidence contributed to this perspective. Firstly, there is a lot of anatomical overlap between extralemniscal pathways and central arousal systems (Bellesi et al., 2014): the non-specific intralaminar and midline nuclei are considered part of the 'ascending reticular activating system' due to their extensive brainstem input (Van Der Werf et al., 2002), which includes monoaminergic inputs such as noradrenergic locus coeruleus fibres and cholinergic pontine projections (French, 1953; Hu, 2003; Jones, 2003; Bellesi et al., 2014). Secondly, functional evidence comes from the observation that low-frequency electrical stimulation of these nuclei causes slow-wave activity across the cortex (similar to that found in deep sleep) as well as somnolence, while stimulation at high-frequencies causes desynchronised cortical activity and arousal (Hunter and Jasper, 1949; Jasper, 1949). Thirdly, behavioural studies have shown that these nuclei produce cortical activations which lead to alert and attentive brain states, allowing faster and more efficient processing of incoming stimuli (reviewed in Van Der Werf et al., 2002). For example, the activity of medial thalamus (measured by positron emission tomography) correlated with levels of vigilance during a task in which participants

had to react to sudden and unexpected *offsets* of stimulus intensity (Paus et al., 1997).

It is important to note that there is probably no single function which can be ascribed to this system. Indeed, the various non-specific thalamic nuclei are not identical, but appear to perform several distinct functions which fall broadly into the domain of arousal and awareness (Bentivoglio et al., 1991; Groenewegen and Berendse, 1994; Van Der Werf et al., 2002). Van Der Werf et al. (2002) divide them into four groups: (1) a *posterior group* involved in the generation of motor responses following awareness of surprising stimuli, (2) a *dorsal group* involved in viscerosensory awareness and motivated arousal, (3) a *lateral group* involved in cognitive awareness and executive function, and (4) a *ventral group* involved in polymodal sensory awareness. These functions are fairly consistent with the hypothesis that the VP reflects a widespread modulation of brain systems, which allows the organism to rapidly react to potentially threatening or rewarding environmental events (Iannetti and Mouraux, 2010; Moayedi et al., 2015; Novembre et al., 2018). For example, neurons in CM-Pf (part of the *posterior group*; Van Der Werf et al., 2002) respond more to unexpected and behaviourally-relevant sensory stimuli (Matsumoto et al., 2001), similar to the sensitivity of the VP to unexpected environmental changes (Chapters 4 & 5). Indeed, a recent study recorded both the ERP (with EEG) and CM-Pf activity (with intracranial recordings) in humans and found similar modulations by deviant target stimuli in an oddball paradigm (Beck et al., 2020). The *posterior group* is also capable of affecting the motor system: lesions of the non-specific CM-Pf complex can abolish escape behaviour in cats (Mitchell and Kaelber, 1966). This result is consistent with findings that VP amplitude correlates with the magnitude of the HBR (Chapter 6) and the reaction time of defensive hand withdrawals (Moayedi et al., 2015). Indeed, these thalamic nuclei may be the common upstream element responsible for the correlation between the HBR and VP magnitudes proposed in Chapter 6. The modulations of applied force seen in Experiment 5.4 may also reflect the CM-Pf complex's actions on the motor system in response

to surprising stimuli. Furthermore, there is some evidence that the VP correlates with transient modulations of *peripheral* arousal (such as the skin conductance response), indicating a general relationship between the VP and arousal (Barry et al., 1993; Mobascher et al., 2009).

With the evidence at hand it seems likely that the VP is a consequence of the activation of the extralemniscal system, rather than the high-fidelity sensory processing of the lemniscal pathways. Given the heterogeneity of the thalamic nuclei within the extralemniscal system, the existing evidence does not clarify exactly what function the VP subserves. It does, however, provide general insights and an exciting new avenue for future research into Vertex Potential function.

8.4 Future directions: high-resolution fMRI in humans & electrophysiological recordings in rodents

The evidence discussed so far is largely consistent with the extralemniscal hypothesis. However, a detailed and systematic study using knowledge about the VP to test this hypothesis is lacking. Following my PhD, I aim to perform such a study.

Specifically, I am organising a collaboration to collect data from both humans and rodents. The human experiments will use high-resolution functional magnetic resonance imaging (fMRI) to allow the best possible distinction between different thalamic nuclei. The rodent experiments will use electrophysiological recordings and/or calcium imaging. These experiments will allow us to explore the thalamic nuclei and cortical areas constituting the lemniscal & extralemniscal systems and compare their functional properties to those of the VP. The experiments will consist of abrupt stimuli of several sensory modalities (auditory, visual and somatosensory) delivered at long interstimulus intervals (e.g. 8-12 s).

In the human experiments, supramodal thalamic nuclei will be identified using a data-driven approach in which nuclei which respond to two or more sensory

modalities will be labelled ‘non-specific’, while those only responding to one modality will be labelled ‘specific’. The identified thalamic nuclei could be compared with the nuclei associated with the extralemniscal pathways, such as the CM-Pf and other intralaminar nuclei (French, 1953; Albe-Fessard and Rougeul, 1958; Albe-Fessard and Bowsher, 1965) or those associated with the lemniscal pathways, such as the (visual) lateral geniculate nucleus, (somatosensory) ventral posterior nucleus and the (auditory) ventral medial geniculate nucleus (Hu, 2003; Clascá et al., 2012). Subsequently, the identified nuclei will be used to extract brain networks according to their functional connectivity (i.e. by correlating their activity with voxels across the cortex). Further comparisons could then be made between these networks and the VP by using more complex experimental designs, in which we vary experimental factors that are known to modulate the VP and test the effects on the fMRI activity. For example, we might expect some networks to have high sensitivity to differential (but not absolute) stimulus intensity (as in Chapter 4), a large degree of overlap in their responses to onsets and offsets of stimulus intensity (as in Chapter 5) and to rapidly habituate when stimuli are repeated at short latency (as in Chapter 5; see also Iannetti et al., 2008).

The rodent experiments will allow comparison of the fMRI results with more direct recordings of neurones in particular thalamic nuclei and cortical regions, as well as larger-scale measurements of the local field potentials and cortical potentials from ECoG (as in Chapter 4). If necessary, we could record Vertex Potentials with EEG in humans to facilitate comparisons between the other experiments.

This study will therefore allow us to (1) exploit knowledge of the functional properties of the Vertex Potential (coming from the evidence described both in this thesis and in the literature) in order to investigate its underlying networks, (2) test the specific hypothesis that the extralemniscal system is the neural substrate of the VP and (3) integrate knowledge about the identified brain regions with knowledge about the VP, in order to elucidate its function.

9 References

Albe-Fessard D, Besson JM (1973) Convergent Thalamic and Cortical Projections - The Non-Specific System. In: Somatosensory System (Iggo A, ed), pp 489–560 Handbook of Sensory Physiology. Berlin, Heidelberg: Springer Berlin Heidelberg.

Albe-Fessard D, Bowsher D (1965) Responses of monkey thalamus to somatic stimuli under chloralose anaesthesia. Electroencephalogr Clin Neurophysiol 19:1–15.

Albe-Fessard D, Kruger L (1962) Duality of unit discharges from cat centrum medianum in response to natural and electrical stimulation. J Neurophysiol 25:3–20.

Albe-Fessard D, Rougeul A (1958) Activités d'origine somesthésique évoquées sur le cortex non-spécifique du chat anesthésié au chloralose: Rôle du centre médian du thalamus. Electroencephalogr Clin Neurophysiol 10:131–152.

Amassian VE (1954) Studies on organization of a somesthetic association area, including a single unit analysis. J Neurophysiol 17:39–58.

Anderson LA, Christianson GB, Linden JF (2009) Stimulus-specific adaptation occurs in the auditory thalamus. J Neurosci 29:7359–7363.

Arendt-Nielsen L (1994) Characteristics, detection, and modulation of laser-evoked vertex potentials. Acta Anaesthesiol Scand Suppl 101:7–44.

Baltzell LS, Billings CJ (2014) Sensitivity of offset and onset cortical auditory evoked potentials to signals in noise. Clin Neurophysiol 125:370–380.

Banakou D, Groten R, Slater M (2013) Illusory ownership of a virtual child body causes overestimation of object sizes and implicit attitude changes. Proc Natl Acad Sci 110:12846–12851.

Bancaud J, Bloch V, Paillard J (1953) Contribution EEG à l'étude des potentiels évoqués chez l'homme au niveau du vertex. Rev Neurol 89:399–418.

Barry RJ, Feldmann S, Gordon E, Cocker KI, Rennie C (1993) Elicitation and habituation of the electrodermal orienting response in a short interstimulus interval paradigm. Int J Psychophysiol 15:247–253.

Baumann S, Meyer M, Jäncke L (2008) Enhancement of auditory-evoked potentials in musicians reflects an influence of expertise but not selective attention. J Cogn Neurosci 20:2238–2249.

Beck AK, Sandmann P, Dürschmid S, Schwabe K, Saryyeva A, Krauss JK (2020) Neuronal activation in the human centromedian-parafascicular complex predicts cortical responses to behaviorally significant auditory events. Neuroimage 211:116583.

Beckmann CF, Smith SM (2004) Probabilistic Independent Component Analysis for Functional Magnetic Resonance Imaging. IEEE Trans Med Imaging 23:137–152.

Bellesi M, Riedner BA, Garcia-Molina GN, Cirelli C, Tononi G (2014) Enhancement of sleep slow waves: Underlying mechanisms and practical consequences. Front Syst Neurosci 8:1–17.

Ben-David BM, Campeanu S, Tremblay KL, Alain C (2011) Auditory evoked potentials dissociate rapid perceptual learning from task repetition without learning. Psychophysiology 48:797–807.

Bentivoglio M, Balercia G, Kruger L (1991) The specificity of the nonspecific thalamus: The midline nuclei. Prog Brain Res 87:53–80.

Beydoun A, Morrow TJ, Casey KL (1997) Pain-related laser-evoked potentials in awake monkeys: Identification of components, behavioral correlates and drug effects. Pain 72:319–324.

Beydoun A, Morrow TJ, Shen JF, Casey KL (1993) Variability of laser-evoked potentials: attention, arousal and lateralized differences. Electroencephalogr Clin Neurophysiol Evoked Potentials 88:173–181.

Biggio M, Bisio A, Ruggeri P, Bove M (2019) Defensive peripersonal space is modified by a learnt protective posture. Sci Rep 9:1–6.

Billington J, Wilkie RM, Field DT, Wann JP (1998) Neural Processing of imminent collision in humans. Proc R Soc 68:48–54.

Bisio A, Garbarini F, Biggio M, Fossataro C, Ruggeri P, Bove M, Bisio XA, Garbarini XF, Biggio XM, Fossataro XC, Ruggeri XP, Bove XM, Bisio A, Garbarini F, Biggio M, Fossataro C, Ruggeri P, Bove M (2017) Dynamic shaping of the defensive peripersonal space through predictive motor mechanisms: When the “near” becomes “far.” J Neurosci 37:2415–2424.

Blum KP, Lamotte D’Incamps B, Zytnicki D, Ting LH (2017) Force encoding in muscle spindles during stretch of passive muscle. PLoS Comput Biol 13:1–24.

Bordi F, LeDoux JE (1994) Response properties of single units in areas of rat auditory thalamus that project to the amygdala - I. Acoustic discharge patterns and frequency receptive fields. Exp Brain Res 98:261–274.

Brainard DH (1997) The Psychophysics Toolbox. Spat Vis 10:433–436.

Bromm B, Treede RD (1991) Laser-evoked cerebral potentials in the assessment of cutaneous pain sensitivity in normal subjects and patients. Rev Neurol (Paris) 147:625–643.

Bufacchi RJ (2017) Approaching threatening stimuli cause an expansion of defensive peripersonal space. J Neurophysiol 118:1927–1930.

Bufacchi RJ, Iannetti G (2016) Gravitational cues modulate the shape of defensive peripersonal space. Curr Biol 26:R1–R3.

Bufacchi RJ, Iannetti GD (2018) An Action Field Theory of Peripersonal Space. Trends Cogn Sci 22:1076-1090.

Bufacchi RJ, Liang M, Griffin LD, Iannetti GD (2016) A geometric model of defensive peripersonal space. J Neurophysiol 115:218–225.

Bufacchi RJ, Magri C, Novembre G, Iannetti GD (2021) Local spatial analysis: An easy-to-use adaptive spatial EEG filter. J Neurophysiol 125:509–521.

Bufacchi RJ, Sambo CF, Di Stefano G, Cruccu G, Iannetti GD (2017) Pain outside the body: defensive peripersonal space deformation in trigeminal neuralgia. Sci Rep 7:1–8.

Calford MB, Aitkin LM (1983) Ascending projections to the medial geniculate body of the cat: Evidence for multiple, parallel auditory pathways through thalamus. J Neurosci 3:2365–2380.

Carpenter AL, Shahin AJ (2013) Development of the N1-P2 auditory evoked response to amplitude rise time and rate of formant transition of speech sounds. Neurosci Lett 544:56–61.

Chait M, Poeppel D, Simon JZ (2008) Auditory temporal edge detection in human auditory cortex. Brain Res 1213:78–90.

Chapman CR, Colpitts YH, Mayeno JK, Gagliardi GJ (1981) Rate of stimulus repetition changes evoked potential amplitude: Dental and auditory modalities compared. Exp Brain Res 43:246–252.

Chen ACN, Chapman RC, Harkins SW (1979) Brain evoked potentials are functional correlates of induced pain in man. Pain 6:365–374.

Clascá F, Rubio-Garrido P, Jabaudon D (2012) Unveiling the diversity of thalamocortical neuron subtypes. Eur J Neurosci 35:1524–1532.

Cohen J (1988) The effect size index: d. In: Statistical power analysis for the behavioural sciences, 2nd ed., pp 77–83. Lawrence Erlbaum Associates.

Colby CL, Duhamel JR, Goldberg ME (1993) Ventral intraparietal area of the macaque: anatomic location and visual response properties. J Neurophysiol 69:902–914.

Cooke DF, Graziano MSA (2003) Defensive Movements Evoked by Air Puff in Monkeys. J Neurophysiol 90:3317–3329.

Creed RS, Denny-Brown D, Eccles JC, Liddell EGT, Sherrington CS (1932) Reflex activity of the spinal cord. Oxford, England: Clarendon Press.

Davis H, Bowers C, Hirsh SK (1968) Relations of the Human Vertex Potential to Acoustic Input: Loudness and Masking. J Acoust Soc Am 43:431–438.

Davis H, Zerlin S (1966) Acoustic Relations of the Human Vertex Potential. 39:179–185.

de Haan AM, Smit M, Van der Stigchel S, Dijkerman HC (2016) Approaching threat modulates visuotactile interactions in peripersonal space. Exp Brain Res 234:1875–1884.

De Vignemont F, Iannetti GD (2015) How many peripersonal spaces? Neuropsychologia 70:327–334.

Delorme A, Makeig S (2004) EEGLAB: an open source toolbox for analysis of single-trial EEG dynamics. J Neurosci Methods 13:9–21.

Duhamel JR, Colby CL, Goldberg ME (1998) Ventral intraparietal area of the macaque: Congruent visual and somatic response properties. J Neurophysiol 79:126–136.

Edeline JM, Manunta Y, Nodal FR, Bajo VM (1999) Do auditory responses recorded from awake animals reflect the anatomical parcellation of the auditory thalamus? Hear Res 131:135–152.

Elfner LF, Gustafson DJ, Williams KN (1976) SIGNAL ONSET AND TASK VARIABLES IN AUDITORY EVOKED POTENTIALS. Biol Psychol 4:197–205.

Ferri F, Tajadura-Jiménez A, Väljamäe A, Vastano R, Costantini M (2015) Emotion-inducing approaching sounds shape the boundaries of multisensory peripersonal space. Neuropsychologia 70:468–475.

Fogassi L, Gallese V, Fadiga L, Luppino G, Matelli M, Rizzolatti G (1996) Coding of peripersonal space in inferior premotor cortex (area F4). J Neurophysiol 76:141–157.

Fossataro C, Bruno V, Gindri P, Garbarini F (2018) Defending the Body Without Sensing the Body Position: Physiological Evidence in a Brain-Damaged Patient With a Proprioceptive Deficit. Front Psychol 9:1–10.

Fossataro C, Tieri G, Grollero D, Bruno V, Garbarini F (2020) Hand blink reflex in virtual reality: The role of vision and proprioception in modulating defensive responses. Eur J Neurosci 51:937–951.

French JD (1953) An Extralemniscal Sensory System in the Brain. Arch Neurol Psychiatry 69:505.

Friesen LM, Tremblay KL (2006) Acoustic change complexes recorded in adult cochlear implant listeners. Ear Hear 27:678–685.

Friston K (2005) A theory of cortical responses. Philos Trans R Soc B Biol Sci 360:815–836.

Friston K (2009) The free-energy principle: a rough guide to the brain? Trends Cogn Sci 13:293–301.

Fruhstorfer H (1971) Habituation and dishabituation of the human vertex response. Electroencephalogr Clin Neurophysiol 30:306–312.

Garcia-Larrea L, Frot M, Valeriani M (2003) Brain generators of laser-evoked potentials: From dipoles to functional significance. Neurophysiol Clin 33:279–292.

García-Larrea L, Peyron R, Laurent B, Mauguière F (1997) Association and dissociation between laser-evoked potentials and pain perception. Neuroreport 8:3785–3789.

Gardner EP, Hämäläinen HA, Warren S, Davis J, Young W (1984) Somatosensory evoked potentials (SEPs) and cortical single unit responses elicited by mechanical tactile stimuli in awake monkeys. Electroencephalogr Clin Neurophysiol 58:537–552.

Geschwind N (1965) Disconnexion syndromes in animals and man. I. Brain 88:237–294.

Graziano MS, Hu XT, Gross CG (1997) Visuospatial properties of ventral premotor cortex. J Neurophysiol 77:2268–2292.

Grech R, Cassar T, Muscat J, Camilleri KP, Fabri SG, Zervakis M, Xanthopoulos P, Sakkalis V, Vanrumste B (2008) Review on solving the inverse problem in EEG source analysis. J Neuroeng Rehabil 5:1–33.

Grillon C, Ameli R, Woods SW, Merikangas K, Davis M (1991) Fear-Potentiated Startle in Humans: Effects of Anticipatory Anxiety on the Acoustic Blink Reflex. Psychophysiology 28:588–595.

Groenewegen HJ, Berendse HW (1994) The specificity of the “nonspecific” midline and intralaminar thalamic nuclei. Trends Neurosci 17:52–57.

Guilbaud G (1968) Évolution au cours du sommeil naturel des réponses somatiques évoquées en différents niveaux corticaux et sous-corticaux chez le chat. (PhD Thesis).

Guo Y, Wang Y, Sun Y, Wang J-Y (2016) A Brain Signature to Differentiate Acute and Chronic Pain in Rats. Front Comput Neurosci 10:1–11.

Han JH, Dimitrijevic A (2015) Acoustic change responses to amplitude modulation: A method to quantify cortical temporal processing and hemispheric asymmetry. Front Neurosci 9:1–15.

He S, Grose JH, Teagle HFB, Woodard J, Park LR, Hatch DR, Roush P, Buchman CA (2015) Acoustically Evoked Auditory Change Complex in Children With Auditory Neuropathy Spectrum Disorder. Ear Hear 36:289–301.

Hébert M, Versace E, Vallortigara G (2019) Inexperienced preys know when to flee or to freeze in front of a threat. Proc Natl Acad Sci U S A 116:22918–22920.

Hegerl U, Gallinat J, Mrowinski D (1994) Intensity dependence of auditory evoked dipole source activity. Int J Psychophysiol 17:1–13.

Herrmann B, Henry MJ, Fromboluti EK, McAuley JD, Obleser J (2015) Statistical context shapes stimulus-specific adaptation in human auditory cortex. J Neurophysiol 113:2582–2591.

Hess A (2015) Importance of knowing your stimulation paradigm. Pain 156:2404–2405.

Hess U, Sabourin G, Kleck RE (2007) Postauricular and eyeblink startle responses to facial expressions. Psychophysiology 44:431–435.

Hillyard SA, Picton TW (1978) ON and OFF components in the auditory evoked potential. Percept Psychophys 24:391–398.

Hird EJ, Jones AKP, Talmi D, El-Deredy W (2018) A comparison between the neural correlates of laser and electric pain stimulation and their modulation by expectation. J Neurosci Methods 293:117–127.

Hoppe U, Wohlberedt T, Danilkina G, Hessel H (2010) Acoustic Change Complex in Cochlear Implant Subjects in Comparison with Psychoacoustic Measures. Cochlear Implants Int 11:426–430.

Hsu MM, Shyu BC (1997) Electrophysiological study of the connection between medial thalamus and anterior cingulate cortex in the rat. Neuroreport 8:2701–2707.

Hu B (2003) Functional organization of lemniscal and nonlemniscal auditory thalamus. Exp Brain Res 153:543–549.

Hu L, Cai MM, Xiao P, Luo F, Iannetti GD (2014a) Human Brain Responses to Concomitant Stimulation of A and C Nociceptors. J Neurosci 34:11439–11451.

Hu L, Iannetti GD (2016) Painful Issues in Pain Prediction. Trends Neurosci 39:212–220.

Hu L, Iannetti GD (2019) Neural indicators of perceptual variability of pain across species. Proc Natl Acad Sci 116:1782–1791.

Hu L, Mouraux A, Hu Y, Iannetti GD (2010) A novel approach for enhancing the signal-to-noise ratio and detecting automatically event-related potentials (ERPs) in single trials. Neuroimage 50:99–111.

Hu L, Valentini E, Zhang ZG, Liang M, Iannetti GD (2014b) The primary somatosensory cortex contributes to the latest part of the cortical response elicited by nociceptive somatosensory stimuli in humans. Neuroimage 84:383–393.

Hu L, Xia XL, Peng WW, Su WX, Luo F, Yuan H, Chen AT, Liang M, Iannetti G (2015) Was it a pain or a sound? Across-species variability in sensory sensitivity. Pain 156:2449–2457.

Huang G, Xiao P, Hung YS, Iannetti GD, Zhang ZG, Hu L (2013) A novel approach to predict subjective pain perception from single-trial laser-evoked potentials. Neuroimage 81:283–293.

Hughes HC (2001) Sensory Exotica: A World beyond Human Experience. Cambridge, Massachusetts: MIT Press.

Hulliger M, Matthews PBC, Noth J (1977) Static and dynamic fusimotor action on the response of IA fibres to low frequency sinusoidal stretching of widely ranging amplitude. J Physiol 267:811–838.

Hunt CC, Wilkinson RS (1980) An analysis of receptor potential and tension of isolated cat muscle spindles in response to sinusoidal stretch. J Physiol 302:241–262.

Hunter J, Jasper HH (1949) Effects of thalamic stimulation in unanaesthetised animals. The arrest reaction and petit Mal-like seizures, activation patterns and generalized convulsions. Electroencephalogr Clin Neurophysiol 1:305–324.

Hyvarinen J, Poranen A (1974) Function of the parietal associative area 7 as revealed from cellular discharges in alert monkeys. Brain 97:673–692.

Iannetti GD, Baumgärtner U, Tracey I, Treede RD, Magerl W (2013) Pinprick-evoked brain potentials: A novel tool to assess central sensitization of nociceptive pathways in humans. J Neurophysiol 110:1107–1116.

Iannetti GD, Hughes NP, Lee MC, Mouraux A (2008) Determinants of laser-evoked EEG responses: pain perception or stimulus saliency? J Neurophysiol 100:815–828.

Iannetti GD, Mouraux A (2010) From the neuromatrix to the pain matrix (and back). Exp Brain Res 205:1–12.

Iannetti GD, Zambreanu L, Cruccu G, Tracey I (2005) Operculoinsular cortex encodes pain intensity at the earliest stages of cortical processing as indicated by amplitude of laser-evoked potentials in humans. Neuroscience 131:199–208.

Jamison JH (1951) Measurement of auditory intensity thresholds in the rat by conditioning of an autonomic response. J Comp Physiol Psychol 44:118–125.

Janssens T, Silva M, Davenport PW, Van Diest I, Dupont LJ, Van Den Bergh O (2014) Attentional modulation of reflex cough. Chest 146:135–141.

Jasper HH (1949) Diffuse projection systems: The integrative action of the thalamic reticular system. Electroencephalogr Clin Neurophysiol 1:405–420.

Jasper HH (1960) Unspecific thalamocortical relations. Neurophysiology II:1307–1321.

Jessop J, Griffiths DE, Furness P, Jones JG, Sapsford DJ, Breckon DA (1991) Changes in amplitude and latency of the p300 component of the auditory evoked potential with sedative and anaesthetic concentrations of nitrous oxide. Br J Anaesth 67:524–531.

Jin QQ, Wu GQ, Peng WW, Xia XL, Hu L, Iannetti GD (2018) Somatotopic Representation of Second Pain in the Primary Somatosensory Cortex of Humans and Rodents. J Neurosci 38:5538–5550.

Jones BE (2003) Arousal systems. Front Biosci 8:s438-451.

Jones EG (1998) Viewpoint: The core and matrix of thalamic organization. Neuroscience 85:331–345.

Jones EG (2001) The thalamic matrix and thalamocortical synchrony. Trends Neurosci 24:595–601.

Jones SJ (1992) AEPs at the onset and offset of repetitive sound modulation, due to mismatch with the contents of an auditory sensory store. Electroencephalogr Clin Neurophysiol Potentials Sect 84:149–156.

Jung T-P, Makeig S, Humphries C, Lee T-W, Mckeown MJ, Iragui V, Sejnowski TJ (2000) Removing electroencephalographic artifacts by blind source separation. Psychophysiology 37:163–178.

Kilintari M, Bufacchi RJ, Novembre G, Guo Y, Haggard P, Iannetti GD (2018) High-precision voluntary movements are largely independent of preceding vertex potentials elicited by sudden sensory events. J Physiol 596:3655–3673.

Knight RT, Brailowsky S, Scabini D, Simpson G V (1985) Surface auditory evoked potentials in the unrestrained rat: component definition. Electroencephalogr Clin Neurophysiol 61:430–439.

Komura Y, Tamura R, Uwano T, Nishijo H, Ono T (2005) Auditory thalamus integrates visual inputs into behavioral gains. Nat Neurosci 8:1203–1209.

Kooi KA, Bagchi BK, Jordan RN (1964) OBSERVATIONS ON PHOTICALLY EVOKED OCCIPITAL AND VERTEX WAVES DURING SLEEP IN MAN*. Ann N Y Acad Sci 112:270–280.

Krahé C, Paloyelis Y, Condon H, Jenkinson PM, Williams SCR, Fotopoulou A (2014) Attachment style moderates partner presence effects on pain: A laser-evoked potentials study. Soc Cogn Affect Neurosci 10:1030–1037.

Kraus N, McGee T, Littman T, Nicol T, King C (1994) Nonprimary auditory thalamic representation of acoustic change. J Neurophysiol 72:1270–1277.

Kulics AT (1982) Cortical neural evoked correlates of somatosensory stimulus detection in the rhesus monkey. Electroencephalogr Clin Neurophysiol 53:78–93.

Leó N L, Casanova-Molla J, Lauria G, Valls-Solé J (2011) The somatosensory blink reflex in upper and lower brainstem lesions. Muscle and Nerve 43:196–202.

Liang M, Mouraux A, Chan V, Blakemore C, Iannetti GD (2010) Functional characterisation of sensory ERPs using probabilistic ICA: Effect of stimulus modality and stimulus location. Clin Neurophysiol 121:577–587.

Liberati G, Algoet M, Klöcker A, Ferrao Santos S, Ribeiro-Vaz JG, Raftopoulos C, Mouraux A (2018) Habituation of phase-locked local field potentials and gamma-band oscillations recorded from the human insula. Sci Rep 8:1–13.

Lindsley DB (1969) Average evoked potentials - achievements, failures and prospects. In: Average evoked potentials: Methods, results, and evaluations. (Donchin E, Lindsley DB, eds). Washington: US National Aeronautics and Space Administration.

Lisney TJ, Rubene D, Rózsa J, Løvlie H, Håstad O, Ödeen A (2011) Behavioural assessment of flicker fusion frequency in chicken Gallus gallus domesticus. Vision Res 51:1324–1332.

Lucia SÁ, Josep L, Álvarez-Blanco S, Leon L, Valls-Solé J (2009) The startle reaction to somatosensory inputs: Different response pattern to stimuli of upper and lower limbs. Exp Brain Res 195:285–292.

Makin TR, Holmes NP, Brozzoli C, Farne A (2012) Keeping the world at hand: Rapid visuomotor processing for hand-object interactions. Exp Brain Res 219:421–428.

Mancini F, Pepe A, Stefano G Di, Mouraux A, Iannetti GD (2018) Characterising the short-term habituation of event-related evoked potentials. eNeuro 5:1–14.

Maris E, Oostenveld R (2007) Nonparametric statistical testing of EEG- and MEG-data. J Neurosci Methods 164:177–190.

Martin BA, Boothroyd A (1999) Cortical, auditory, event-related potentials in response to periodic and aperiodic stimuli with the same spectral envelope. Ear Hear 20:33–44.

Martin BA, Boothroyd A (2000) Cortical, auditory, evoked potentials in response to changes of spectrum and amplitude. J Acoust Soc Am 107:2155–2161.

Mathew R, Undurraga J, Li G, Meerton L, Boyle P, Shaida A, Selvadurai D, Jiang D, Vickers D (2017) Objective assessment of electrode discrimination with the auditory change complex in adult cochlear implant users. Hear Res 354:86–101.

Matsumoto N, Minamimoto T, Graybiel AM, Kimura M (2001) Neurons in the thalamic CM-Pf complex supply striatal neurons with information about behaviorally significant sensory events. J Neurophysiol 85:960–976.

Mitchell CL, Kaelber WW (1966) Effect of medial thalamic lesions in responses elicited by tooth pulp stimulation. Am J Physiol 210:263–269.

Miwa H, Nohara C, Hotta M, Shimo Y, Amemiya K (1998) Somatosensory-evoked blink response: Investigation of the physiological mechanism. Brain 121:281–291.

Moayedi M, Di Stefano G, Stubbs MT, Djeugam B, Liang M, Iannetti GD (2016) Nociceptive-evoked potentials are sensitive to behaviorally relevant stimulus displacements in egocentric coordinates. eNeuro 3:399–418.

Moayedi M, Liang M, Sim AL, Hu L, Haggard P, Iannetti GD (2015) Laser-evoked vertex potentials predict defensive motor actions. Cereb Cortex 25:4789–4798.

Mobascher A, Brinkmeyer J, Warbrick T, Musso F, Wittsack HJ, Stoermer R, Saleh A, Schnitzler A, Winterer G (2009) Fluctuations in electrodermal activity reveal variations in single trial brain responses to painful laser stimuli - A fMRI/EEG study. Neuroimage 44:1081–1092.

Mouraux A, Iannetti GD (2008) Across-trial averaging of event-related EEG responses and beyond. Magn Reson Imaging 26:1041–1054.

Mouraux A, Iannetti GD (2009) Nociceptive Laser-Evoked Brain Potentials Do Not Reflect Nociceptive-Specific Neural Activity. J Neurophysiol 101:3258–3269.

Mouraux A, Iannetti GD (2018) The search for pain biomarkers in the human brain. Brain:3290–3307.

Mulert C, Juckel G, Augustin H, Hegerl U (2002) Comparison between the analysis of the loudness dependency of the auditory N1/P2 component with LORETA and dipole source analysis in the prediction of treatment response to the selective serotonin reuptake inhibitor citalopram in major depression. Clin Neurophysiol 113:1566–1572.

Murray MM, Brunet D, Michel CM (2008) Topographic ERP analyses: A step-by-step tutorial review. Brain Topogr 20:249–264.

Näätänen R, Picton T (1987) The N1 Wave of the Human Electric and Magnetic Response to Sound: A Review and an Analysis of the Component Structure. Psychophysiology 24:375–425.

Neville HJ, Foote SL (1984) Auditory event-related potentials in the squirrel monkey: Parallels to human late wave responses. Brain Res 298:107–116.

Nishihara M, Inui K, Motomura E, Otsuru N, Ushida T, Kakigi R (2011) Auditory N1 as a change-related automatic response. Neurosci Res 71:145–148.

Noel JP, Grivaz P, Marmaroli P, Lissek H, Blanke O, Serino A (2015) Full body action remapping of peripersonal space: The case of walking. Neuropsychologia 70:375–384.

Novembre G, Pawar VM, Bufacchi RJ, Kilintari M, Srinivasan M, Rothwell JC, Haggard P, Iannetti GD (2018) Saliency detection as a reactive process: Unexpected Sensory Events Evoke Corticomuscular Coupling. J Neurosci 38:2385–2397.

Novembre G, Pawar VM, Kilintari M, Bufacchi RJ, Guo Y, Rothwell JC, Iannetti GD (2019) The effect of salient stimuli on neural oscillations, isometric force, and their coupling. Neuroimage 198:221–230.

Onishi S, Davis H (1968) Effects of Duration and Rise Time of Tone Bursts on Evoked V Potentials. J Acoust Soc Am 44:582–591.

Oostenveld R, Fries P, Maris E, Schoffelen J-M (2011) FieldTrip: Open Source Software for Advanced Analysis of MEG, EEG, and Invasive Electrophysiological Data. Comput Intell Neurosci 2011:1–9.

Paloyelis Y, Krahé C, Maltezos S, Williams SC, Howard MA, Fotopoulou A (2016) The Analgesic Effect of Oxytocin in Humans: A Double-Blind, Placebo-Controlled Cross-Over Study Using Laser-Evoked Potentials. J Neuroendocrinol 28.

Parker DM, Salzen EA, Lishman JR (1982) Visual-evoked responses elicited by the onset and offset of sinusoidal gratings: Latency, waveform, and topographic characteristics. Investig Ophthalmol Vis Sci 22:675–680.

Paus T, Zatorre RJ, Hofle N, Caramanos Z, Gotman J, Petrides M, Evans AC (1997) Time-related changes in neural systems underlying attention and arousal during the performance of an auditory vigilance task. J Cogn Neurosci 9:392–408.

Peck TC, Seinfeld S, Aglioti SM, Slater M (2013) Putting yourself in the skin of a black avatar reduces implicit racial bias. Conscious Cogn 22:779–787.

Peschanski M, Guilbaud G, Gautron M (1981) Posterior intralaminar region in rat: Neuronal responses to noxious and nonnoxious cutaneous stimuli. Exp Neurol 72:226–238.

Phipson B, Smyth GK (2010) Permutation P-values should never be zero: Calculating exact P-values when permutations are randomly drawn. Stat Appl Genet Mol Biol 9:1–12.

Picton TW, Alain C, Woods DL, John MS, Scherg M, Valdes-Sosa P, Bosch-Bayard J, Trujillo NJ (1999) Intracerebral Sources of Human Auditory-Evoked Potentials. Audiol Neuro-Otology 4:64–79.

Picton TW, Hillyard SA (1974) Human auditory evoked potentials. II: effects of attention. Electroencephalogr Clin Neurophysiol 36:191–199.

Pierrel-Sorrentino R, Raslear TG (1980) Loudness Scaling in Rats and Chinchillas. J Comp Physiol Psychol 94:757–766.

Pineda JA, Foote SL, Neville HJ (1989) Effects of locus coeruleus lesions on auditory, long-latency, event-related potentials in monkey. J Neurosci 9:81–93.

Polich J (2007) Updating P300: An integrative theory of P3a and P3b. Clin Neurophysiol 118:2128–2148.

Pratt H, Starr A, Michalewski HJ, Dimitrijevic A, Bleich N, Mittelman N (2010) A comparison of auditory evoked potentials to acoustic beats and to binaural beats. Hear Res 262:34–44.

Raslear TG (1989) Discriminability, Loudness and Masking in the Rat (Rattus norvegicus): A Confirmation and Extension. J Comp Psychol 103:289–296.

Ritter W, Vaughan HG, Costa LD (1968) Orienting and habituation to auditory stimuli: A study of short terms changes in average evoked responses. Electroencephalogr Clin Neurophysiol 25:550–556.

Ronga I, Valentini E, Mouraux A, Iannetti GD (2013) Novelty is not enough: laser-evoked potentials are determined by stimulus saliency, not absolute novelty. J Neurophysiol 44:692–701.

Sambo CF, Forster B, Williams SC, Iannetti GD (2012a) To Blink or Not to Blink: Fine Cognitive Tuning of the Defensive Peripersonal Space. J Neurosci 32:12921–12927.

Sambo CF, Iannetti GD (2013) Better safe than sorry? The safety margin surrounding the body is increased by anxiety. J Neurosci 33:14225–14230.

Sambo CF, Liang M, Cruccu G, Iannetti GD (2012b) Defensive peripersonal space: the blink reflex evoked by hand stimulation is increased when the hand is near the face. J Neurophysiol 107:880–889.

Sandrini G, Serrao M, Rossi P, Romaniello A, Cruccu G, Willer JC (2005) The lower limb flexion reflex in humans. Prog Neurobiol 77:353–395.

Scherg M, Vajsar J, Picton TW (1989) A source analysis of the late human auditory evoked potentials. J Cogn Neurosci 1:336–355.

Schweitzer PK (1977) Auditory evoked brain responses: Comparison of ON and OFF responses at long and short durations. Percept Psychophys 22:87–94.

Schweitzer PK, Tepas DI (1974) Intensity effects of the auditory evoked brain response to stimulus onset and cessation. Percept Psychophys 16:396–400.

Shahin A, Bosnyak DJ, Trainor LJ, Roberts LE (2003) Enhancement of neuroplastic P2 and N1c auditory evoked potentials in musicians. J Neurosci 23:5545–5552.

Simpson TP, Manara AR, Kane NM, Barton RL, Rowlands CA, Butler SR (2002) Effect of propofol anaesthesia on the event-related potential mismatch negativity and the auditory-evoked potential N1. Br J Anaesth 89:382–388.

Simpson G V, Knight RT (1993) Multiple brain systems generating the rat auditory evoked potential. II. Dissociation of auditory cortex and non-lemniscal generator systems. Brain Res 602:251–263.

Snyder E, Hillyard SA (1976) Long-latency evoked potentials to irrelevant, deviant stimuli. Behav Biol 16:319–331.

Somervail R, Bufacchi RJ, Guo Y, Kilintari M, Novembre G, Swapp D, Steed A, Iannetti GD (2019) Movement of environmental threats modifies the relevance of the defensive eye-blink in a spatially-tuned manner. Sci Rep 9:1–9.

Somervail R, Zhang F, Novembre G, Bufacchi RJ, Guo Y, Crepaldi M, Hu L, Iannetti GD (2021) Waves of Change: Brain Sensitivity to Differential, not Absolute, Stimulus Intensity is Conserved Across Humans and Rats. Cereb Cortex 31:949–960.

Spackman L, Boyd S, Towell T (2006) Identification and characterization of somatosensory off responses. Brain Res 1114:53–62.

Spychala P, Rose DE, Grier JB (1969) Comparison of the “ON” And “OFF” Characteristics of the Acoustically Evoked Response. Int Audiol 8:416–423.

Squintani G, Brugnoli MP, Pasin E, Segatti A, Concon E, Polati E, Bonetti B, Matinella A (2018) Changes in laser-evoked potentials during hypnotic analgesia for chronic pain: A pilot study. Ann Palliat Med 7:7–16.

Staikou C, Kokotis P, Kyrozis A, Rallis D, Makrydakis G, Manoli D, Karandreas N, Stamboulis E, Moschovos C, Fassoulaki A (2017) Differences in Pain Perception Between Men and Women of Reproductive Age: A Laser-Evoked Potentials Study. Pain Med 18:316–321.

Taffou M, Viaud-Delmon I (2014) Cynophobic fear adaptively extends peri-personal space. Front Psychiatry 5:3–9.

Thomson JM, Goswami U, Baldeweg T (2009) The ERP signature of sound rise time changes. Brain Res 1254:74–83.

Tiemann L, Hohn VD, Ta Dinh S, May ES, Nickel MM, Gross J, Ploner M (2018) Distinct patterns of brain activity mediate perceptual and motor and autonomic responses to noxious stimuli. Nat Commun 9:1–12.

Torta DM, Liang M, Valentini E, Mouraux A, Iannetti GD (2012) Dishabituation of laser-evoked EEG responses: Dissecting the effect of certain and uncertain changes in stimulus spatial location. Exp Brain Res 218:361–372.

Tran TD, Lam K, Hoshiyama M, Kakigi R (2001) A new method for measuring the conduction velocities of Aβ-, Aδ- and C-fibers following electric and CO2 laser stimulation in humans. Neurosci Lett 301:187–190.

Treede RD, Kief S, Hölzer T, Bromm B (1988) Late somatosensory evoked cerebral potentials in response to cutaneous heat stimuli. Electroencephalogr Clin Neurophysiol 70:429–441.

Treede RD, Lorenz J, Baumgärtner U (2003) Clinical usefulness of laser-evoked potentials. Neurophysiol Clin 33:303–314.

Uglem M, Omland PM, Stjern M, Gravdahl GB, Sand T (2017) Habituation of laser-evoked potentials by migraine phase: a blinded longitudinal study. J Headache Pain 18.

Valentini E, Hu L, Chakrabarti B, Hu Y, Aglioti SM, Iannetti GD (2012) The primary somatosensory cortex largely contributes to the early part of the cortical response elicited by nociceptive stimuli. Neuroimage 59:1571–1581.

Valentini E, Torta DME, Mouraux A, Iannetti GD (2011) Dishabituation of Laser-evoked EEG Responses: Dissecting the Effect of Certain and Uncertain Changes in Stimulus Modality. J Cogn Neurosci 23:2822–2837.

Valeriani M, Betti V, Le Pera D, De Armas L, Miliucci R, Restuccia D, Avenanti A, Aglioti SM (2008) Seeing the pain of others while being in pain: A laser-evoked potentials study. Neuroimage 40:1419–1428.

Valeriani M, Liguori S, Vollono C, Testani E, Bangrazi S, Petti F, Liguori A, Germanotta M, Padua L, Pazzaglia C (2021) Homotopic reduction in laser-evoked potential amplitude and laser-pain rating by abdominal acupuncture. Eur J Pain 25:659–667.

Van Der Werf YD, Witter MP, Groenewegen HJ (2002) The intralaminar and midline nuclei of the thalamus. Anatomical and functional evidence for participation in processes of arousal and awareness. Brain Res Rev 39:107–140.

von Uexküll J (1909) Umwelt und Innenwelt der Tiere. Berlin: Springer.

Wagner M, Roychoudhury A, Campanelli L, Shafer VL, Martin B, Steinschneider M (2016) Representation of spectro-temporal features of spoken words within the P1-N1-P2 and T-complex of the auditory evoked potentials (AEP). Neurosci Lett 614:119–126.

Wallwork SB, Talbot K, Camfferman D, Moseley GL, Iannetti GD (2016) The blink reflex magnitude is continuously adjusted according to both current and predicted stimulus position with respect to the face. Cortex 81:168–175.

Walter WG (1964) The convergence and interaction of visual, auditory, and tactile responses in human nonspecific cortex. Ann N Y Acad Sci 112:320–361.

Wang AL, Mouraux A, Liang M, Iannetti GD (2010) Stimulus novelty, and not neural refractoriness, explains the repetition suppression of laser-evoked potentials. J Neurophysiol 104:2116–2124.

Wang CA, Munoz DP (2015) A circuit for pupil orienting responses: Implications for cognitive modulation of pupil size. Curr Opin Neurobiol 33:134–140.

Weise A, Schröger E, Fehér B, Folyi T, Horváth J (2012) Auditory event-related potentials reflect dedicated change detection activity for higher-order acoustic transitions. Biol Psychol 91:142–149.

Weise A, Schröger E, Horváth J (2018) The detection of higher-order acoustic transitions is reflected in the N1 ERP. Psychophysiology 55:1–14.

Woods DL, Clayworth CC, Knight RT, Simpson G V., Naeser MA (1987) Generators of middle- and long-latency auditory evoked potentials: implications from studies of patients with bitemporal lesions. Electroencephalogr Clin Neurophysiol Evoked Potentials 68:132–148.

Woods DL, Knight RT, Neville HJ (1984) Bitemporal lesions dissociate auditory evoked potentials and perception. Electroencephalogr Clin Neurophysiol 57:208–220.

Xia XL, Peng WW, Iannetti GD, Hu L (2016) Laser-evoked cortical responses in freely-moving rats reflect the activation of C-fibre afferent pathways. Neuroimage 128:209–217.

Yamashiro K, Inui K, Otsuru N, Kida T, Akatsuka K, Kakigi R (2008) Somatosensory off-response in humans: An ERP study. Exp Brain Res 190:207–213.

Zanker JM, Harris JP (2002) On temporal hyperacuity in the human visual system. Vision Res 42:2499–2508.

Zaslansky R, Sprecher E, Katz Y, Rozenberg B, Hemli JA, Yarnitsky D (1996) Pain-evoked potentials: What do they really measure? Electroencephalogr Clin Neurophysiol - Evoked Potentials 100:384–391.

Zhang F, Wang F, Yue L, Zhang H, Peng W, Hu L (2019) Cross-Species Investigation on Resting State Electroencephalogram. Brain Topogr 32:808–824.

Zhang M, Zhang Y, Li Z, Hu L, Kong Y (2021) Sexism-Related Stigma Affects Pain Perception. Neural Plast 2021:1–11.

10 Glossary

AEP – auditory-evoked potential

ANOVA – analysis of variance

AUC – area under curve

CM-Pf – Centromedian–Parafascicular Complex

EcoG – electrocorticography

EEG – electroencephalography

ERP – event-related potential

FDR – false discovery rate

fMRI – functional magnetic resonance imaging

GFP – global field power

GoF – goodness of fit

HBR – hand blink reflex

IC – independent component (s)

ICA – independent component analysis (also pICA: *probabilistic* independent component analysis)

LEP – laser-evoked potential

LME – linear mixed-effect model

PPS – peripersonal space

VP – Vertex Potential (s)

VR – Virtual Reality